DYNAMICS OF JACK-UP PLATFORMS IN ELEVATED CONDITION

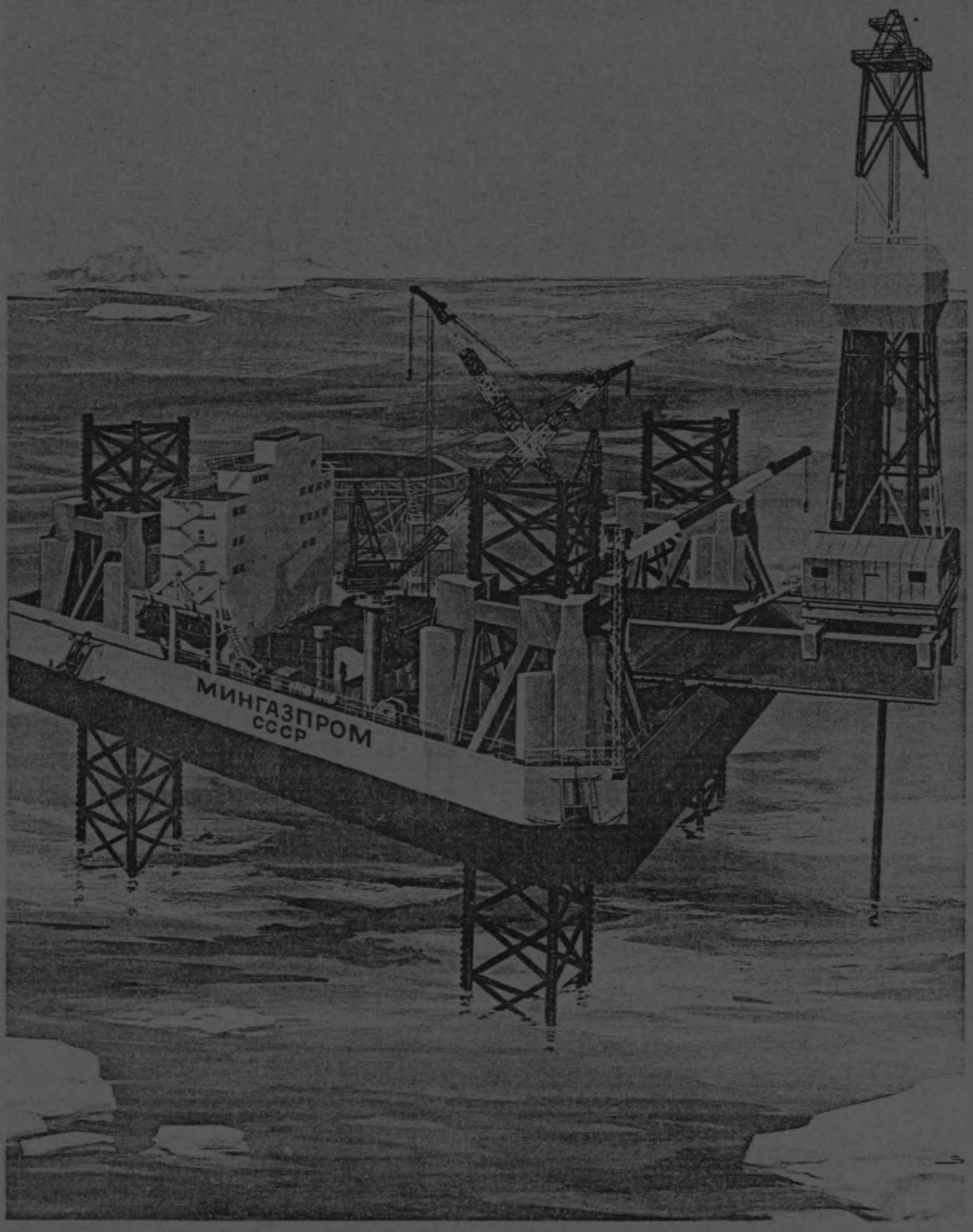

S.A. Nagy
GUSTO ENGINEERING C.V.
Schiedam, The Netherlands
February, 1986

PREFACE

This report is the result of a graduation project of the Delft University of Technology, Department of Civil Engineering, under the supervision of Prof. E. W. Bijker and Prof. A. L. Bouma. The project was carried out in order of Gusto Engineering, Schiedam, The Netherlands.

Apart from both professors, I would like to thank D. J. Lub at Gusto Engineering, and C. van Soven, E. Klaver and W. W. Massie, all at the Delft University of Technology, for their contributions and support during this study. Furthermore, I would like to mention Wim Janse at Gusto Engineering for his great support concerning hydrodynamics and computer programming.

S. A. Nagy

CONTENTS

1 INTRODUCTION

1.1 PURPOSE

The main objective of this study is to get an insight into the dynamic behaviour of a jack-up platform with lattice legs, in elevated condition. The main parameters to be examined are:

a. Water loads

b. Deck motions

c. Hydrodynamic damping

These parameters will be investigated for the excitation of the platform by a regular wave as well as a stochastic sea state represented by a JONSWAP wave spectrum.

An attempt will be made to find statistical distribution functions for the water loads and the platform motions for the case of a spectral reprentation of the waves at sea.

A numerical approach to handle jack-up dynamics is developed, together with the necessary computer programs, applicable to a wide range of jack-up platforms and environmental conditions.

Much attention will be paid to comparing frequency domain analysis and time domain analysis.

In order to get a verification of the general results, the resulting numerical model will be applied to a Russian platform, the Kolskaya, which is shown on the cover of this report. Its properties are described in paragraph 1.3.

1.2 GENERAL DESCRIPTION OF JACK-UP PLATFORMS

Jack-up platforms have been in use since about 1955. This type of platform has become a standard tool for operations in water with depths up to 100 metres. In the offshore industry, it is mainly used for exploration and drilling activities, because of its mobility. Basically, a jack-up is a self-elevating pontoon, which is carried by retractable legs resting on the sea bed. This is the case during operation, which is the situation to be studied in this report.

If the legs are pulled up by means of jacking mechanisms, the platform can be towed by tugboats or carried by a heavy transportation vessel to another location at sea.

The number of legs of the platform depends on the design and varies from three to eight. The legs are either designed as

tubulars with circular or square cross-section, or as lattice structures with triangular or square cross-section.

1.3 RUSSIAN JACK-UP PLATFORM

1.3.1 General

The platform to be studied is of the three-legged type with the derrick cantilevered over the side. It was ordered from Rauma Repola Offshore Division, Finland by the Russian Ministry of Gas in 1982. It is designed by Gusto Engineering, Schiedam, for operation under arctic conditions of Kara, Baltic, Barents, and Okhotsk Seas and the Black Sea of the USSR. All data concerning the structure have been derived from reports by Gusto Engineering.

1.3.2 Particulars

The pontoon of the Russian platform is triangular, with a cantilevered derrick (see figures 1.1 and 1.2). Its main properties are:

Length	69.28	m
Breadth	80.00	m
Depth at centre line	8.55	m
Pontoon mass	7960	tons

The legs are of the triangular lattice type with vertical, horizontal and diagonal elements. The vertical elements are called chords and are interconnected by the diagonal elements, the so-called braces. The buckling length of these braces is reduced by means of spanbreakers, which interconnect the centres of all braces in one bay of the legs (see figures 1.3 and 1.4). Because of their configuration in this type of leg design the braces are called X-braces (see figures 1.2 and 1.3). The cross-sections of the chords are triangular shaped, while the other elements are tubular.

At the lower end of each leg there is a spud can to reduce penetration into the soil (see figure 1.2).

The main leg properties are:

Bay height	5.76	m
Length overall	141.50	m
Centre chord to centre chord	10.50	m
Nominal mass, incl. spud can	1160	tons
Spud can mass	60	tons
Spud can area	180	m
Equivalent spud can radius	7.57	m

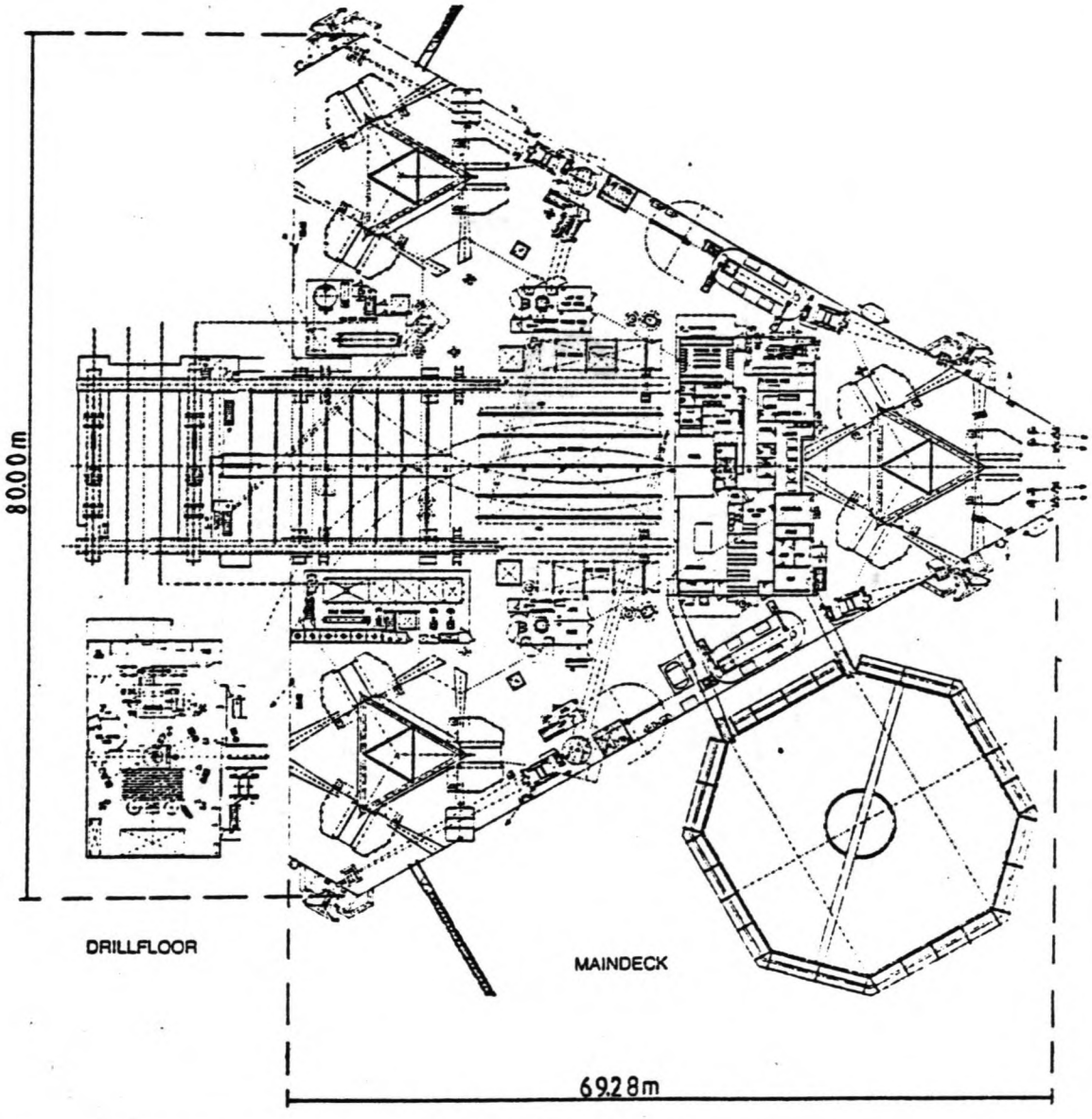

Figure 1.1: Topview of the jack-up platform Kolskaya

As the spud can has an octagonal shape, the equivalent spud can radius is defined as the radius of a circle with the same area as the spud can (see figure 1.5).

In the connection of the legs to the hull, moments and horizontal forces are carried by a guiding system, consisting of twelve steel pads, the guides. The six lower guides are attached to the pontoon itself, near its bottom, and the six upper guides are supported by a framework (see figure 1.6).

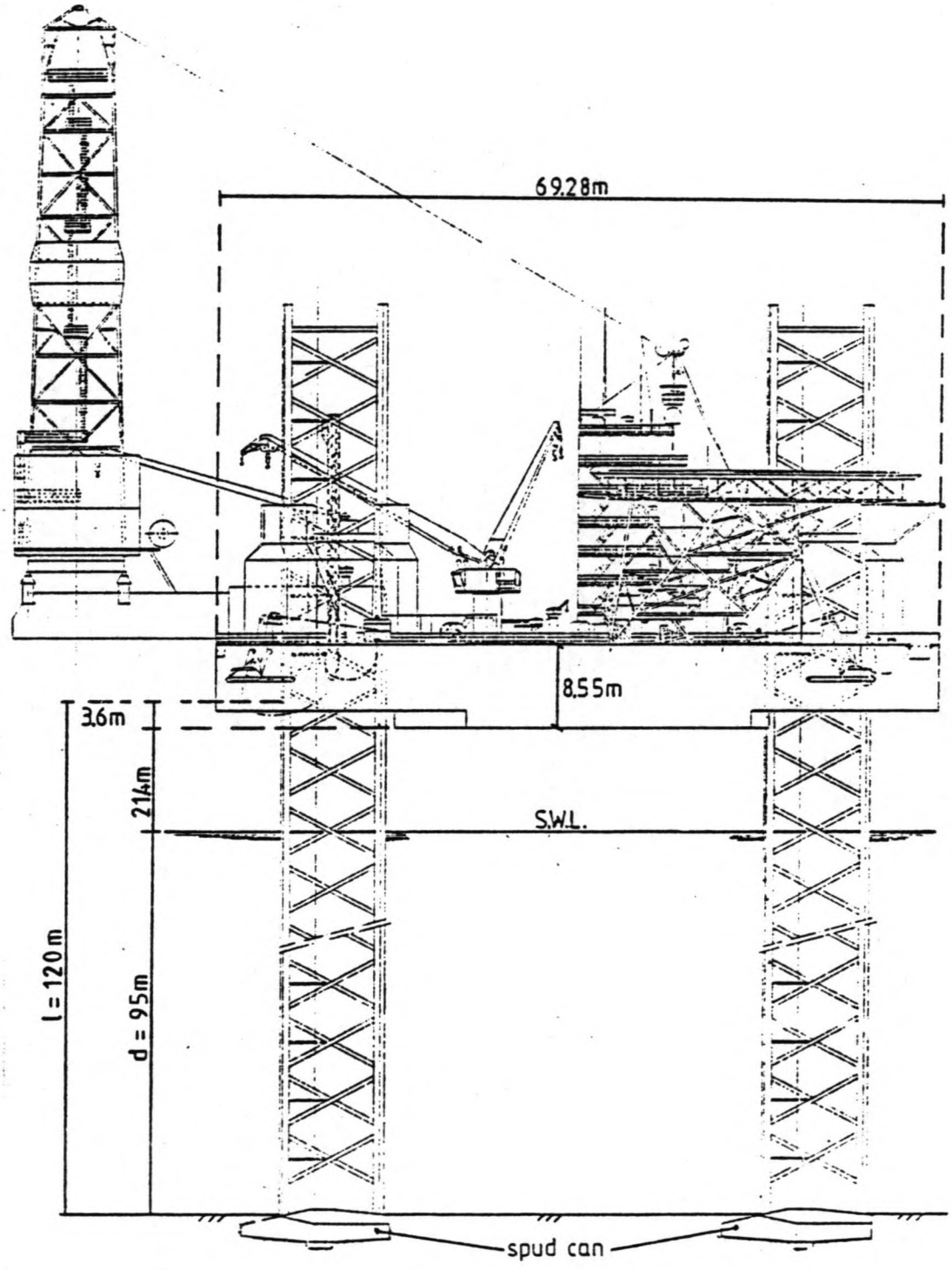

Figure 1.2: Sideview of the jack-up platform Kolskaya

The pontoon is elevated by an electrically driven rack and pi-

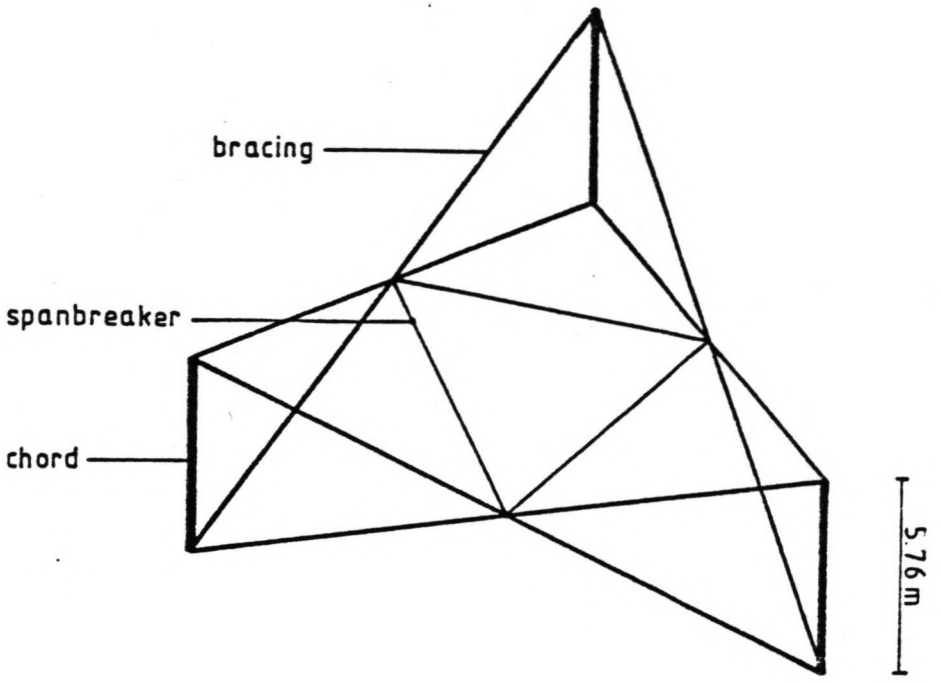

Figure 1.3: One bay of the leg

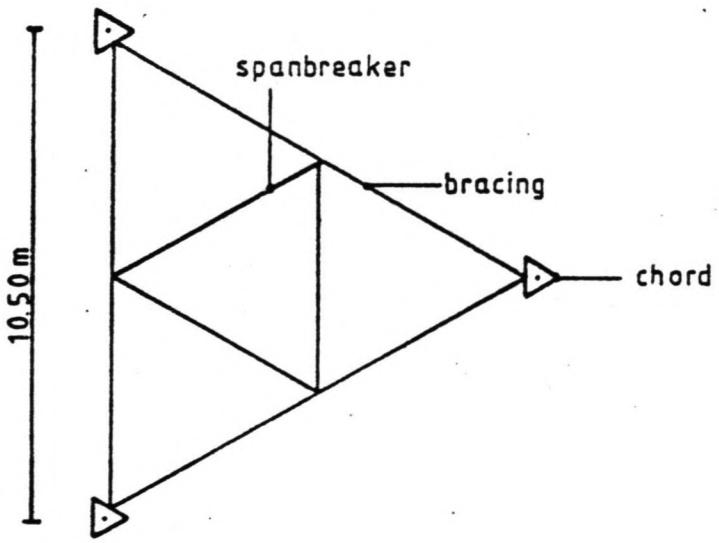

Figure 1.4: Cross-section of one leg

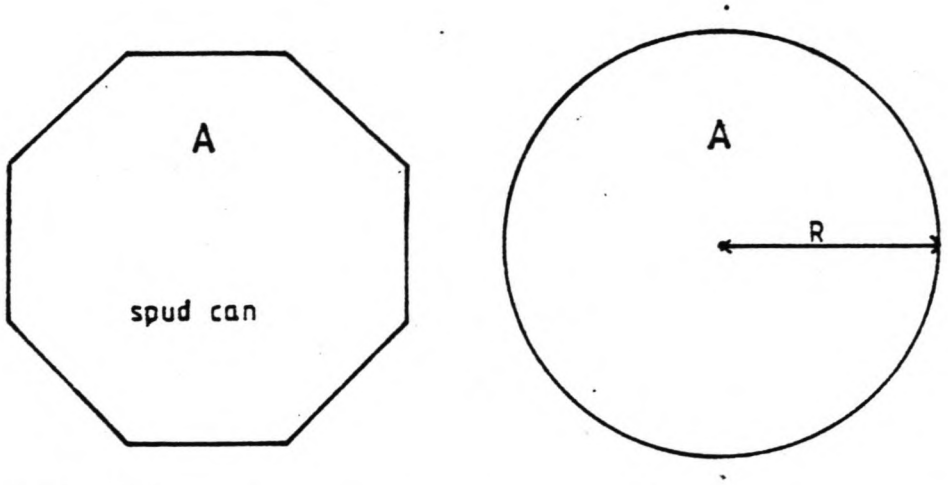

Figure 1.5: Equivalent spud can area

nion system, which is integrated in the framework supporting the upper guides. The elevated condition of the pontoon is maintained by means of brakes acting on the motor units, so the vertical forces within the leg-hull connection are always carried by the toothing of the racks and the pinion wheels. There is on rack per chord of the leg and there are four pinion wheels acting on each rack. Each wheel has its own motor and brake.

As the toothing of the racks and the pinion wheels is relatively vulnerable, it is desirable to minimize the forces in the toothing. For this reason, the twelve motor units per leg, including the brakes, are linked hydraulically by a load sharing device, keeping the forces equal in all pinion wheels under all conditions. This means that the rack and pinion system is not loaded by moments but only by the vertical forces in the leg-hull connection.

The main properties of the alevating system are:

Distance centre lower guide and bottom hull	3.60	m
Vertical guide distance	16.50	m
Holding force of the brakes, per leg	73920	kN

The upper point of fixation of the leg is assumed to be at the centre of the lower guides, from now on refered to as the lower guide level.

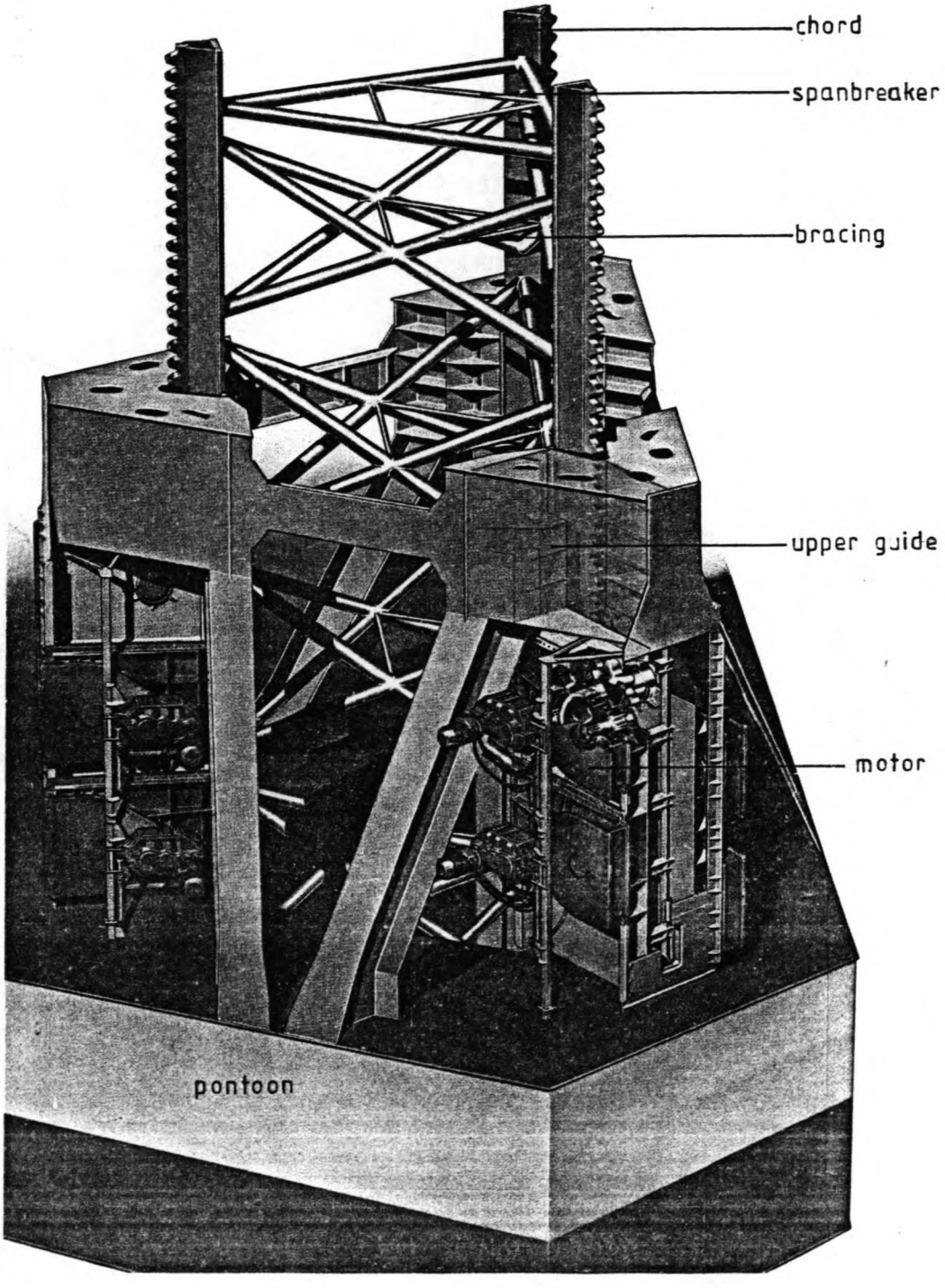

Figure 1.6: Jacking system of the Kolskaya

In this study, the free leg length, l, is defined as the dis-

tance between the tip of the spud can and the lower guides.

The design conditions as stated by Gusto are listed for operation and survival conditions:

	Operation	Survival	
Maximum payload	2650	2300	tons
Pontoon mass	7960	7960	tons
Total elevated mass	10610	10260	tons
Free leg length for maximum elevation	120	120	m

1.4 LOCATION

Since it is virtually impossible to obtain the necessary environmental data for the operational sea areas of the Russian jack-up platform, a North Sea location has been chosen for the tests of the numerical model. It is assumed that the jack-up is located on the Forties field, as shown in figure 1.7.

The following design conditions have been derived from Noble and Denton:

Water depth (including tide and storm surge)	95	m
50 year wave height	28	m
50 year wave period	17.5	s
Wind speed (1 min. sust.)	43	m/s
Current at surface	0.8	m/s
Airgap between hull bottom and still water level	21.4	m

The airgap between the hull bottom and still water level is found by assuming that the maximum elevation of the water surface due to the design wave is 70 % of its wave height, as shown in figure 1.8.

This is the approximate surface elevation computed for a fifth order Stokes wave of the above properties. Most classification rules require an airgap of 6 feet on top of the design wave. This yields the following airgap computation:

Maximum surface elevation due to the 50 year wave:	70 % * 28 m =	19.6 m
6 feet airgap:	+	1.8 m
Airgap between hull bottom and still water level:		21.4 m

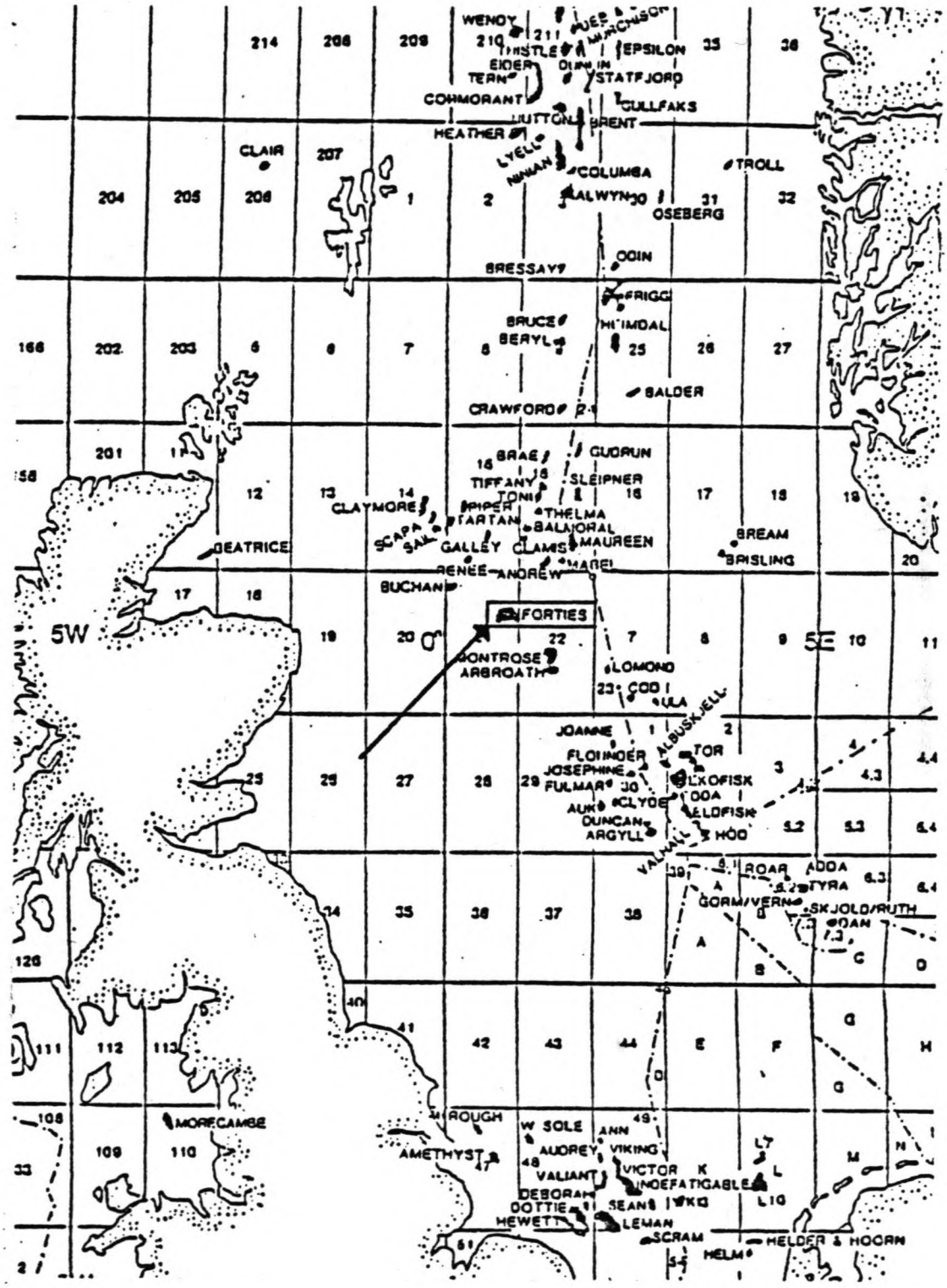

Figure 1.7: Location of the Forties field

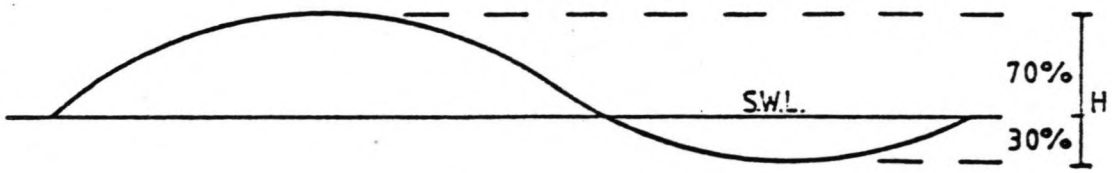

Figure 1.8: Height distribution of the design wave

Application of its definition yields the free leg length:

Water depth (including tide and storm surge):	95 m
Airgap between hull bottom and still water level:	21.4 m
Distance between lower guide level and hull bottom:	3.6 m
Free leg length	120.0 m

For the purpose of a stochastic wave representation by means of a wave spectrum, it has been derived from scatter diagrams, that the 50 year design wave has the largest probability of occuring in the sea state with a peak period of 12 s and a significant wave height of 14 m. In order to enable the analysis of dynamic amplification effects on the platform response due to sea states with peak periods near the natural periods of the jack-up, the following range of sea states will be examined:

Peak period [s]	Significant wave height [m]
8.0	6.0
8.5	7.0
9.0	8.0
9.5	9.0
10.0	10.0
10.5	11.0
11.0	12.0
11.5	13.0
12.0	14.0

Table 1.1: Design sea states
of the Forties field

2 PARAMETER STUDY

2.1 INTRODUCTION

In this chapter all parameters that are needed for a dynamic response analysis of a jack-up, are examined. For this purpose the data listed in paragraph 1.3 are used. The parameters to be examined are:

a. Mass distribution of the legs

b. Mass distribution of the deck

c. Stiffness of the legs

d. Stiffness of the leg-soil connection

e. Stiffness of the leg-hull connection

f. Second order bending

g. Damping

h. Loads

The formulas are derived for the Russian platform, but most of them apply to a wide range of jack-ups.

For many of the computations it is very convenient to use a coordinate system that is fixed to the platform. Figure 2.1 shows the the orientation of the axes used in this report. The origin is located at the sea bottom, vertically below the gravity centre of the pontoon.

The basis of the parameter study in this chapter is the general dynamic model presented in paragraph 2.2. A more detailed model will be highlighted in chapter 5.

Before the above parameters are analysed, a closer look is taken at the leg-soil connection.

It should be noted that it is inevitable that some of the results in this chapter are based on the results stated later. This is due to the links between several parameters.

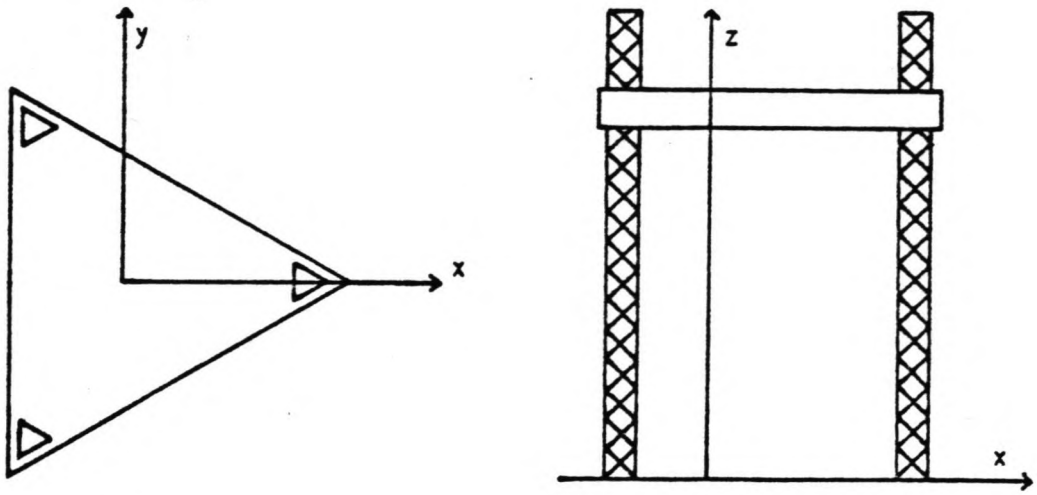

Figure 2.1: Platform-fixed coordinate system

2.2 GENERAL DYNAMIC MODEL

In this paragraph the basis is presented of a dynamic model, that will be refined in the next chapters. The main structural property underlying this model is the lateral flexibility of a jack-up platform, which is large compared to its vertical flexibility. Due to this, vertical translations of the deck and rotation of the deck about a horizontal axis are negligible, if the amplitude of the lateral motions is small compared to the free leg length. This means that the dynamic response of the platform is dominated by lateral motions and that there are three degrees of freedom (see figure 2.2):

a. Two orthogonal translations.

b. Rotation about the vertical axis through the gravity centre of the platform.

According to theory, this three-degrees-of-freedom system can be split into three single-degree-of-freedom systems, if the following conditions are satisfied:

a. Low damping percentages.

b. Platform symmetry about an axis parallel to the loading direction. This implies that the motion modes are not linked physically.

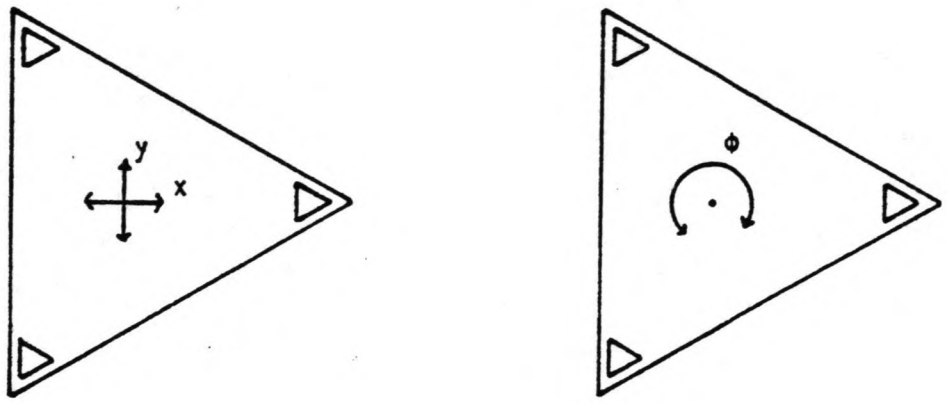

Figure 2.2: Degrees of freedom of a jack-up platform

For jack-up platforms in general, maximum damping percentages are about 5 %, so the first condition is satisfied. In the case of the Russian platform the second condition is satisfied for the loading directions shown in figure 2.3.

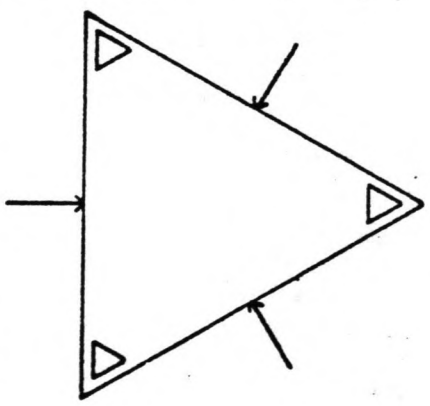

Figure 2.3: Symmetrical loading directions of the Kolskaya

As a first approximation, the three motion modes will be considered separately in this chapter. The frequency domain computer program, however, applies to the general three-degrees-of-freedom system. This is outlined in chapter 6.

The theory for both of the translational modes is identical,

and therefore the parameters involved are only examined for one direction. However, this does not imply that the motion amplitudes of both translational motions are equal, as this depends on the loading conditions.

The two remaining single-degree-of-freedom systems to be studied are described by the following parameters, as shown in figure 2.4:

M_{DYN} = dynamic deck mass

k_{TR} = translational stiffness

c_{TR} = translational damping

J = mass moment of inertia

k_{ROT} = rotational stiffness

c_{ROT} = rotational damping

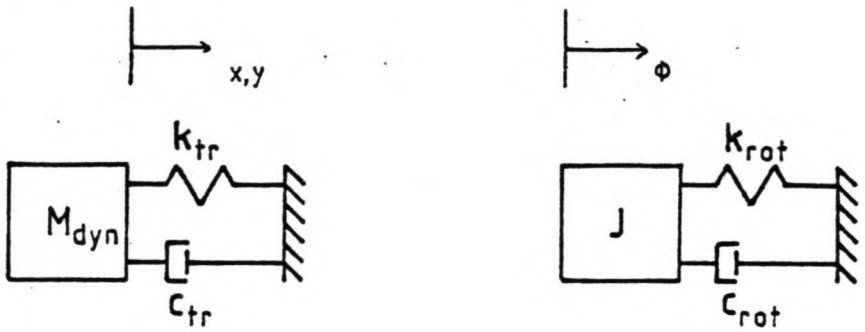

Figure 2.4: Single-degree-of-freedom systems replacing the platform

It should be noted that the frequency domain computer program that has been developed does not use the three single-degree-of-freedom systems, but the 'original' three-degrees-of-freedom system, and therefore it is capable of handling assymetric platform configurations and relatively high damping percentages.

2.3 LEG-SOIL CONNECTION

The damping and stiffness properties of the leg-soil connection are of great importance for the dynamic behaviour of a jack-up platform, but their evaluation is troubled by the following problems and uncertainties:

a. The effect of cyclic loading on soil.

b. Possible non-linearity of the relationship between loads and displacements.

c. Degree of spud can penetration into the soil.

d. The influence of bottom slopes.

e. Possible plastic behaviour of the soil near failure.

f. Due to the mobility of jack-ups it is virtually impossible to predict soil parameter values. Strong fluctuations occur even within relatively small areas.

Remarks a. to e. reflect the poor knowledge about the mechanisms governing the interaction between the sea bed and the spud can and even for a simplified model of interaction there are no adequate formulas available describing the soil damping and stiffness.

The problems arising from the lack of knowledge about the leg-soil interaction are handled by making the following assumptions:

a. Horizontal motions of the spud can are negligible.

b. Vertical motions of the spud can are negligible.

c. Deck motions cause the leg to rotate about a horizontal axis through the tip of the spud can (see figure 2.5).

d. The rotational soil restraint is independent of the penetration depth of the leg.

ad b. In appendix 1.7.2 it is found that the variation of the axial leg load, due to deck motions, is less than 7.5 % of the average axial leg load, and therefore the vertical spud can displacements will be small.

ad c. Since the amplitude of the dynamic soil stress due

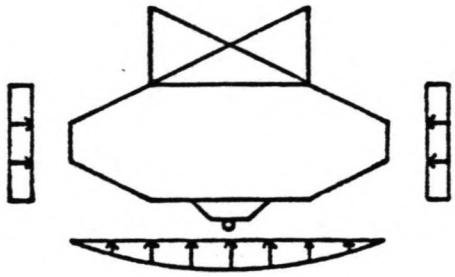

Figure 2.5: Rotation axis of the spud can

to deck motions increases, going from the tip of the spud can to the edge. This is shown in figure 2.6. As a result of this, the effect of soil weakening, which is caused by dynamic loading, will have its maximum near the edge and the soil stresses will concentrate at the tip of the spud can, thus allowing rotation about the spud can tip.

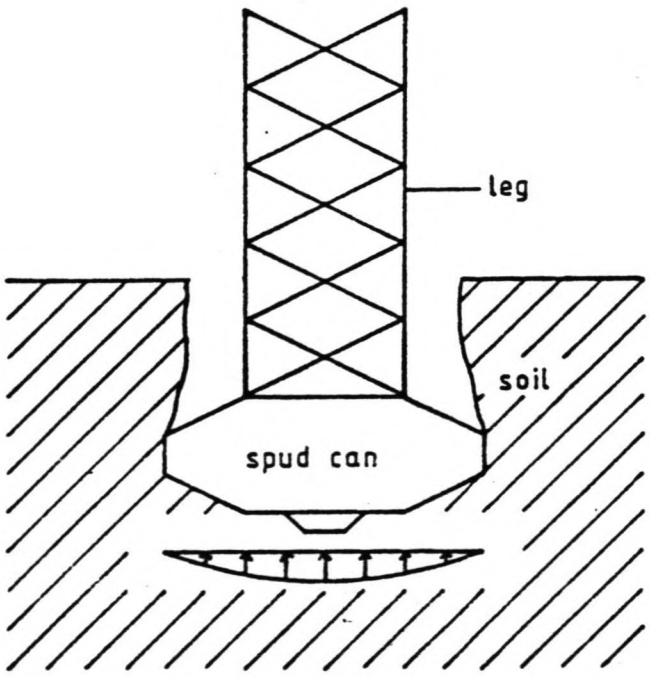

Figure 2.6: Penetration of the spud can

ad d. This reflects the assumption that all soil resistance is generated in the contact area of the spud can bottom and the soil and that there is no contact of the soil with the top of the spud can or the penetrated part of the leg. This is due to the fact that the soil does not completely return to is original position after being pushed aside by the penetrating spud can (see figure 2.6). However, there is no certainty wether this assumption is valid for all soils.

The assumptions stated above reduce the leg-soil connection to a hinged support with a certain amount of rotational restraint and, of particular importance for the dynamic response analysis, an amount of rotational damping (see figure 2.7).

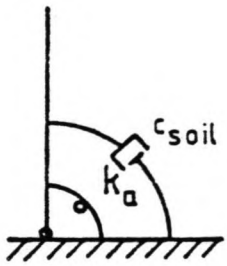

Figure 2.7: Model of leg-soil interaction

In an attempt to predict the order of magnitude of soil stiffness, the following D.N.V formula is used:

$$k_A = \frac{8GR^3}{3(1-\nu)} \qquad (2.01)$$

where:

k_A = rotational stiffness of leg-soil connection

G = shear modulus of soil

R = spud can radius

ν = Poisson's ratio

D.N.V. states the following limitations of expression (2.01):

a. It applies to static loading conditions.

b. It is valid only for soil stresses up to 40 % of the maximum bearing capacity.

c. Bottom slope is not accounted for.

The soil parameters needed for the computation of rotational restraint and damping are the shear modulus of soil and Poisson's ratio. As information about the soil conditions in the operational areas of the Russian platform is not available, the values that are given here apply to approximate conditions for some parts of the North Sea:

$$G = 15000 \text{ kN/m}^2$$

$$\nu = 0.4$$

Together with the value of equivalent spud can radius:

$$R = 7.57 \text{ m}$$

this yields the result for the rotational stiffness of the leg-soil connection:

$$k_A = 3*10^7 \text{ kNm/rad}$$

Although this result is well in line with values found by D.N.V.; it is again pointed out that this figure only indicates an order of magnitude and certain soil conditions could yield much less rotational restraint. Such an underestimation could cause a significant underprediction of jack-up motions.

The estimation of soil damping values is troubled by the same uncertainties. For this reason, platform motions will be computed for a number of leg-soil stiffness and soil damping values. The following range of rotational stiffness values will be used:

$$k_A = 0 \text{ kNm/rad} \quad \text{to} \quad 4*10^7 \text{ kNm/rad}$$

As mentioned in paragraph 2.6, D.N.V. states the following range of soil damping values for a jack-up, similar to the one studied here:

$$c_{SOIL} = 0 \% \quad \text{to} \quad 2 \%$$

2.4 MASS DISTRIBUTION

2.4.1 Legs

Going upwards from the spud can, the leg mass per unit length is slightly increasing, due to an increasing cross-sectional area of the chords (see table 1.1 of the appendix). In further computations this effect is neglected, causing a maximum error in the order of 10 %. Due to deck motions the legs will rotate about an horizontal axis through the tip of the spud can (see figure 2.7), and therefore the mass of the spud can will not influence the dynamic behaviour of the jack-up platform significantly. It is neglected for the computation of the leg mass per unit length, which then becomes (see appendix 2.1):

$$m_l = 8 \text{ tons/m}$$

2.4.2 Deck

For the dynamic response analysis of a jack-up platform, the following mass parameters are of importance:

a. The mass causing second order bending of the legs, called total deck mass, M_D. It is consisting of the pontoon mass, the maximum payload and mass of the leg parts above lower guide level (see figure 2.8).

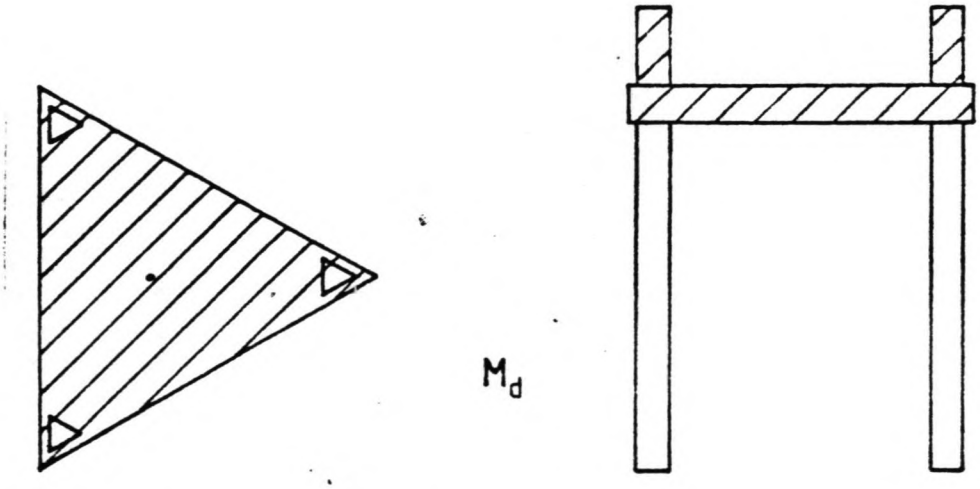

Figure 2.8: Total deck mass

b. The so-called dynamic deck mass, M_{DYN}, which is used for translational modes of the platform. It in-

corporates the total deck mass, M_D, and a mass contribution from the free leg length, M_L, as shown in figure 2.9.

c. The mass moment inertia of the deck about the vertical axis through the centre of gravity, J. Again, contrbutions from the legs are included. It is derived from D.N.V. computations for a similar jack-up platform (see figure 2.9).

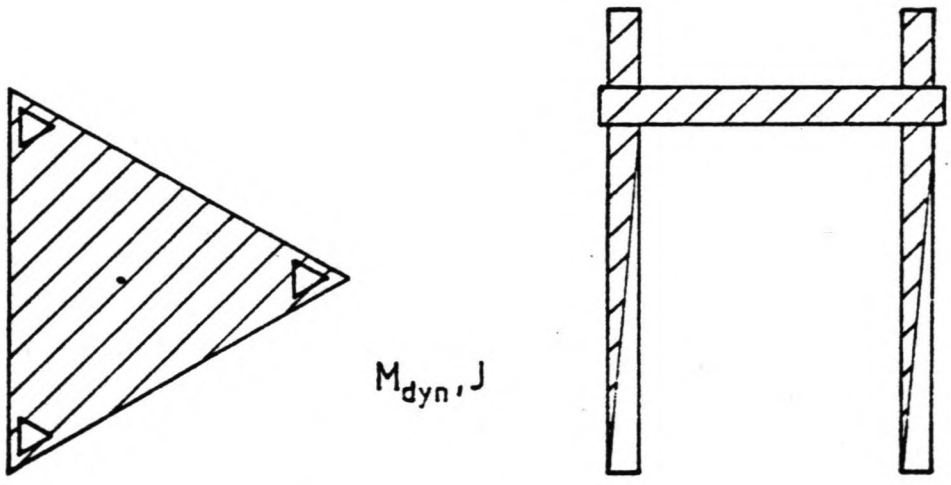

Figure 2.9: Dynamic deck mass and mass moment of inertia

The mass contribution from the free leg length is computed in appendix 2.1 by assuming that the leg motions are quasi-static in the frequency range relevant for the dynamic behaviour of the platform. This assumption can be checked by comparing the natural period of the complete platform to the natural period of the legs.

The natural period of a leg can be calculated by considering the motions of one leg, while the pontoon is assumed to be fixed. It depends on the stiffness of the leg-hull connection and the leg-soil connection. The two extreme cases are shown in figure 2.10.

Case A, in which both ends of the leg are fixed, will yield the lowest possible value of the natural period, while case B, with two hinges, yields an upper boundary. The following expression for the natural period of one leg is derived from structural mechanics:

$$T_\ell = \frac{2n}{C}\sqrt{\frac{m_\ell l^4}{EI'}} \qquad (2.02)$$

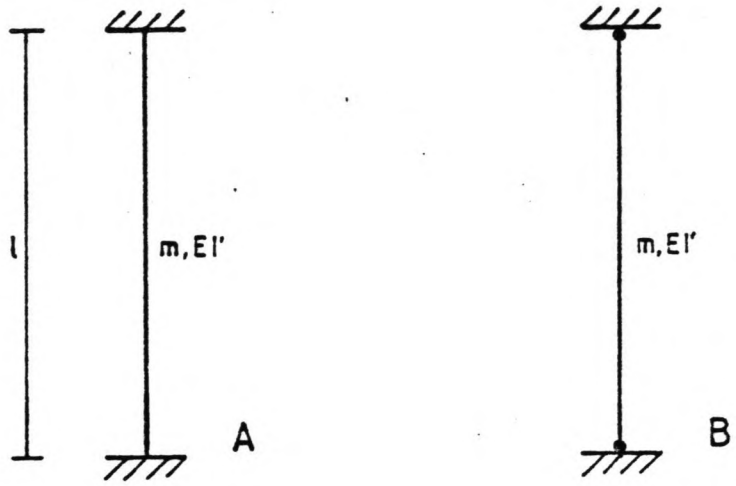

Figure 2.10: Two extreme cases of leg support

where:

T_ℓ = natural period of one leg

m_ℓ = leg mass per unit length

l = free leg length

C = coefficient, depending on the degree of rotational restraint at both ends of the free leg length

EI' = reduced leg stiffness (see paragraph 2.5)

For cases A and B shown in figure 2.10, the values of coefficient C are respectively 22.4 and 9.87. Substitution of these values together with the data from the Kolskaya into expression (2.02) yields the following range of natural periods for one leg:

T_ℓ = 0.26 s to 0.59 s

For the computation of the natural periods of the complete platform the mass contributions from the free leg length are neglected. This is sufficiently accurate for the purpose of

comparing both natural periods. The natural periods for the two relevant types of platform motion , horizontal translation of the deck and rotation about the vertical axis through the gravity centre, can be computed by considering the two mechanisms as separate single-degree-of-freedom systems (see figure 2.11).

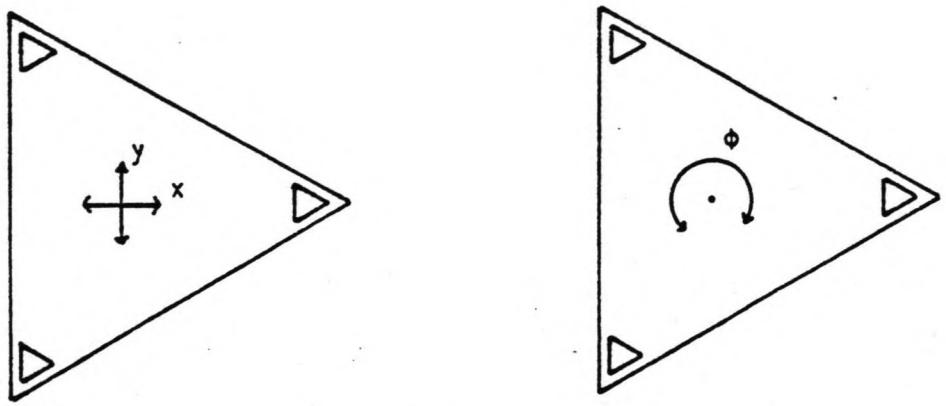

Figure 2.11: Degrees of freedom of the jack-up platform

This yields the following approximation of the natural periods of the complete platform, for translation:

$$T_{TR} = 5.9 \text{ s to } 11.8 \text{ s}$$

and for rotation:

$$T_{ROT} = 4.2 \text{ s to } 8.5 \text{ s}$$

From comparision of the various natural periods listed above the following conclusions can be drawn:

a. The natural period of one leg and the natural periods of the complete platform differ one order of magnitude.

b. The natural period of the legs is well outside the range of relevant wave periods at sea, approximatly 4 s to 18 s.

This means that the motions of the legs can be regarded as quasi-static, which is an important conclusion for the analysis of jack-up dynamics.

With this conclusion, the static leg deflection, x(z), can be written as a dimensionless deflection parameter, h(z), defined as:

$$h(z) = \frac{x(z)}{x(l)} \qquad (2.03)$$

where:

h(z) = dimensionless static deflection

x(z) = static deflection of the leg

x(l) = static deflection at lower guide level

This is shown in figure 2.12.

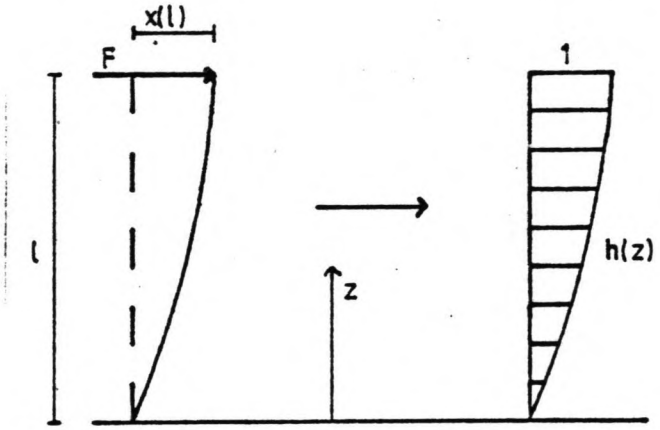

Figure 2.12: Dimensionless leg deflection

Using this dimensionless leg deflection, the expression for the mass contribution from the free leg length, M_2, is given by (see appendix 2.1):

$$M_2 = m_l \int_0^l h(z)dz \qquad (2.04)$$

Substitution of (2.03) into (2.04) and using the expression for x(z) found in the next paragraph yields the following contributing leg mass:

M_2 = 479 tons to 561 tons

It is stressed that this is the mass contribution from the leg part below lower guide level only and that the mass of the upper leg part is already included in the total deck mass, M_D.

Further computations yield (see appendix 2.2):

M_D = 11090 tons

M_{DYN} = 12527 tons to 12773 tons

J = $6.1*10^6$ tonm^2 to $6.4*10^6$ tonm^2

The following should be noted:

a. The above mass parameters are defined for the dry condition, which means that no added water mass is included. This is done at the computation of the water loads.

b. Fluid motions of the liquid payload could have a significant effect on the dynamic behaviour of the platform, but this will not be the case here. The preloading tanks are the only tanks aboard with a significant size, but they are empty during severe weather conditions, which are dominant for the dynamic response of the platform. The mass of the remaining liquid payload during survival conditions is less than 2 % of the total deck mass, M_p. Therefore the liquid payload is included in M_D.

c. For the computations described above it is assumed that the centre of gravity of the platform coincides with the geometrical centre of the deck. The computer program, that has already been mentioned, allows the definition of any other realistic gravity centre.

2.5 STIFFNESS

2.5.1 Combined leg stiffness

For the dynamic response analysis, the jack-up platform is modelled as a system of masses, springs and dashpots. As the mass is concentrated at the deck and the legs act as springs in this system, it is convenient to replace the legs by horizontal springs at lower guide level, where the fixation point of the legs is assumed to be (see figure 2.13). For this purpose, all relevant stiffness parameters of the leg are replaced by the so-called combined leg stiffness, denoted as k_c.

The combined leg stiffness is defined as the spring constant

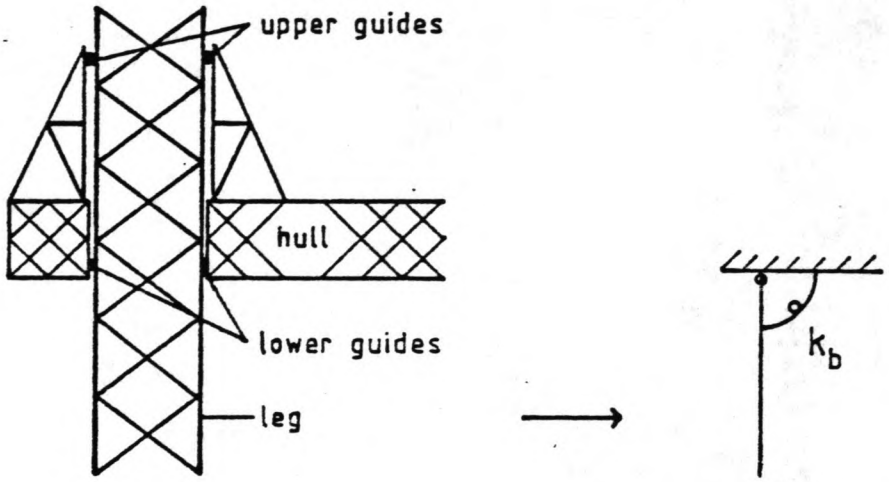

Figure 2.13: Model of the leg-hull connection

of a translational spring replacing the lateral stiffness of the leg at lower guide level. Actually, it is not a stiffness parameter of the leg, but a combination of various parameters governing the behaviour of the leg in dynamic model of the platform, so the name 'stiffness' is not correct. However, it will be used in this report for convenience.

2.5.2 Assumptions

The computation of the combined leg stiffness, as presented in appendix 1, is based on the following assumptions:

a. The deck is rigid compared to the legs.

b. Axial deformation of the legs is neglected.

c. The bending forces of the leg are carried by the chords. Steiner's rule is used for the computation of EI.

d. The shear forces of the leg are carried by the braces.

e. The displacements of the lower guides are negligible.

f. The springs at the leg-hull connection and the leg-soil connection are linear.

g. The axial force in the leg is independent of the vertical coordinate and equal to the axial leg load at lower guide level.

ad f. This assumption is not correct for all types of jack-ups. For example, slack in the guiding system will allow a certain amount of free rotation, before rotational stiffness builds up (see figure 2.14). Slack in the leg-hull connection can only be avoided by the use of wedges, otherwise the relationship between moment and rotation will be non-linear. At the Russian platform, no wedges are used for fixation of the leg-hull connection.

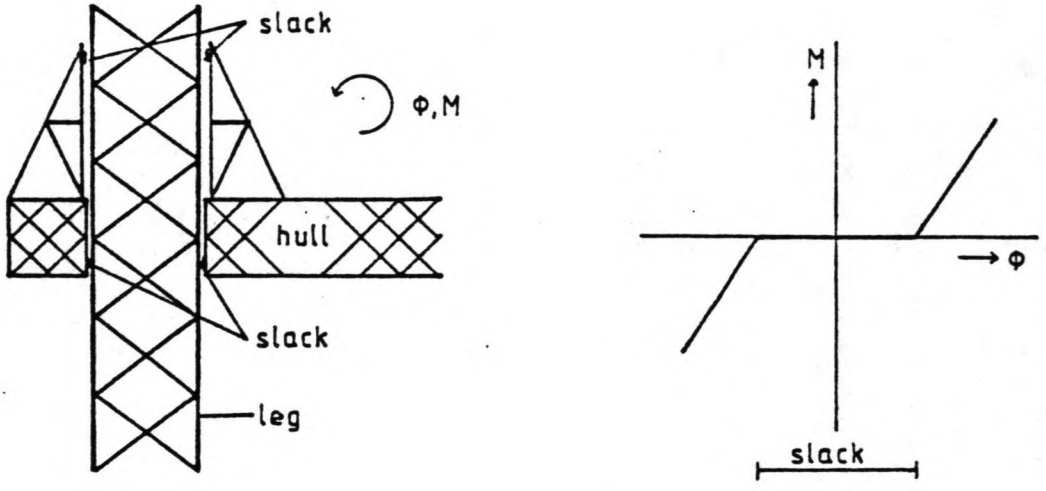

Figure 2.14: Slack in the guiding system

ad g. Due to the mass of the leg the axial force in the leg will increase going downward from the lower guides. For a three-legged platform the axial leg load at lower guide level is proportional to one third of the total deck mass, so in this case about 3680 tons. The mass of the free leg length is about 960 tons and thus the maximum increase of the axial leg load is 26 %. This seems quite significant, but for the upper part of the free leg length, which governs second order bending, the increase of the axial leg load will be in the order of 10 %. This can be neglected for the computation of the combined leg stiffness.

2.5.3 Computation procedure

The combined leg stiffness includes the following parameters and influences (see figure 2.15):

a. EI = bending stiffness of the leg

b. k_{sb} = shear stiffness of one bay of the leg

c. k_B = rotational stiffness of the leg-hull connection

d. k_A = rotational stiffness of the leg-soil connection

e. F_z = axial leg load, causing second order bending of the leg. This axial leg load is excerted by the total deck mass, M_D.

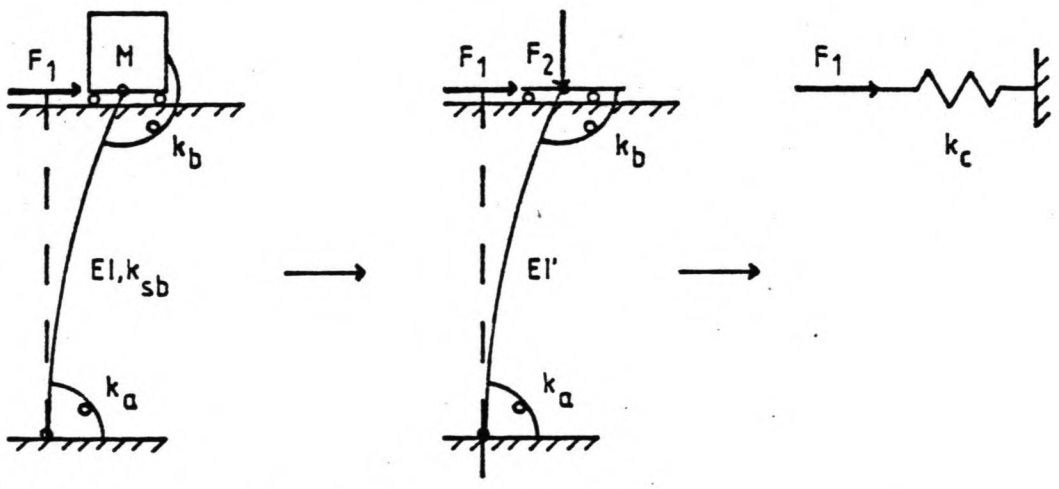

Figure 2.15: Modelling of the combined leg stiffness

In chapter 1.1 of the appendix it is shown that all of the above parameters are independent of the loading direction, except for the shear stiffness. This means that the combined leg stiffness is independent of the loading direction as well, if the shear stiffness has only little influence on the combined leg stiffness. This assumption is verified in section 2.4.3.

The exact procedure for computing and combining parameters listed above is given in appendix 1 and will not be reproduced here, only a general description. First the bending stiffness

of the leg, EI, and the shear stiffness of one bay, k_{sb}, are combined to one parameter, called the reduced bending stiffness, EI', (see appendix 1.4). This is done by regarding the leg as a cantilever with bending and shear stiffness and replacing it by a cantilever with 'reduced' bending stiffness and the same ratio of load and displacement at lower guide level (see figure 2.16).

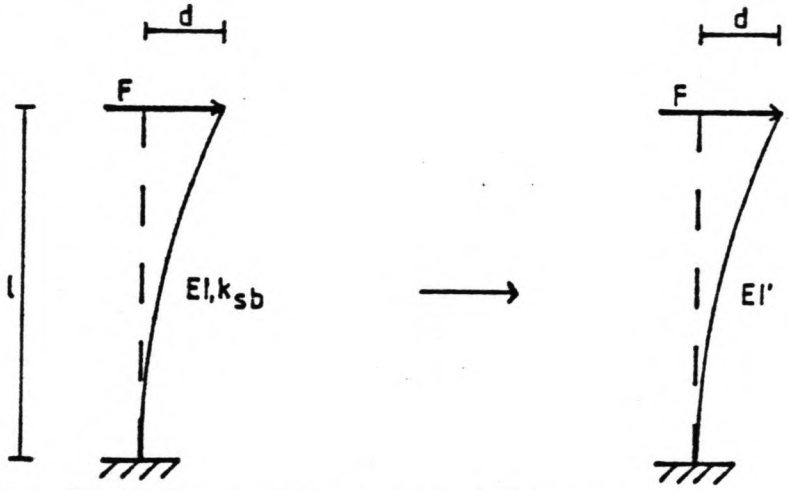

Figure 2.16: Definition of the reduced leg bending stiffness

After this, the differential equation for the leg bending moments is solved. This equation includes the influence of the reduced bending stiffness of the leg, EI', the rotational stiffness of the leg-soil connection, k_A, and the rotational stiffness of the leg-hull connection, k_B. The resulting expression is given by equations (2.05) to (2.08):

$$x(z) = c_2 F_1 \sin(\alpha z) + c_3 F_1 (\cos(\alpha z)-1) - \frac{F_1 z}{EI'} \qquad (2.05)$$

where:

$$c_2 = \frac{-k_B}{\alpha^2 EI'} c \qquad (2.06)$$

$$c_3 = \frac{k_A k_B}{\alpha^3 EI'^2} c + \frac{k_A}{\alpha^4 EI'^2} \qquad (2.07)$$

$$c = \frac{1+k_A\cos(\alpha l)/k_\beta + k_A\sin(\alpha l)/\alpha EI'}{(EI'\alpha^2 - k_A k_\beta/EI')\sin(\alpha l) - (k_A+k_\beta)\alpha\cos(\alpha l)} \qquad (2.08)$$

$$\alpha = \sqrt{\frac{F_2}{EI'}}$$

$x(z)$ = leg displacement

F_2 = axial leg load

EI' = reduced leg bending stiffness

k_A = rotational stiffness of the leg-soil connection

k_β = rotational stiffness of the leg-hull connection

l = free leg length

F_1 = horizontal load at lower guide level

It should be noted that this solution is valid only for an axial leg load, F_2, less than the buckling load of the leg. If both sides of equation (2.05) are divided by the horizontal load at lower guide level, F_1, and the vertical coordinate of the lower guides is substituted:

$$z = l$$

then the reciproke of the combined leg stiffness, k, is found:

$$\frac{1}{k_c} = \frac{x(l)}{F_1}$$

$$\frac{1}{k_c} = c_2\sin(\alpha l) + c_3(\cos(\alpha l)-1) - \frac{1}{\alpha^2 EI'} \qquad (2.09)$$

The computation of the various stiffness parameters in appendix 1 yields:

$$EI = 2.03*10^9 \text{ kNm}^2$$

$$k_{sb} = 8.26*10^6 \text{ kNm/rad}$$

$$EI' = 1.93*10^9 \text{ kNm}^2$$

$$k_\beta = 3.9*10^7 \text{ kNm/rad} \quad \text{to} \quad 9.6*10^7 \text{ kNm/rad}$$

The computation of the rotational stiffness of the leg-hull connection, k_β, includes the following effects:

a. Horizontal displacement of the upper guides.

b. Bending of the chords facing the guides.

Both effects are due to guide forces.

As can be seen, the reduction of the bending stiffness, EI, caused by the shear stiffness, $k_{s\beta}$, is only 5 %, so the shear deformation of the legs will only have a minor effect on the dynamic behaviour of the platform and the assumption, that the combined leg stiffness is independent of the loading direction, is correct.

2.5.4 Axial leg load

Due to deck motions, the distribution of the axial leg loads will change. In this section it is examined, wether this influences the dynamic behaviour of the platform.

From the equilibrium of forces and moments of a two-dimensional platform model, as shown in appendix 1.7.2, it can be seen that a displacement of the deck causes a change of the individual axial leg loads (see figure 2.17). As the total vertical load on the legs remains constant, the decrease of the axial force in one leg is canceled by the increase in the other leg.

In the appendix it is found that, for a maximum deck displacement of 2 m, the fluctuation of the axial leg load, F_z, is in the following range:

$$F_z = 3.36*10^4 \text{ kN} \quad \text{to} \quad 3.90*10^4 \text{ kN}$$

In this range, there is a linear relationship between the combined leg stiffness and the axial leg load, as is shown in figure 2.18.

It can be concluded that the fluctuations of the combined leg stiffness of the individual legs cancel each other and thus will have no effect on the dynamic behaviour of the platform. This means that these fluctuations can be neglected and that the axial load on each leg can be taken as a constant value:

$$F_z = 3.63*10^4 \text{ kN}$$

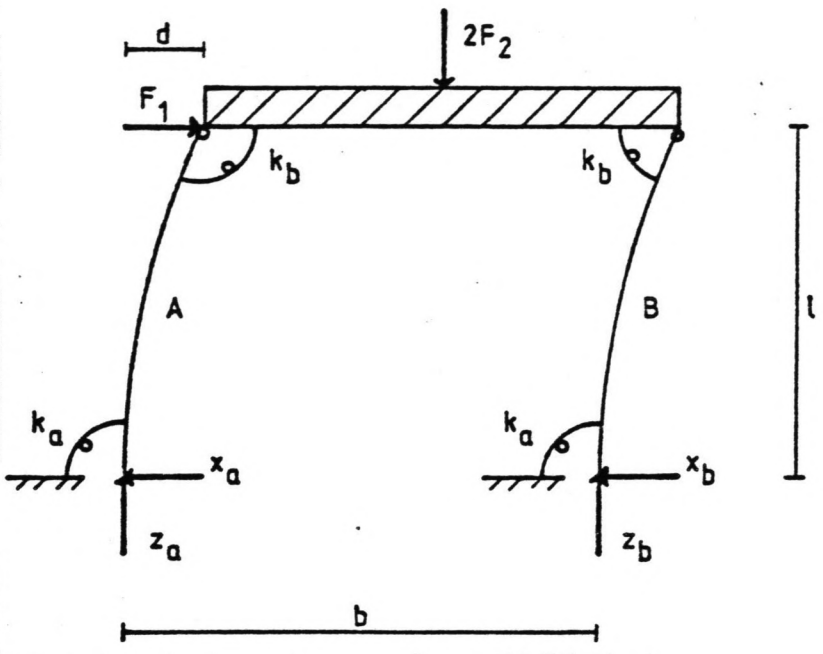

Figure 2.17: Variation of the axial leg loads due to deck displacement

FIG. 2.18: COMBINED LEG STIFFNESS VERSUS AXIAL LEG LOAD

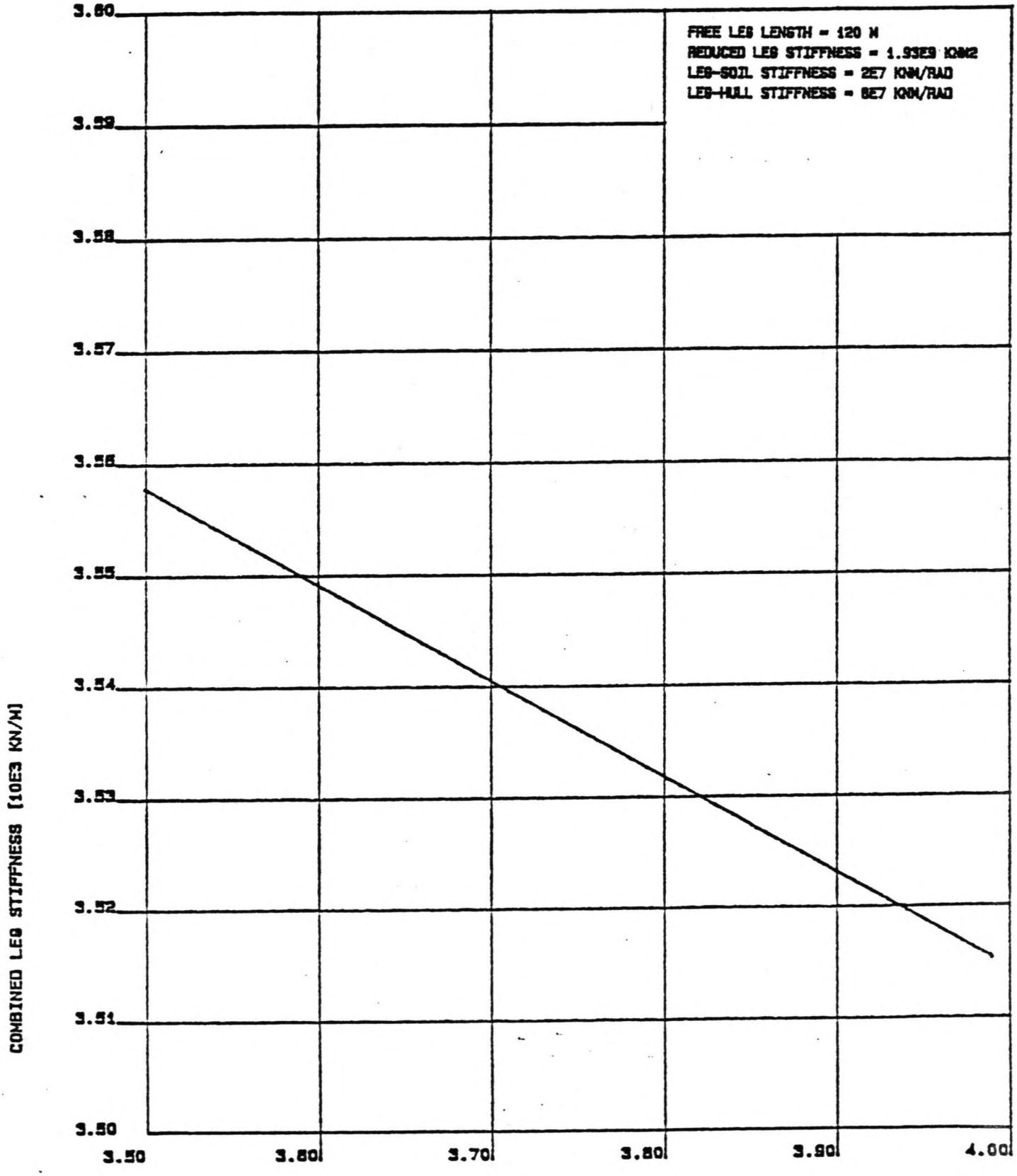

2.5.5 Results

Substitution of the previous results for F_2, k_β and EI', together with the following range of soil stiffness values:

$$k_A = 0 \text{ kNm/rad} \quad \text{to} \quad 4*10^7 \text{ kNm/rad}$$

into equation (2.09) yields the combined leg stiffness, k_C:

$$k_C = 1.2*10^3 \text{ kN/m} \quad \text{to} \quad 4.8*10^3 \text{ kN/m}$$

In order to get a verification of the leg stiffness computations, this result is compared to the stiffness of a cantilever of the same length and reduced bending stiffness, EI' (see figure 2.19).

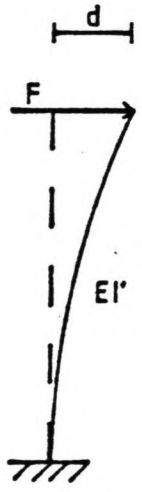

Figure 2.19: Cantilever with bending stiffness equal to the reduced leg bending stiffness

According to its definition, the combined leg stiffness of a cantilever with the same reduced bending stiffness EI' is found to be:

$$k_{C,CANT} = 3.4*10^3 \text{ kN/m} \qquad (2.10)$$

As to be expected, the order of magnitude of both results agrees quite well. This indicates that the expression found for the leg deflection is correct.

In figure 2.20 the deflection of one leg due to a horizontal

load of 1000 kN has been plotted for several values of the rotational leg-soil stiffness, k . In figure 2.21 the same has been done for a number of values of the rotational leg-hull stiffness. The main conclusions that can drawn from these figures are:

a. In the range of realistic values of the leg-hull stiffness, $3.9*10^7$ kNm/rad to $9.6*10^7$ kNm/rad, the change of the deck displacement is relatively small.

b. The presence of any rotational restraint at the spud can reduces the deck displacements considerably. The assumption of no restraint at all causes a significant increase of the deck displacement.

In figure 2.22 the deck displacement has been plotted as a function of the axial leg load, F_z, for several values of the rotational leg-soil stiffness, k_A. The horizontal load at lower guide level is 1000 kN. In figure 2.23 the same has been done for a number of values of the rotational leg-hull stiffness. The axial load at the vertical branches of the figures represents the buckling load of the leg. The conclusions are identical to those stated above.

The translational and rotational stiffness of the complete platform with n_l legs are now given by (see figure 2.24):

$$k_{TR} = \sum_{i_l=1}^{n_l} k_{c,i_l} \qquad (2.11)$$

$$k_{ROT} = \sum_{i_l=1}^{n_l} r_{i_l} k_{c,i_l} \qquad (2.12)$$

where:

k_{TR} = translational stiffness of the platform

k_{ROT} = rotational stiffness of the platform

k_{c,i_l} = combined leg stiffness of leg i_l

r_{i_l} = distance between leg i_l and the gravity centre of the platform

For the Russian platform with three equal legs at an equal distance, r, to the centre of gravity this reduces to:

$$k_{TR} = 3k_c \qquad (2.13)$$

$$k_{ROT} = 3rk_c \qquad (2.14)$$

FIG. 2.20: LEG DEFLECTION FOR SEVERAL VALUES OF THE LEG-SOIL STIFFNESS, KA

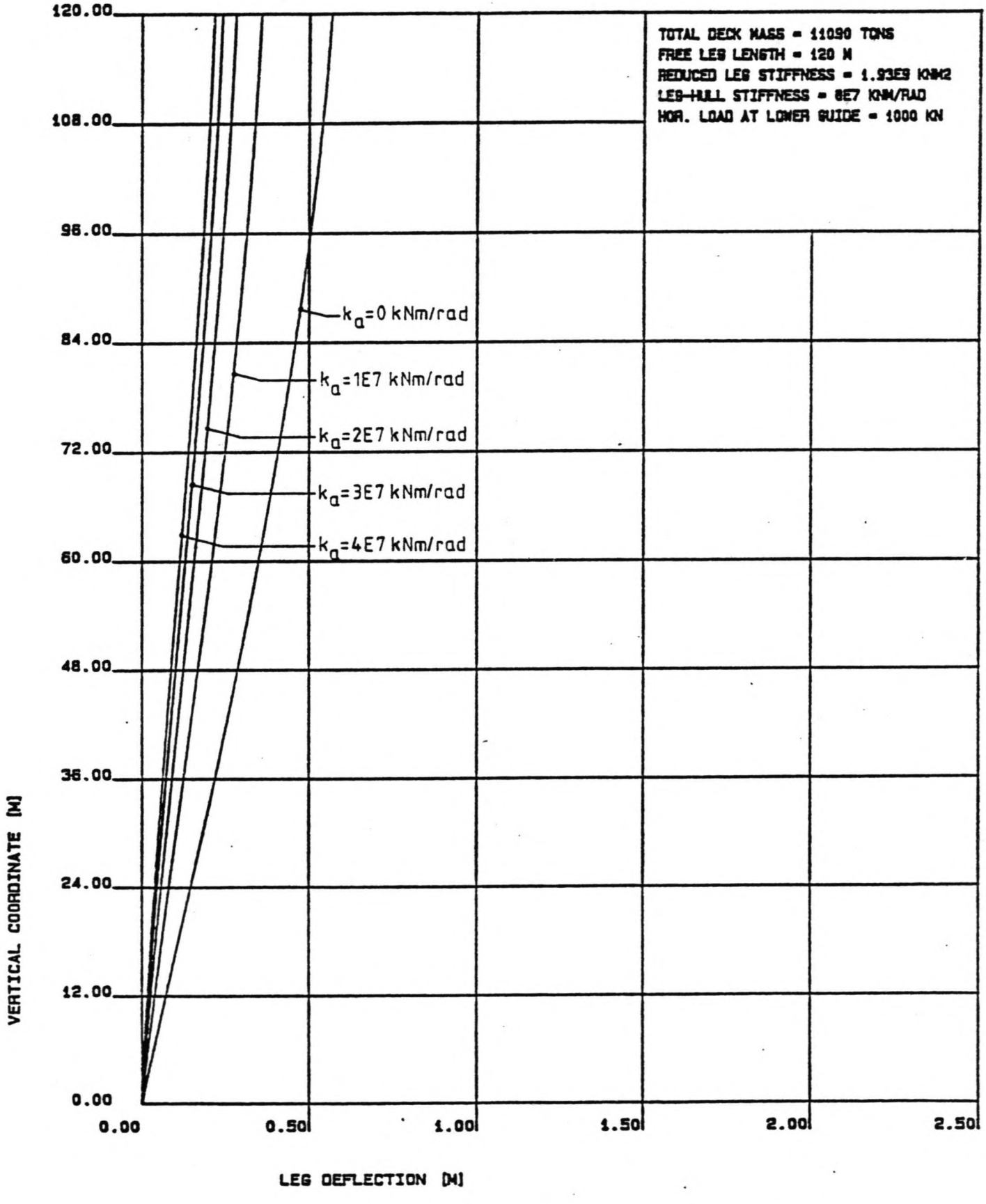

FIG. 2.21: LEG DEFLECTION FOR SEVERAL VALUES OF THE LEG-HULL STIFFNESS, KB

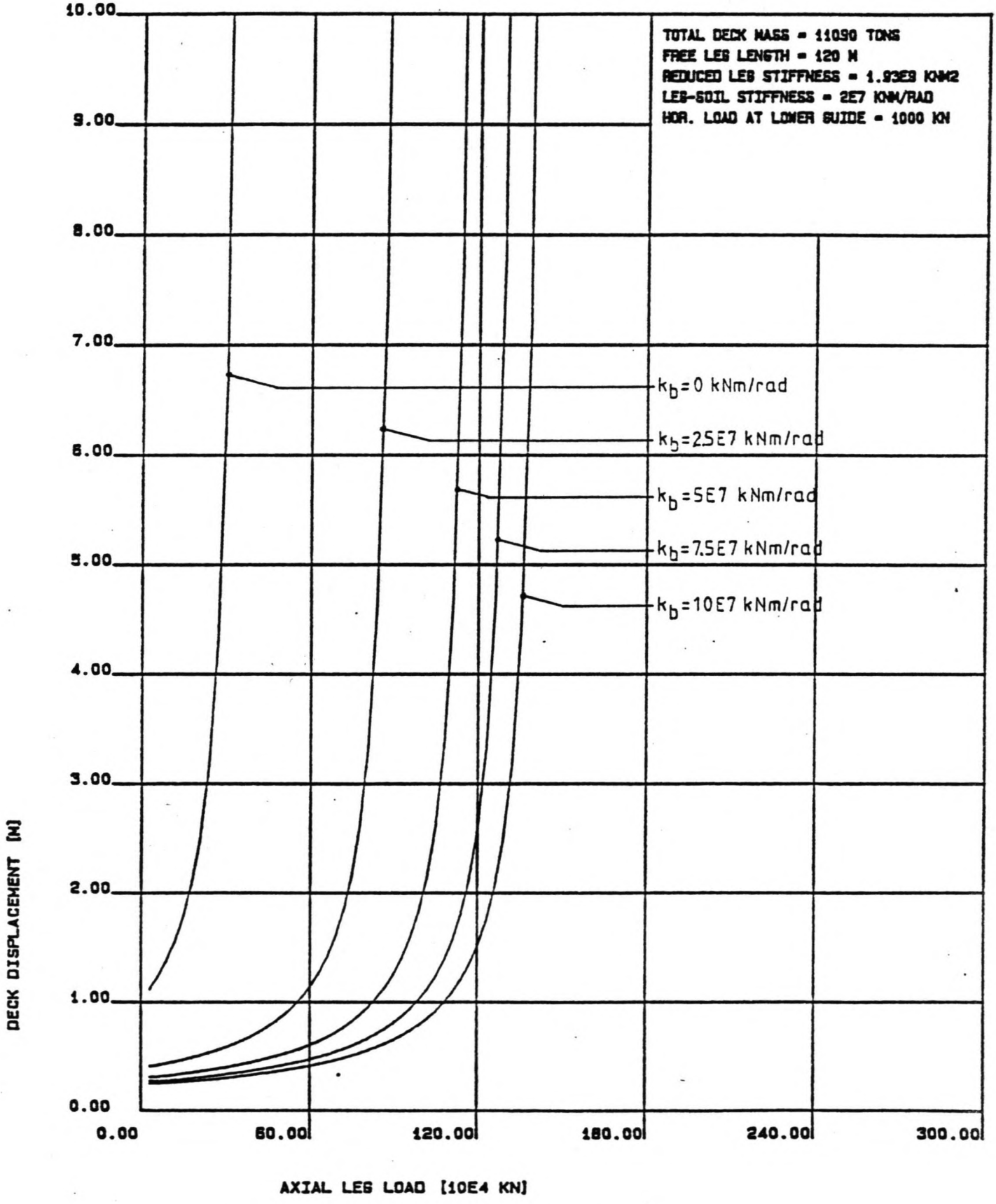

FIG. 2.22: DECK DISPLACEMENT VERSUS AXIAL LEG LOAD FOR SEVERAL VALUES OF THE LEG-SOIL STIFFNESS, KA

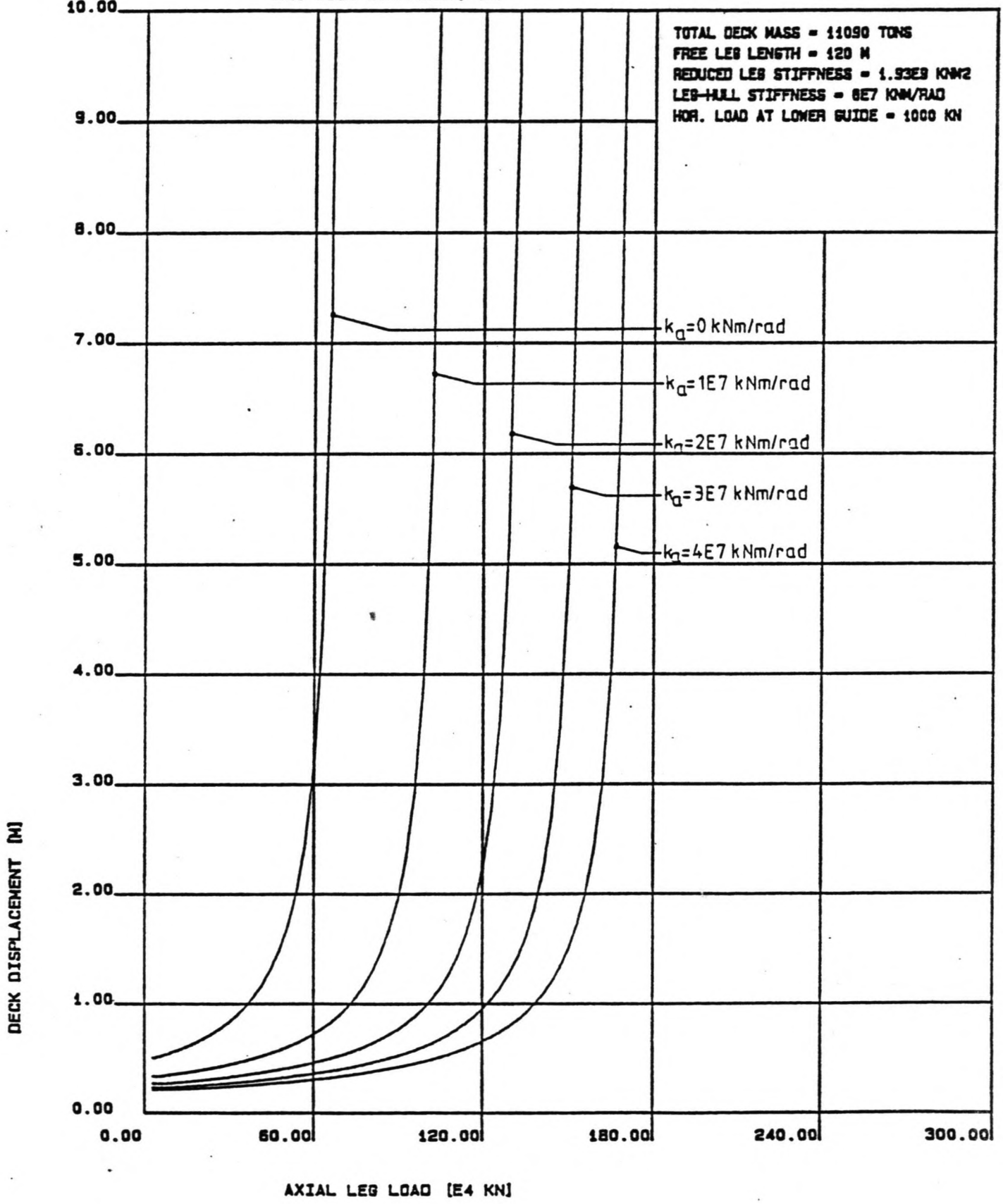

FIG. 2.23: DECK DISPLACEMENT VERSUS AXIAL LEG LOAD FOR SEVERAL VALUES OF THE LEG-HULL STIFFNESS, KB

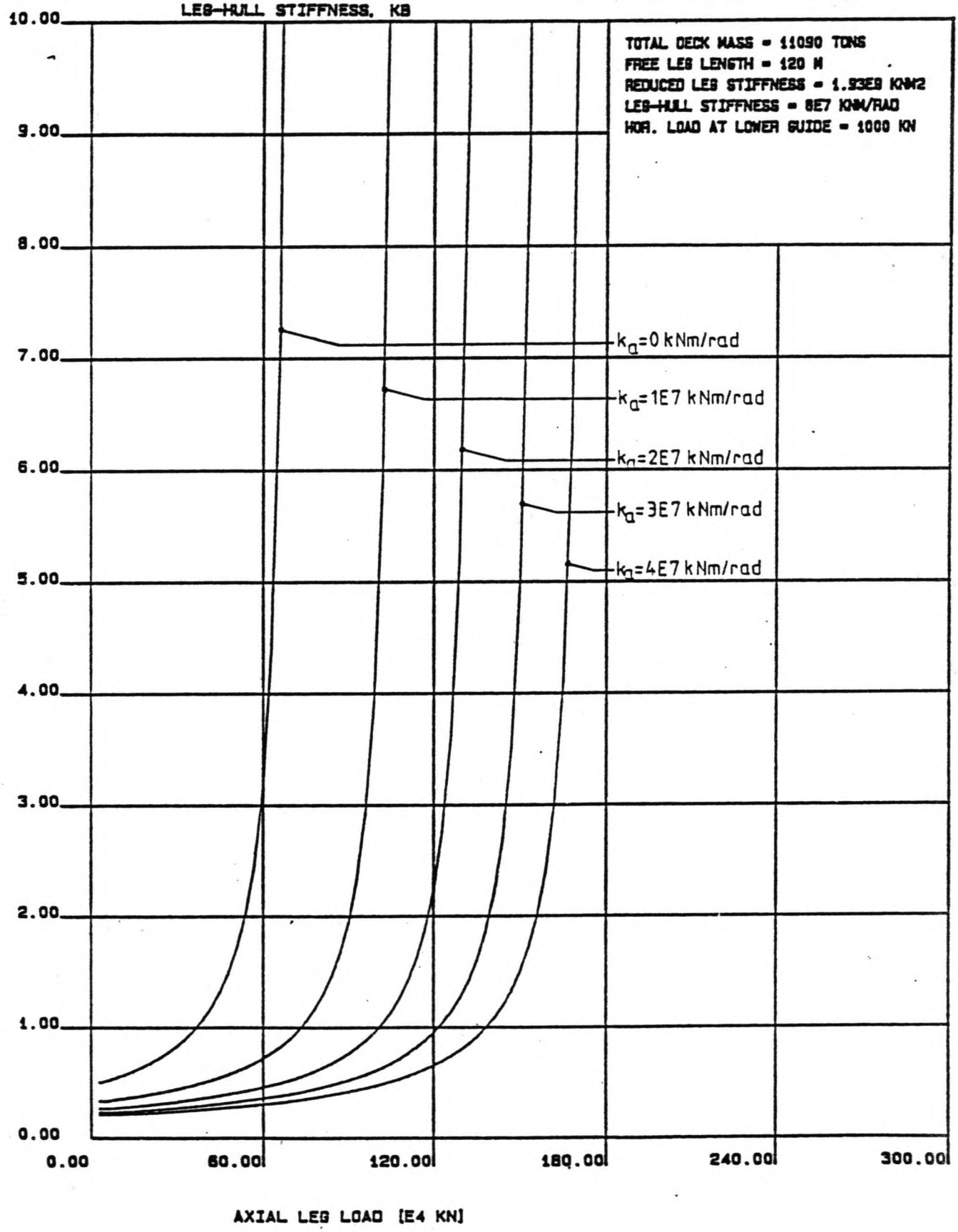

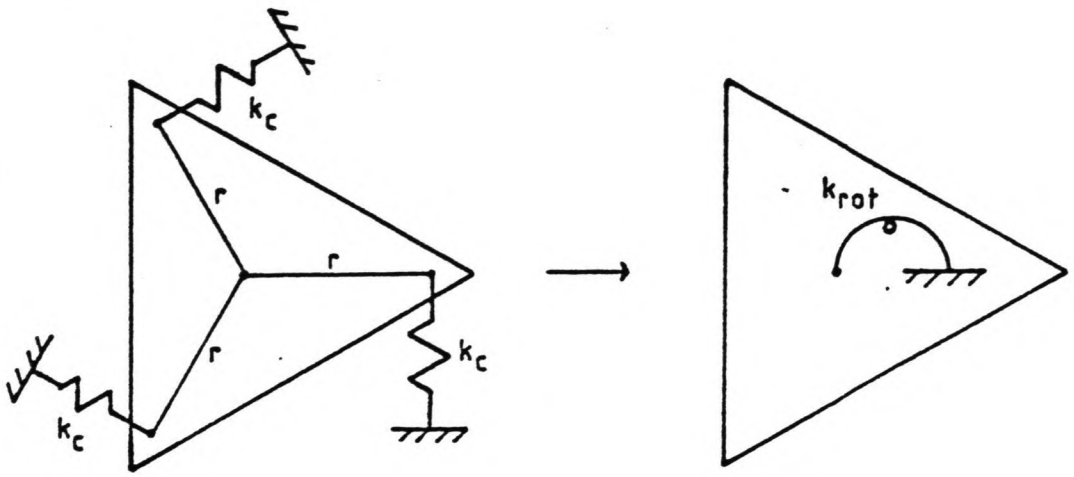

Figure 2.24: Rotational stiffness of the platform

2.6 DAMPING

The parameter damping stands for the energy dissipation in a vibrating dynamic system. It is often described by the damping percentage, which is a percentage of the critical damping of a structure. For the translational motion modes of the jack-up platform the critical damping is defined as:

$$\zeta_{CRIT,TR} = 2\sqrt{k_{TR} M_{DYN}} \qquad (2.15)$$

where:

$\zeta_{CRIT,TR}$ = critical damping for the translational mode of the platform

k_{TR} = translational stiffness of the platform

M_{DYN} = dynamic deck mass

The critical damping for rotation is given by:

$$\zeta_{CRIT,ROT} = 2\sqrt{k_{ROT} J} \qquad (2.16)$$

where:

$\zeta_{CRIT,ROT}$ = critical damping for the rotational mode of the platform

k_{ROT} = rotational stiffness of the platform

J = mass moment of inertia of the platform

The total damping coefficient consists of three parts:

a. Soil damping

b. Structural damping

c. Hydrodynamic damping

ad a. Soil damping represents the energy dissipation in the soil, mainly due to local plastic deformations. It depends on soil conditions and spud can design and will be design- and site-dependent. According to D.N.V., soil damping ranges from 0 % to 2 %.

ad b. Structural damping consists of energy dissipation in the framework of the leg and dissipation in the leg-hull connection. The latter will be governed by the displacements of the upper guides and bending of the chords facing the guides. It is estimated by D.N.V. at 1 % to 3 %.

ad c. Hydrodynamic damping is caûsed by fluid-structure interaction and will consequently be dependent of the drag coefficients and sea state. It is determined during dynamic response analysis. D.N.V. states values for hydrodynamic damping in the order of 2 % to 4 %.

The damping values stated by D.N.V. apply to a jack-up similar to the Russian platform refered to in this report. It is felt that the D.N.V. figures concerning soil damping are on the high side. Most of the arguments for the neglection of soil restraint, as listed in paragraph 2.3 apply to soil damping as well. Generally speaking, it is very hard to obtain any reliability of soil damping figures proposed, and therefore in this report all soil damping is neglected for the computation of the maximum platform response:

c_{SOIL} = 0 %

As the damping properties used in a dynamic analysis of a jack-up are, to a large extant, governing the magnitude of the response, particular consideration should be given to evaluating their influence on the dynamic behaviour. This is done by performing the dynamic response analysis for several values of the structural and soil damping, together denoted as c_{SS} from now on, in the following range:

c_{ss} = 0 % to 4 %

The case of c_{ss} = 0 % is of special interest, as it allows comparison of several hydrodynamic conditions.

3 WAVE REPRESENTATION

3.1 INTRODUCTION

The motions of a jack-up platform at sea are mainly caused by waves and in order to allow the computation of these motions, a mathematical description of the waves is needed. In this chapter the waves are modelled in two ways.

In the first approach, the stochastic nature of the waves at sea is neglected and the waves are assumed to be sine-shaped, with a constant wave height and a constant period. This deterministic wave model is not very realistic, as it implies a regular sea surface. However, it allows a mathematical description of several wave-induced phenomena, like fluid velocities and accelerations, pressure gradients and transport of energy, by means of short wave theory.

In order to account for the irregularity of the sea surface, a stochastic wave model is introduced. In this model, the excursion of the sea surface is assumed to be a stochastic process in time, with a Gaussian distribution. The frequency-dependent variance of the excursion of the water surface is described by a wave spectrum. It is assumed that the sea state is stationary for a certain period of time and thus is represented by one wave spectrum. The stochastic wave model is described in paragraph 3.3.

At sea, all waves have a different direction of propagation. Compared to a one directional wave train, this effect will cause a reduction of the jack-up motions. In order to account for the directional spreading of the waves, a cosine-square distribution is introduced in paragraph 3.4.

3.2 DETERMINISTIC WAVE MODEL

In the deterministic wave model, the waves are assumed to be regular and their stochastic nature is neglected. Several deterministic wave models are known, for example:

a. Short wave theory

b. Cnoidal theory

c. Stokes theory

Since short wave theory is the least cumbersome, it will be used in this study. According to this theory, the waves are assumed to be sine-shaped. The expressions for the wave-induced fluid velocities and accelerations, pressure gradients and wave energy are relatively simple. Their derivation will not be

given here, only the expressions most often used in this report:

$$\zeta(t,x) = \frac{H}{2}\sin(\omega t - kx) \qquad (3.01)$$

$$\dot{u}(t,x,z) = \hat{u}(z)\sin(\omega t - kx) \qquad (3.02)$$

$$\ddot{u}(t,x,z) = \hat{u}(z)\omega\cos(\omega t - kx) \qquad (3.03)$$

$$u(z) = \frac{H\omega}{2}\frac{\cosh(kz)}{\sinh(kd)} \qquad (3.04)$$

where:

$\zeta(t,x)$ = excursion of the sea surface

t = time

x = horizontal coordinate

z = vertical coordinate

H = wave height

$\omega = \frac{2\pi}{T}$

T = wave period

$k = \frac{2\pi}{L}$

L = wave length

$\dot{u}(t,x,z)$ = fluid velocity

$\ddot{u}(t,x,z)$ = fluid acceleration

$\hat{u}(z)$ = amplitude of fluid velocity

d = water depth

For all of the above expressions, the orientation of the coordinate system is shown in figure 3.1.The term kx describes the phase difference between different locations of, for instance, the platform legs.It is left out if only one location is considered, as is the case for the one leg model.

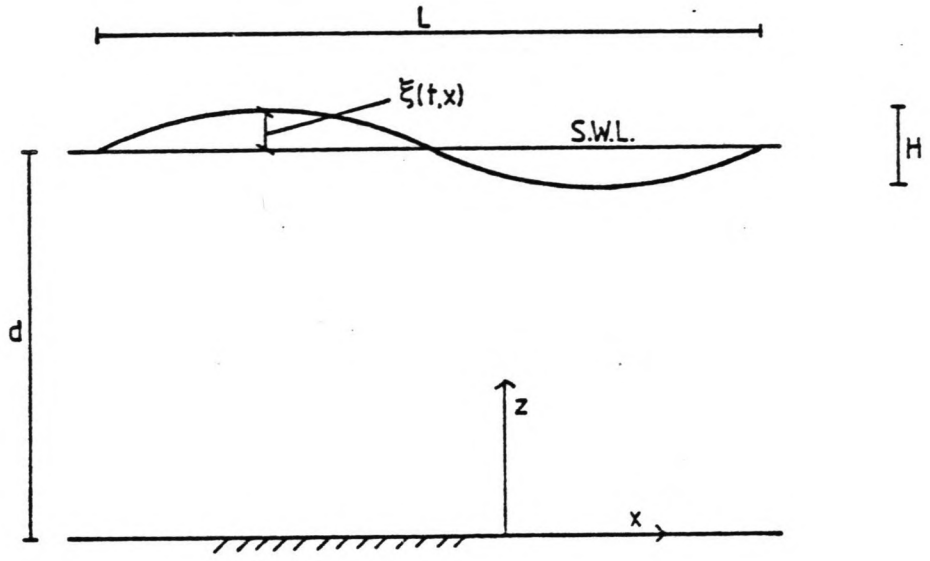

Figure 3.1: Sinusoidal wave

The general expression for the wave length, L, is:

$$L = L_0 \tanh(kd) \qquad (3.05)$$

$$L_0 = \frac{gT^2}{2\pi} \qquad (3.06)$$

where:

g = gravity acceleration

For deep water, tanh(kd) = 1 and expression (3.05) reduces to (3.06), which represents the deep water wave length. Deep water is assumed if the following condition is satisfied:

$$\frac{d}{L} > 0.5 \qquad (3.07)$$

Substitution of:

$$g = 9.81 \text{ m/s}^2$$

yields the following approximation of the deep water wave length, in SI-units:

$$L_0 = 1.56T^2 \qquad (3.08)$$

In the next chapters, the expressions listed above will be used without further derivation.

In this report some attention is given to the dynamic response of one leg due to a regular, sinusoidal wave. This method of dynamic analysis, called deterministic analysis from now on, does not incorporate a description of the irregularity of the sea surface, and therefore is rather unrealistic. Nevertheless, deterministic analysis is intoduced for the following reasons:

a. It can easily be expanded to dynamic analysis methods using wave spectra.

b. It provides a basis for the comparison of frequency domain and time domain analysis.

c. It is a link to the current design methods, which are used, for example, by D.N.V. These methods involve regular waves as well.

For the purpose of deterministic analysis, the wave height is related to the wave period by means of an average relationship, as stated by D.N.V., in SI-units:

$$H = \frac{(T-1)^2}{34} \qquad (3.09)$$

According to D.N.V., the wave height is limited by the 100 year wave height, H_{100} , which may be taken as:

$$H_{100} = 32 \text{ m}$$

The wave periods need not be examined above the following value:

$$T = 18 \text{ s}$$

For the analysis of survival conditions, steep waves are of particular interest, since they will cause severe platform motions. Using the 100 year wave steepness, as defined by D.N.V., the wave height is related to the wave period as follows:

$$H = \frac{gS_{100}\, T^2}{2n} \qquad (3.10)$$

$$S_{100} = \begin{cases} \frac{1}{7} & , T \leq 6 \text{ s} \\ \frac{1}{7+0.93(T^2-36)/H_{100}} & , T > 6 \text{ s} \end{cases} \qquad (3.11)$$

where:

S = 100 year wave steepness

These relationships are shown in figure 3.2.

The range of wave periods and wave heights for the purpose of deterministic analysis has been derived from the 100 year wave steepness criterion, since they will cause severe motions. This range is shown in table 3.1.

Wave period [s]	Wave height [m]
8.00	12.79
9.00	15.22
10.00	17.62
11.00	19.95
12.00	22.18
13.00	24.28
14.00	26.27
15.00	28.12
16.00	29.84
17.00	31.44
18.00	32.00

Table 3.1: Range of regular waves

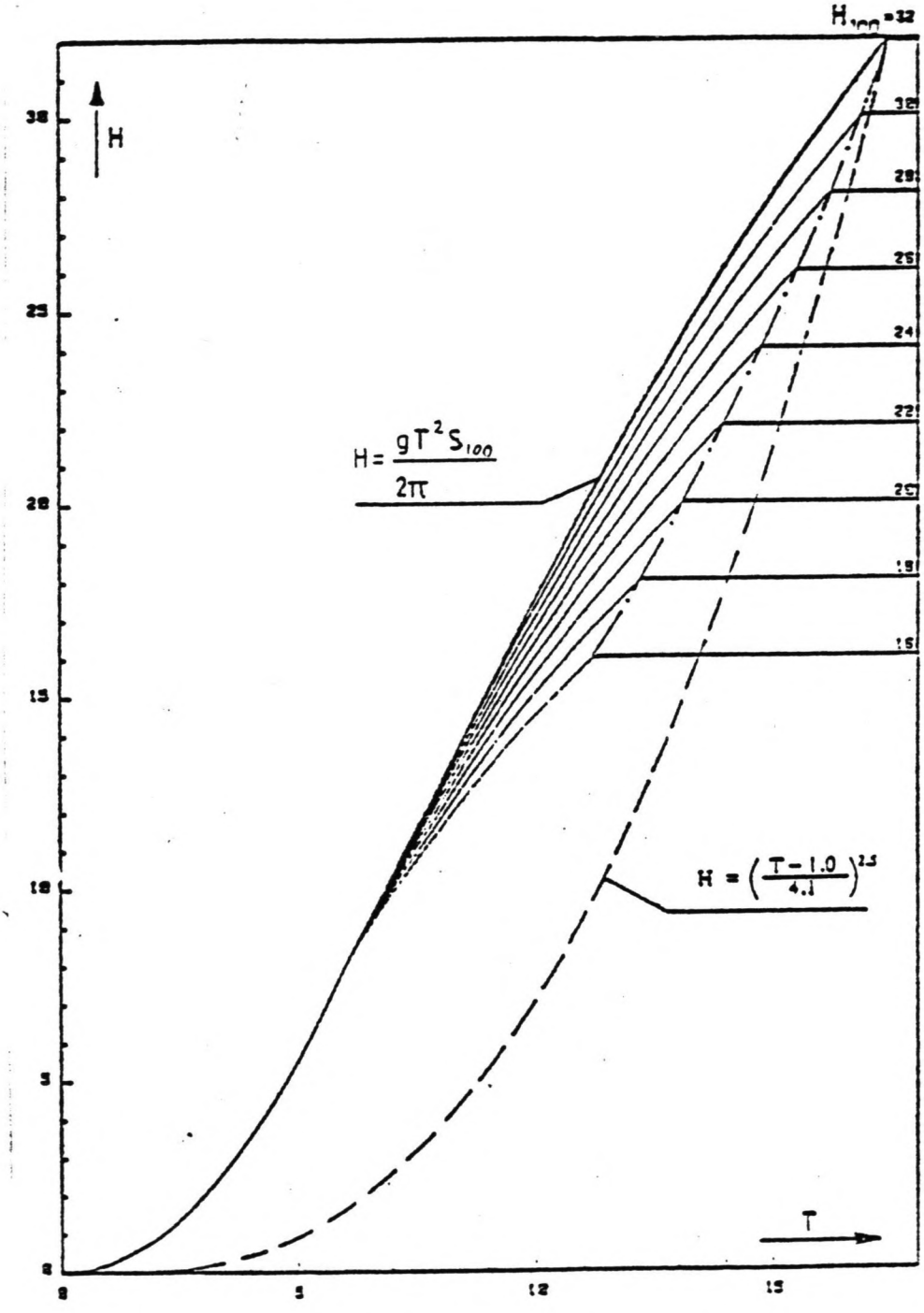

Figure 3.2: Relationships between wave period and wave height

3.3 STOCHASTIC WAVE MODEL

3.3.1 General

For the stochastic wave model, the excursion of the sea surface is assumed to be a Gaussian process in time. For a Gaussian variable, x, the probability of occurence of a certain value X, denoted as p(x=X) or p(X), is given by:

$$p(X) = \frac{1}{\sigma_x \sqrt{2\pi}} \exp\left\{\frac{-(X-\mu_x)^2}{2\sigma_x^2}\right\} \qquad (3.12)$$

where:

p(X) = probability of occurence of value X

σ_x = standard deviation

μ_x = mean value

Expression (3.12) is known as the distribution function of variable x. The Gaussian distribution is shown in figure 3.3, with the horizontal axis scaled by means of the standard deviation. This scaling will be used for all statistical plots in this report.

The probability of exceedance of value X, denoted as p(x>X) or P(X), is given by the following integral:

$$P(X) = \int_X^\infty p(x)dx \qquad (3.13)$$

This probability of exceedance is represented by the shaded part of figure 3.3.

Due to the stochastic nature of the wave model, it is not possible to define a maximum wave height. Instead of this, each wave height, and thus each design value of water loads and platform motions has a certain probability of exceedance.

FIG. 3.3: GAUSSIAN DISTRIBUTION

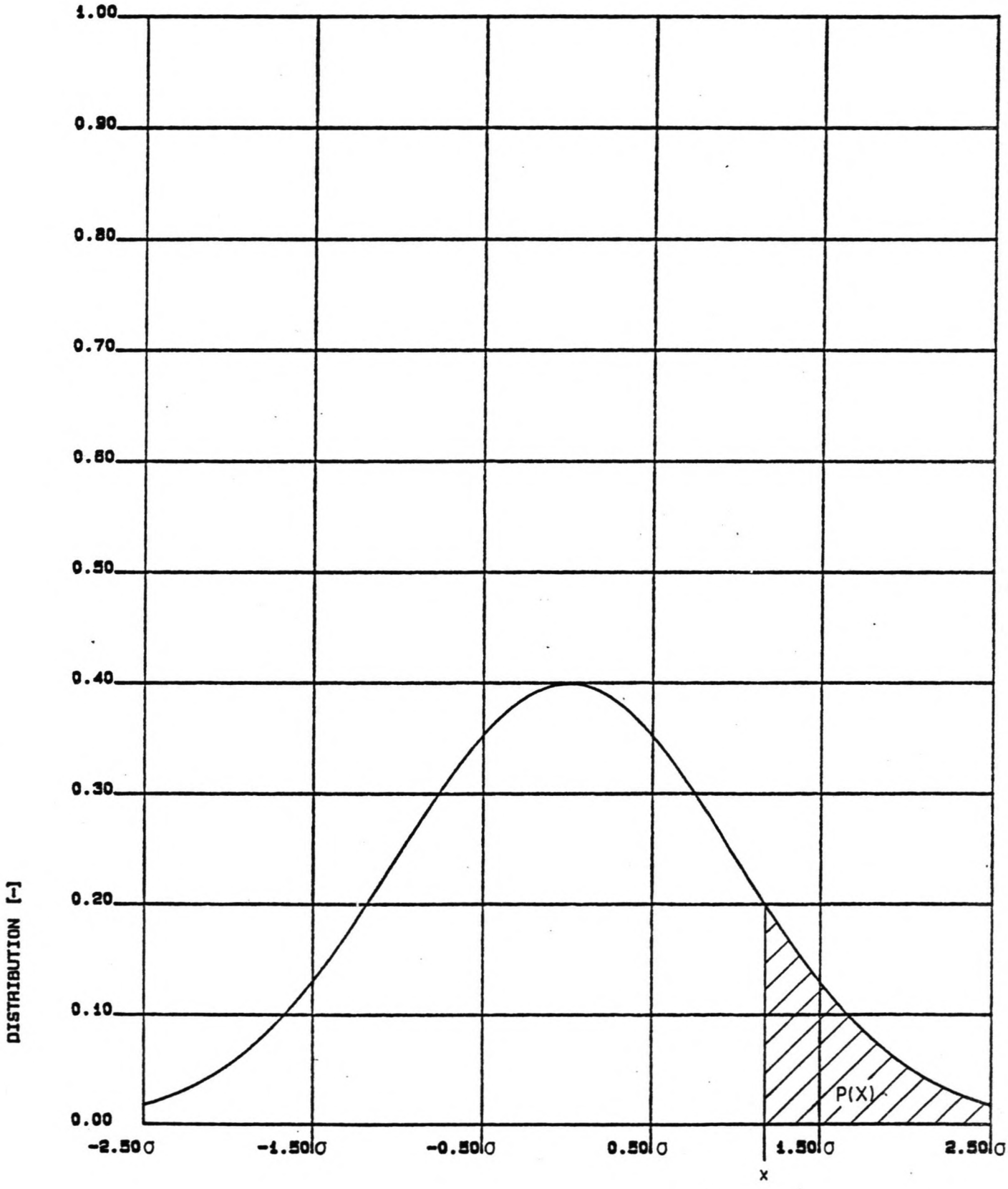

3.3.2 Wave spectrum

In the case of a stochastic wave model, the state of the sea is represented by a wave spectrum, which describes the distribution of wave energy over a relevant frequency interval. Actually, the spectral value is given in terms of variance of the excursion of the sea surface per wave frequency. This variance parameter is related linearly to the wave energy.

The state of the sea is assumed to be stationary for a certain period of time. During this period, the total amount of wave energy and its distribution over the frequencies is constant, and therefore such a stationary period is described by one set of spectral parameters. A duration time generally accepted for a stationary sea state, or rather a quasi-stationary sea state, is three hours. In this report, such a three hour sea state will be refered to as the sea state, without further notice.

The properties of a wave spectrum, and thus the properties of the sea state it is representing,can be characterized by means of several parameters. In this report, the following parameters are used:

a. The peak period, T_p

b. The significant wave height, H_{SIG}

The significant wave height is approximately equal to the average of the upper third of all waves. It is related to the area enclosed by the graph of the wave spectrum in the following way:

$$H_{SIG} = 4\sqrt{m_o} \qquad (3.14)$$

where:

m_o = area enclosed by the graph of the wave spectrum

This enclosed area is related proportionally to the overall wave energy, so the significant wave height is a measure for this energy.

There are several empirical expressions available for wave spectra , all applying to different sea areas, for example:

a. Pierson Moskowitz spectrum

b. JONSWAP spectrum

Both wave spectra are shown in figure 3.4.

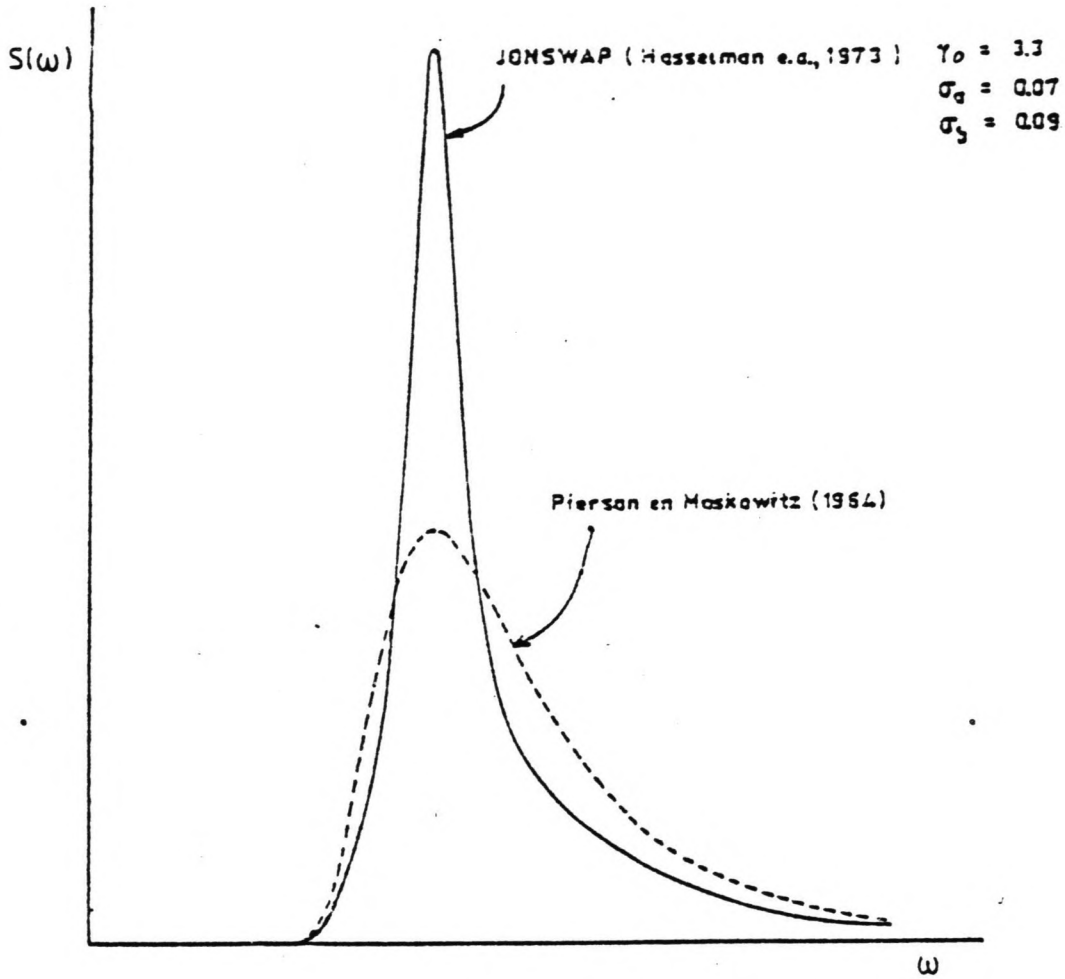

Figure 3.4: Examples of wave spectra

For the tests of the numerical model, the Russian jack-up is assumed to be located on the Forties field. The North Sea wave conditions, which apply to this field, are well described by the JONSWAP spectrum, and therefore this type of spectrum will be used in this study. Characterized by its significant wave height and its peak period, the JONSWAP spectrum is given by:

$$S(\omega) = C H_{SIG}^2 \frac{\omega_p^4}{\omega^5} \exp\{-1.25(\frac{\omega}{\omega_p})^{-4}\} \gamma_0^P \qquad (3.15)$$

where:

$$C = 0.3125\{1-0.287\log(\gamma_0)\}$$

$$p = \exp\left\{\frac{-(\omega-\omega_p)^2}{2\sigma^2\omega_p^2}\right\}$$

H_{sig} = significant wave height

γ_0 = peak enhancement factor

$$\omega = \frac{2\pi}{T}$$

T = wave period

$$\omega_p = \frac{2\pi}{T_p}$$

T_p = peak period

σ = shape factor

Since the significant wave height is directly related to the overall wave energy of the sea state considered, it is possible to compare spectra with the same overall wave energy but different energy distributions, by choosing one significant wave height and varying the peak period.

The average zero-crossing period of the spectrum, T_0, is computed by means of the following expression:

$$T_0 = 2\pi\sqrt{\frac{m_0}{m_2}} \qquad (3.16)$$

where:

$$m_n = \int \omega^n S(\omega)\, d\omega \qquad (3.17)$$

3.3.3 Numerical approach

For the use of the wave spectrum in the dynamic response analysis, the wave frequency range considered is divided into a number of intervals (see figure 3.5).

Each of the spectrum sections generated in this way, represents an amount of wave energy. Per section, i, this wave energy, E_i, is equal to the area of the section:

$$E_i = S_i \Delta \omega_i \qquad (3.18)$$

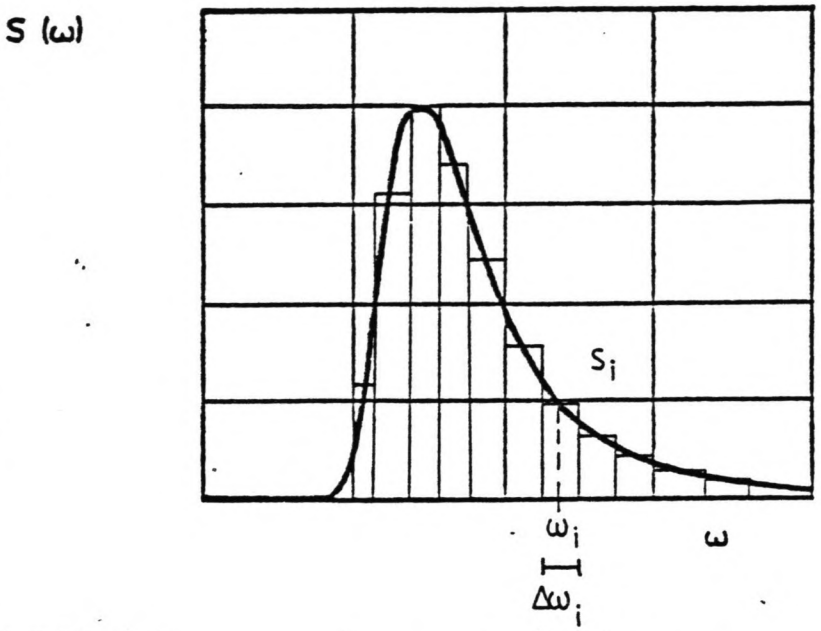

Figure 3.5: Division of wave spectrum into sections

where:

S_i = average spectral value of the section

$\Delta \omega_i$ = frequency interval

This energy is related to a sinusoidal wave with a frequency equal to the centre frequency of the interval considered. The surface excursion due to this wave, ζ_i, is given by:

$$\zeta_i = \frac{H_i}{2} \sin(\omega_i t) \qquad (3.19)$$

where:

ζ_i = surface excursion

ω_i = centre frequency of the spectrum section

t = time

The wave height, H_i, is given by:

$$H_i = 2\sqrt{2S_i\Delta\omega_i} \qquad (3.20)$$

Now the spectrum is represented by a number of sinusoidal waves, each with their own wave height and frequency. The individual fluid velocities and accelerations are found by means of the expressions from short wave theory listed in the previous paragraph.

In the frequency domain the dynamic response of the platform is computed for each of the sinusoidal waves mentioned above. After this, the results are added to find the overall loads and motions. This procedure is highlighted in chapter 6.

In a time domain analysis the sinusoidal waves are added, in order to generate a wave train, and so are their fluid velocities and accelerations. This is the basis for the simulation of the platform response for a number of time steps. Further details of this method are given in chapter 7.

In order to obtain true irregularity of the wave train used for time domain analysis, the following should be noted. If all frequency intervals have the same size, and therefore the frequencies of the sinusoidal waves are equidistant , then the wave pattern resulting from superposition of these waves will have the following return period:

$$T = \frac{2\pi}{\Delta\omega} \qquad (3.21)$$

where:

T = return period

$\Delta\omega$ = frequency interval

There are two ways of avoiding a repeating wave pattern during the desired simulation time:

a. Using a return period longer than the desired simulation time, in other words, making the constant frequency interval small enough.

b. Generating frequency intervals with a random size.

In this study, the second method is used.

For a realistic description of the sea surface, the number of frequency intervals should not be taken to small. This can be checked by adding the areas of all spectrum sections generated

numerically and using the resulting spectrum area to find the significant wave height:

$$H_{s16} = 4\sqrt{\sum_{i=1}^{n} S_i \Delta\omega_i} \qquad (3.22)$$

This result is compared to the original significant wave height. If both values differ significantly, this indicates that the spectrum sections generated numerically do not represent the area of the wave spectrum accurately. This means that the number of spectrum sections should be increased.

For the range of spectra to be examined a number of parameters have been computed with the expressions presented above. The frequency range was taken as:

ω = 0 rad/s to 2 rad/s

This range was divided into 70 sections of random size. The result of this is shown in table 3.2.

Peak period [s]	Significant wave height [m]	Test of significant wave height [m]	Zero-crossing period [s]	Actual number of spectrum sections [-]
8.0	6.0	5.95	6.68	56
8.5	7.0	6.95	7.04	57
9.0	8.0	7.96	7.41	57
9.5	9.0	8.96	7.78	58
10.0	10.0	9.97	8.15	59
10.5	11.0	10.98	8.52	59
11.0	12.0	11.99	8.89	60
11.5	13.0	12.98	9.27	60
12.0	14.0	13.99	9.65	61

Table 3.2: Spectrum computations for design sea states of the Forties field

As can be seen from table 3.2, the difference between the actual significant wave heights and the test values computed numerically is less than 1 %,. It can be concluded that the numerical reprentation of the wave spectra is sufficiently accurate.

In order to save computer time in both analysis methods, the spectrum sections with a resulting wave height less than 1 mm are neglected. The remaining number of spectrum sections is

printed in the last column of table 3.2.

3.3.4 Verification

The wave train generated for the purpose of time domain analysis, can also be used to verify the numerical conversion of the wave spectrum in a number of sinusoidal waves. Since it is assumed that the excursion of the water surface is a Gaussian process, sampling of the water excursion in the wave train that is generated numerically, and computation of the distribution function should yield a Gaussian curve again. This has been done for the two JONSWAP spectra with the following properties:

$$T_p = 10 \text{ s} \quad , \quad H_{s/6} = 10 \text{ m}$$

and

$$T_p = 12 \text{ s} \quad , \quad H_{s/6} = 14 \text{ m}$$

The simulation time is 3600 s.

The histograms of both wave trains are shown in figures 3.6 and 3.7, together with the theoretical Gaussian distribution function. It can be seen that the curves agree very well, which means that the numerical generation of the wave train yields realistic results.

FIG. 3.6: HISTOGRAM OF SURFACE EXCURSION

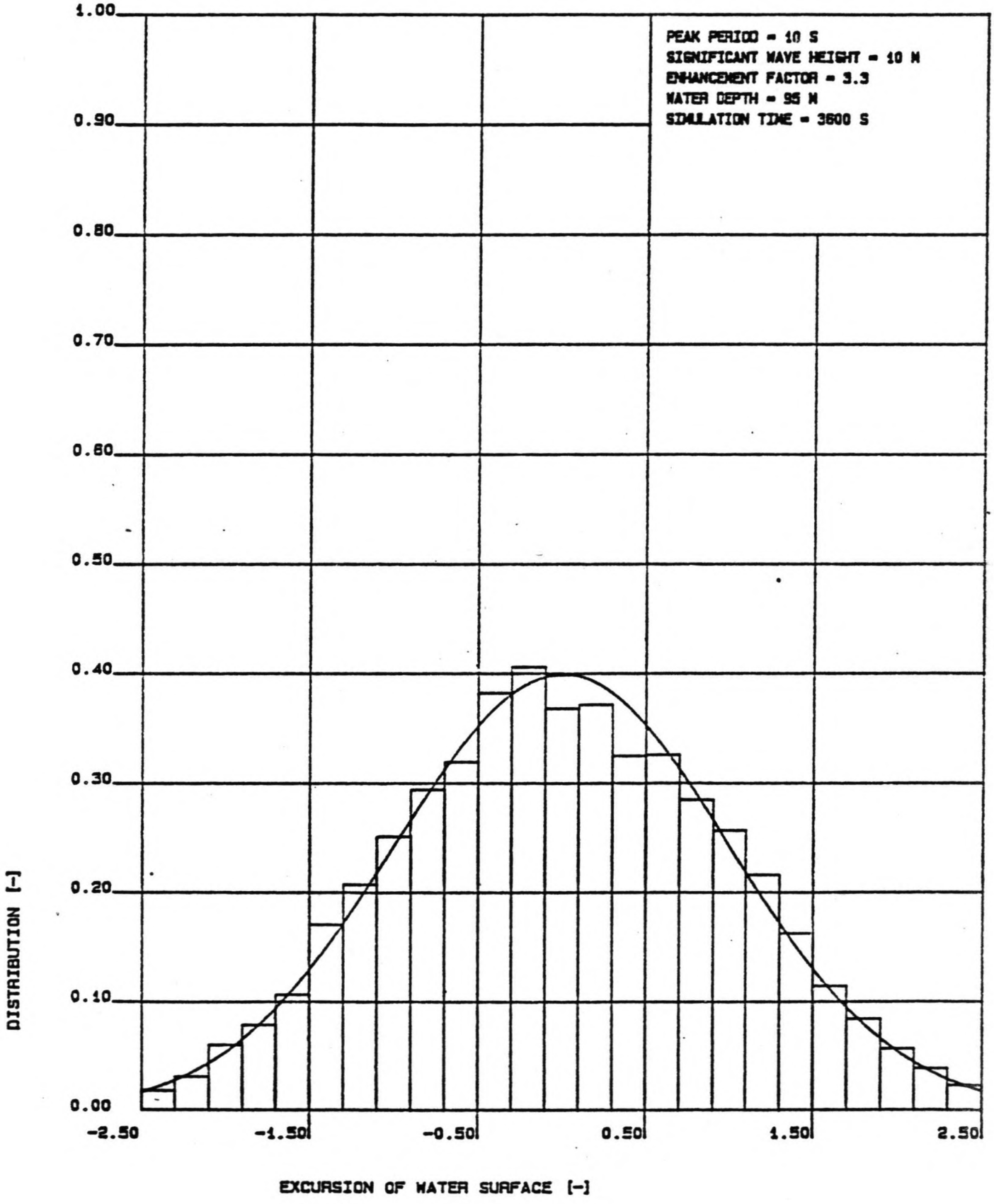

FIG. 3.7: HISTOGRAM OF SURFACE EXCURSION

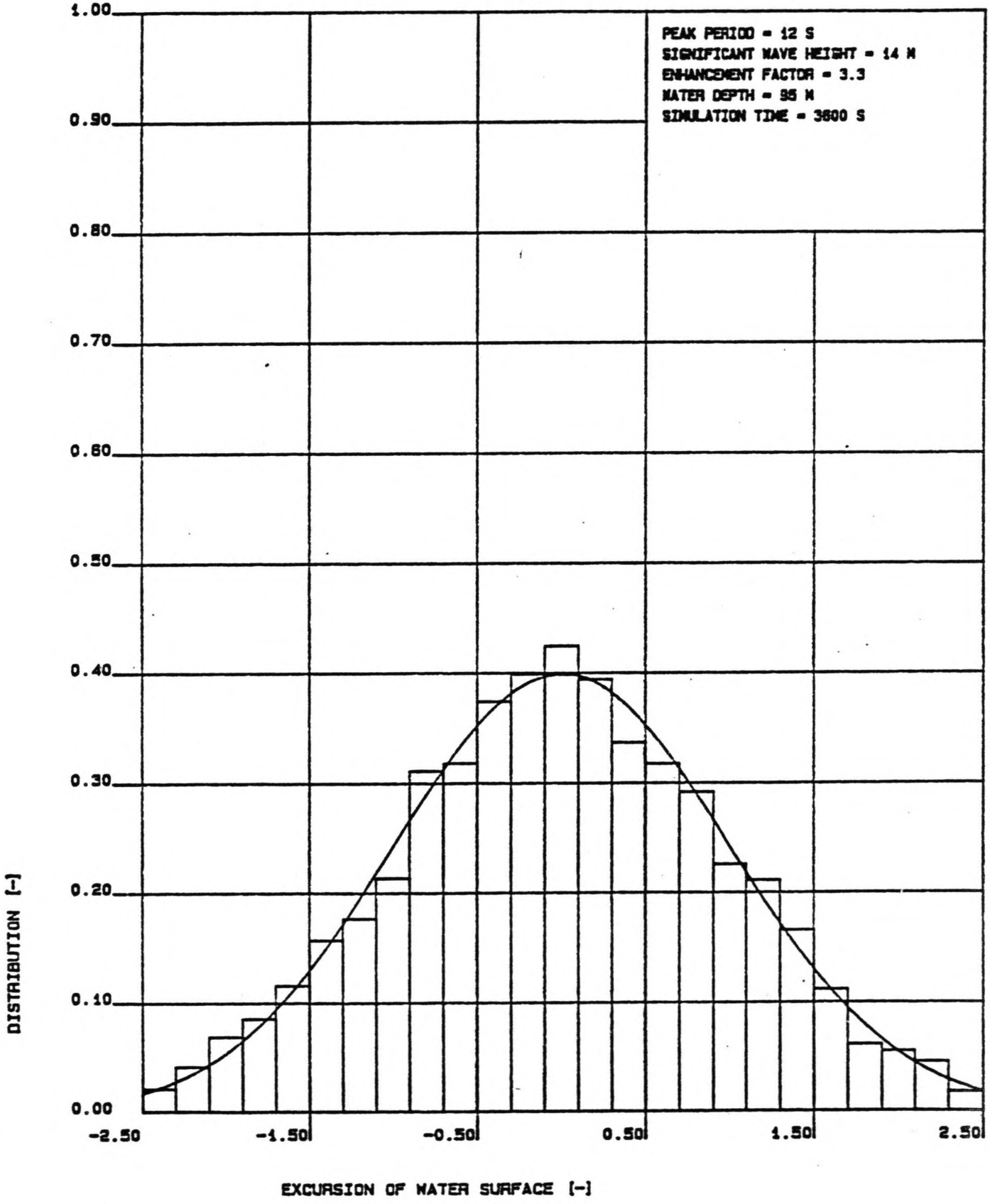

3.4 DIRECTIONAL SPREADING

The model of directional wave spreading, that is introduced in this chapter, is based on the following assumptions:

a. There is a main wave direction, which is constant during one sea state.

b. There is no transport of wave energy in the direction opposite to the main wave direction.

The second assumption indicates that all possible directions of wave propagation during one sea state lie within a semicircle around the main wave direction as shown in figure 3.8.

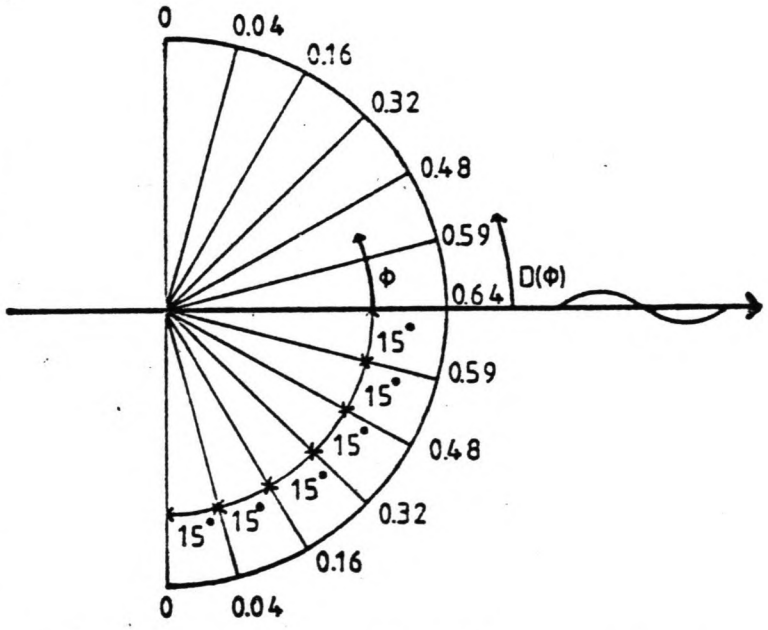

Figure 3.8: Wave spreading factor

The wave energy of a certain sea state is distributed over this semicircle by means of a dimensionless wave spreading factor, $D(\phi)$. Although only little empirical information is available about the wave spreading factor, the following expression is often used:

$$D(\phi) = \frac{2}{\pi} \cos^2(\phi) \qquad (3.23)$$

where:

ϕ = wave direction with respect to the main wave direction

$D(\phi)$ = spreading factor

This expression is known as the cosine square distribution and will be used in this study. The main wave direction is represented by:

$$\phi = 0$$

According to its definition, the integral of $D(\phi)$ with respect to ϕ is equal to unity:

$$\int_{-\pi/2}^{+\pi/2} D(\phi)\,d\phi = 1 \qquad (3.24)$$

Directional wave spreading will only be accounted for in the frequency domain, and for this reason the application of the wave spreading factor is outlined in chapter 6.

4 LOADS

4.1 INTRODUCTION

For the dynamic response analysis of a jack-up platform, there are two relevant types of loading:

a. Payload

b. Environmental loads

Payload has already been accounted for in the previous chapter. This paragraph deals with the environmental loads, which are subdivided into:

b1. water loads

b2. wind loads

As far as the dynamic part of these loads is concerned, two loading conditions are of special interest because of the relative heavy platform motions they will cause:

a. Survival condition. Platform motions are governed by the magnitude of the loads.

b. A concentration of loads with frequencies around the natural frequency of the platform. Apart from the magnitude of the loads, the motions are strongly influenced by the dynamic amplification, which occurs in this frequency range.

The next paragraph deals with water loads and special attention is given to their computation. Wind loads are briefly discussed in paragraph 4.3.

4.2 WATER LOADS

4.2.1 General

The water loads on a jack-up are caused by:

a. Waves

b. Tidal current

c. Wind-driven current

The fluid velocities induced by a sinusoidal wave, are given by short wave theory:

$$\dot{u}_w(t,z) = \hat{\dot{u}}_w(z)\sin(\omega t) \qquad (4.01)$$

$$\hat{\dot{u}}_w(z) = \frac{\omega H}{2}\,\frac{\cosh(kz)}{\sinh(kd)} \qquad (4.02)$$

where:

$\dot{u}_w(t,z)$ = amplitude of wave-induced fluid velocity

ω = angular wave frequency

t = time

H = wave height

$k = \frac{2\pi}{L}$

L = wave length

z = vertical coordinate

d = water depth

According to the D.N.V. Rules, the wind-driven current, u_{w_1}, is taken as:

$$u_{w_1}(z) = v_{w_{1,0}}\,\frac{z-d_0}{d_0} \qquad (4.03)$$

$$v_{w_{1,0}} = 0.017 v_{10} \qquad (4.04)$$

where:

$v_{w_{1,0}}$ = wind-driven current at still water level

v_{10} = reference wind velocity at 10 m above still water level

d_0 = reference depth = 50 m

The tidal fluid velocity is assumed to have a rectangular profile. Figure 4.1 shows the profiles of all fluid velocity profiles.

In the next section, it is shown that the relationship between water loads and fluid velocities is non-linear. In order to account for this, the velocity profiles from figure 4.1 are added before computing the water loads. In order to obtain the

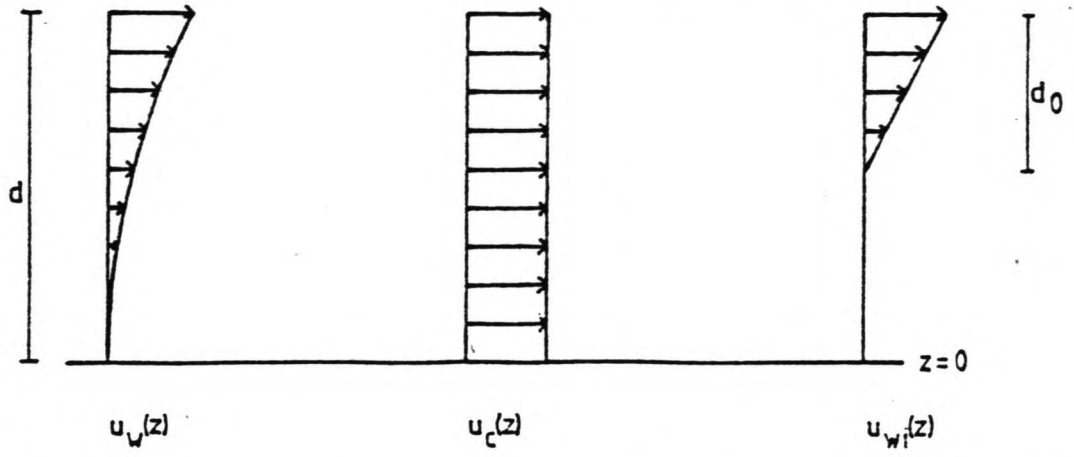

Figure 4.1: Fluid velocity profiles due to waves, tide and wind

relative velocity, structure velocity is included as well. Due to their different sources, the various velocity components will have different directions, and therefore they are added as vectors. The result of this is a relative velocity profile having a time-dependent shape and a time-dependent direction. The problems arising from this for frequency domain analysis are handled in chapter 5.

The computation of the water loads exerted by fluid accelerations is less cumbersome, since these are only wave-induced. In the next paragraph it is also found that these loads are related to the fluid accelerations in a linear way, which simplifies their computation even further.

Additionally, the magnitude of the water loads is influenced by the following factors:

a. The directional spreading of wave attack on each leg.

b. The different phase of wave loads on each leg.

c. Variation of the submerged portion of the legs.

The variation of the submerged portion of the legs will have two effects:

c1. A variation of buoyancy. For a lattice leg buoyancy is not very significant and its variation is as-

sumed to be negligible.

c2. A changing point of action of the water loads. This will cause asymetry of the loading pattern during one wave period, as is shown in figure 4.2. In time domain analysis, the waterdepth is updated at each time step, so the simulation includes this effect. This is not the case for frequency domain analysis. The nature of this method does not allow the computation of the waterdepth variations.

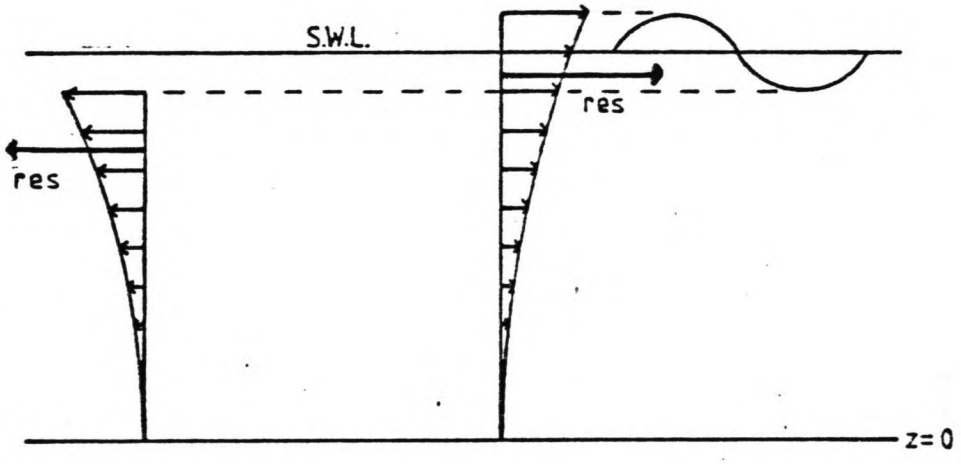

Figure 4.2: Asymmetrical profiles of wave-induced fluid velocity

4.2.2 Morison equation

In this report, the water loads on a jack-up platform are computed by means of the Morison equation. This is an empirical formula and its use is restricted by certain conditions, which will be discussed in this section. For a slender element of a structure, say the lattice leg of a jack-up , the Morison equation is given by:

$$f(t,z) = \frac{C_D \rho D\{\dot{u}(t,z)-\dot{x}(t,z)\}|\dot{u}(t,z)-\dot{x}(t,z)|}{2} + C_A \rho A\{\ddot{u}(t,z)-\ddot{x}(t,z)\} + \rho A\ddot{u}(t,z) \qquad (4.05)$$

where:

$f(t,z)$ = water load per unit length

C_D = drag coefficient

ρ = water density

D = diameter of the member

$\dot{u}(t,z)$ = fluid velocity

$\dot{x}(t,z)$ = structure velocity

C_A = added mass coefficient

A = cross-sectional area of the member

$\ddot{u}(t,z)$ = fluid acceleration

$\ddot{x}(t,z)$ = structure acceleration

The first term on the right of equation (4.05) represents the so-called drag force, while the other terms describe the mass forces. The third term covers the mass displaced by the structure considered, while the the second term describes the contribution from the water mass which is excitated by the motions of the structure. The ratio of this so-called added mass and the displaced water mass is given by the added mass coefficient.

The Morison equation is only valid if the following conditions are satisfied:

a. Wave scattering negligible (diffraction = 100 %). This means that the structure does not disturbe the flow pattern considerably.

b. Quasi-uniform flow. This condition can be understood by looking at figure 4.3, which shows a tubular element loaded by waves, at one point in time. The wave loads are computed by means of the Morison equation, using the velocity profile at cross-section A, but if the diameter of the tube is not small enough, this velocity profile will not represent the fluid velocities at cross-section B, or in other words, the flow pattern will not be quasi uniform and thus the calculated forces will not be correct.

The validity of the Morison equation can be checked by considering a cilinder with radius r loaded by waves and comparing the wave loads found by means of Morison's equation with the wave loads found by means of diffraction theory. From litera-

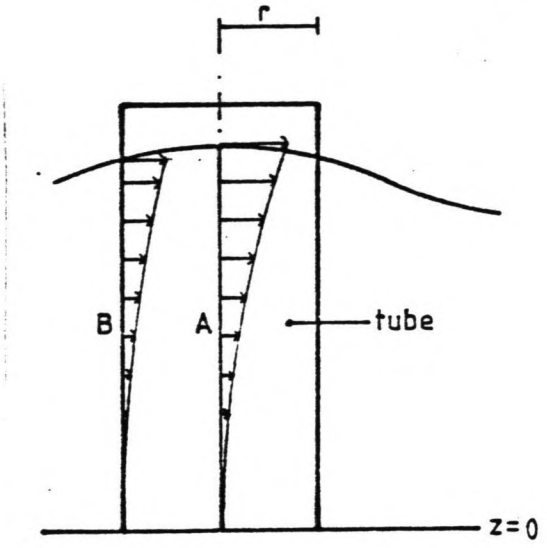

Figure 4.3: Quasi-uniform flow

ture it was found that this comparison yields the following approximate limitation for the use of Morison's equation:

$$kr < 0.5 \qquad (4.06)$$

where:

$$k = \frac{2n}{L}$$

L = wave length

r = radius of the element loaded

This expression represents both conditions stated above. Together with the deep water relationship between the wave period, T, and the wave length:

$$L = 1.56T \qquad (4.07)$$

this limitation can be written as:

$$T > 2.84\ r \qquad (4.08)$$

As the leg is a lattice structure, this condition applies to all separate members. The chords, which are the members with the largest diameter, will cause the most stringent limita-

tion. They have a radius in the following order of magnitude:

$$r \simeq 0.5$$

This yields the following limitation for the use of Morison's equation:

$$T > 2\ s \qquad (4.09)$$

At sea, no wave energy is to be expected below wave periods of about 4 s. This means that wave scattering is negligible for all relevant wave periods. This conclusion is valid for most jack-up platforms with lattice legs. In the case of tubular legs, however, wave scattering could be considerable and the validity of Morison's equation should be examined carefully.

Before looking at the second condition, concerning quasi-uniform flow, some attention is given to the conversion of the drag and mass coefficients, as performed by Gusto Engineering.

In order to obtain one drag coefficient and one mass coefficient per leg, the coefficients of all members of the lattice leg are used to find the wave loads for survival flow conditions. The lattice leg is replaced by a tubular leg, of which the overall drag coefficient and mass coefficient are scaled by means of these survival flow conditions and wave loads. The diameter of this tubular leg is taken as the distance between two chords of the original lattice leg and is called the equivalent leg diameter (see figure 4.4).

Since the introduction of the equivalent tubular leg implies the substitution of equivalent leg diameter and cross-section values, respectively D and A, but the displaced water mass has to remain unchanged, the third term on the right of the Morison equation is multiplied by the conversion factor of the added mass coefficient, c, which is given by:

$$c = \frac{A_l}{A_T} \qquad (4.10)$$

where:

A_l = cross-sectional area of the lattice leg

A_T = cross-sectional area of the equivalent tubular leg

In this way the equivalent tubular leg will have an added water mass equal to that of the lattice leg. After this operation, the lattice leg with separate drag and mass coefficients for all members is replaced by the equivalent tubular leg with

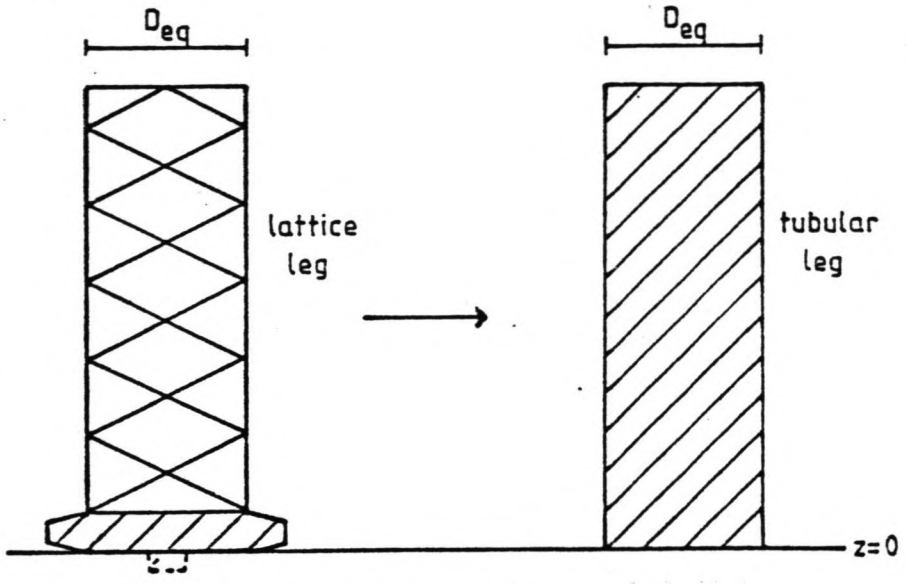

Figure 4.4: Definition of equivalent tubular leg

only one set of coefficients. The Morison equation for the equivalent tubular leg becomes:

$$f(t,z) = \frac{C_{D,EQ}\,\rho\,D_{EQ}\{\dot{u}(t,z)-\dot{x}(t,z)\}\,|\dot{u}(t,z)-\dot{x}(t,z)|}{2}$$

$$+ C_{A,EQ}\,\rho\,A_{EQ}\{\ddot{u}(t,z)-\ddot{x}(t,z)\} + c\rho A_{EQ}\ddot{u}(t,z) \qquad (4.11)$$

where:

$C_{D,EQ}$ = equivalent drag coefficient

ρ = water density

D_{EQ} = equivalent leg diameter

$C_{A,EQ}$ = equivalent added mass coefficient

A_{EQ} = cross-sectional area of the equivalent leg

c = conversion factor of the added mass coefficient

The equivalent drag and added mass coefficients, $C_{D,EQ}$ and $C_{A,EQ}$, and the conversion factor are listed in table 1 of ap-

pendix 5, for twenty-four loading directions with intervals of 15 degrees. As the legs are of the lattice type, drag forces will be large compared to mass forces. Due to leg geometry the drag coefficient slightly depends on the direction of flow, while the mass coefficient remains constant for all directions.

Now the second condition for the use of the Morison equation is considered. As the fluid velocity profile which will be used for the computation of the water loads, now applies to one complete leg, the second condition for the use of Morison's equation, concerning quasi-uniform flow, should apply to the dimensions of the complete leg, instead of one chord. For this reason, condition b. is written as:

$$kR < 0.5 \qquad (4.12)$$

where:

$R = D_{EQ}/2$

D_{EQ} = distance between two chords

Performing the same computations as listed above, using:

$D_{EQ} = 10.5$ m

yields:

$$T > 6 \text{ s} \qquad (4.13)$$

As can be seen from this, the uniform flow condition is more stringent than the wave scattering condition. This is typical of lattice structures, as they combine relatively large overall dimensions with only minor disturbances of the flow pattern. Apart from the above limitations of Morison's equation, which can be represented by a mathematical expression, some critical remarks are made in a more general way about the use of drag and mass coefficients:

a. Marine growth can influence the drag coefficient of the leg substantially.

b. The overall drag and mass coefficients of the equivalent leg are influenced by the hydrodynamic interaction between the members of the lattice leg. This interaction is dependent of wave frequency and direction. At the conversion of the lattice leg to an equivalent tubular leg, this effect can only be accounted for in a very approximate way.

c. Lift forces, acting in the direction normal to the

direction of drag and mass forces, are neglected.

In the next chapters, the Morison equation will be used very often. For reasons of convenience, the following substitutions are made:

$$C_1 = \frac{\rho C_{D,EQ} D_{EQ}}{2} \qquad (4.14)$$

$$C_2' = \frac{\pi \rho C_{A,EQ} D_{EQ}^2}{4} \qquad (4.15)$$

$$C_2'' = cA_{EQ} \qquad (4.16)$$

$$\dot{r}(t,z) = \dot{u}(t,z) - \dot{x}(t,z) \qquad (4.17)$$

$$\ddot{r}(t,z) = \ddot{u}(t,z) - x(t,z) \qquad (4.18)$$

where:

C_1, C_2', C_2'' = modified coefficients

$\dot{r}(t,z)$ = relative velocity

$\ddot{r}(t,z)$ = relative acceleration

The Morison equation then becomes:

$$f(t,z) = C_1 \dot{r}(t,z)|\dot{r}(t,z)| + C_2'\ddot{r}(t,z) + C_2''\ddot{u}(t,z) \qquad (4.19)$$

This expression will be used without further explanation.

4.3 WIND LOADS

As a storm always precedes the high waves it is causing, maximum wind loads and maximum wave loads will not coincide, but if the period of waves preceding these nigh waves is near the natural period of the platform, the combined effect of wind and water loads could become important. In this study, however wind loads will not be examined.

5 DYNAMIC RESPONSE ANALYSIS

5.1 INTRODUCTION

The main purpose of this study is a dynamic response analysis of jack-up platforms under realistic sea conditions. In order to enlarge the understanding of the processes involved and to allow a thorough development of computer programs, this goal is achieved stepwise. The following cases will be studied:

a. Motions of one leg, due to a regular wave.

b. Motions of one leg, due to a wave spectrum.

c. Motions of the platform, due to a wave spectrum.

This way of working is not as cumbersome as it appears to be, because each step incorporates the procedures developed in the previous steps.

This sequence is performed for two methods of analysis:

a. Frequency domain analysis (see chapter 6).

b. Time domain analysis (see chapter 7).

Both methods differ fundamentally, as is highlighted in the next paragraph, but they apply to one and the same dynamic model, described in paragraph 4. The assumptions underlying the dynamic analysis in general, are listed in paragraph 3, while the way to handle directional wave spreading is outlined in the last paragraph of this chapter.

5.2 FREQUENCY DOMAIN VERSUS TIME DOMAIN

As stated before, frequency domain analysis and time domain analysis differ fundamentally. Time domain analysis is a numerical simulation, which is the most accurate method for the following reasons:

a. Non-linear properties of the structure, due to non-linear springs or slack in the leg-hull connection, can be included.

b. Non-linear loads, like the drag force in Morison's equation, can be included.

c. The changing point of action of the water loads, due to the varying immersion of the legs, can be accounted for.

Time domain analysis allows the computation of transient state response as well as steady state response.

The results can be used for statistical analysis of all time-dependent parameters. This yields statistical information, like the probability of exceedance of certain load and motion values, which is indispensable for a jack-up design method with a probabilistic nature.

In this report, an attempt will be made to find mathematical expressions for the distribution functions of the water loads and platform motions by means of simulations. Such a mathematical description of the statistics of the dynamic behaviour would simplify the probabilistic design of a platform considerably, since the probabilities of exceedance are then available for all levels of loads and motions.

The main disadvantage of time domain analysis is the large consumption of computer time.

As opposed to this, frequency domain analysis, also known as spectral analysis, requires much less computer time, but all non-lineair effects need to be linearized, which introduces uncertainty about the accuracy of the method. It is only applicable to steady state response and statistical analysis of the results is not possible. On the other hand, the hydrodynamic damping percentage is computed, which is not the case in time domain analysis.

One of the major advantages of frequency domain analysis is the easy access to the spectral representation of water loads of the water loads and platform motions, which offers very clear information about frequency-characteristics of these parameters. Since loads and motions are computed for a number of separate frequency intervals before the results are put together to yield the overall values, the frequency-dependent information needed for load and wave spectra is readily available in the frequency domain. This is also one of the reasons for the use of spectral analysis methods for fatigue analysis, which will not be discussed in this report.

The time domain results, on the other hand, first have to be transformed in order to obtain load and motion spectra. This can be done by means of a Fourier transformation, but this method can be quite eleborate, which means even more consumption of computer time.

With the same information used for the motion spectrum it is possible to compute the frequency-characteristics of the dynamic system. for this purpose, the so-called Dynamic Amplification Factor (D.A.F.) is introduced, which offers a dimensionless representation of the frequency characteristics. Its

exact definition is given in section 6.6.3.

The main advantages and disadvantages of time domain and frequency analysis are listed in table 5.1.

Time domain	Frequency domain
	+ Direct spectral representation
	+ Computation of hydrodynamic damping
+ Inclusion of non-linearities	- Linearization of all non-linearities
+ Computation of transient and steady state	- Steady state computation only
+ Statistical analysis of loads and motions	
- Large consumption of computer time	

Table 5.1: Frequency domain versus time domain

By starting with the analysis of one leg of the jack-up, a number of complicating effects, caused by the interaction between the legs of the platform, is ruled out. This allows an accurate comparison of frequency domain analysis and time domain analysis. For the same purpose some computations are made for one leg loaded by a regular wave, before introducing a wave spectrum.

5.3 ASSUMPTIONS

In the previous chapters, a number of assumptions have been made concerning the structure and the environmental conditions. The major assumptions, applying to all cases to be analysed, are listed below:

a. The bending forces of the leg are carried by the chords. This allows the use of Steiner's rule for the computation of the bending stiffness of the leg.

b. The shear forces of the leg are carried by the bra-

ces.

c. The pontoon is rigid compared to the legs.

d. The axial deformation of the legs is negligible.

e. The rotational stiffness of the leg-hull can be replaced by a linear spring constant.

f. The rotational stiffness of the leg-soil can be replaced by a linear spring constant.

g. All moments and horizontal forces in the elevating system are carried by the guides. This means that the rack and pinion system only carries the pontoon mass and the payload.

h. All legs carry an equal part of the pontoon mass and the payload.

i. Fluctuations of axial loading of the legs, due to deck motions, do not influence the overall response of the platform.

j. The leg motions are quasi-stacic.

k. Spud can displacements are negligible.

l. Platform motions cause the legs to rotate about horizontal axes through the tips of the spud cans.

m. The spud can mass does not contribute to the dynamic mass of the leg.

n. There is no bottom slope.

o. The excursion of the water surface is a Gaussian process in time, except for deterministic analysis.

p. Short wave theory is applicable.

q. Variation of buoyancy of the legs is negligible.

The assumptions and restrictions, which apply only to specific cases of dynamic analysis, will be mentioned at the description of these cases.

5.4 DYNAMIC MODEL

5.4.1 General

As highlighted in chapter 2.2, the jack-up platform is represented by a three-degrees-of-freedom system, which , under certain conditions, can be subdivided into three independent single-degree-of-freedom systems. As shown in figure 5.1, the first two motion modes are translational and the third mode is a rotation about a vertical axis through the gravity centre of the platform. The two translational modes are identical.

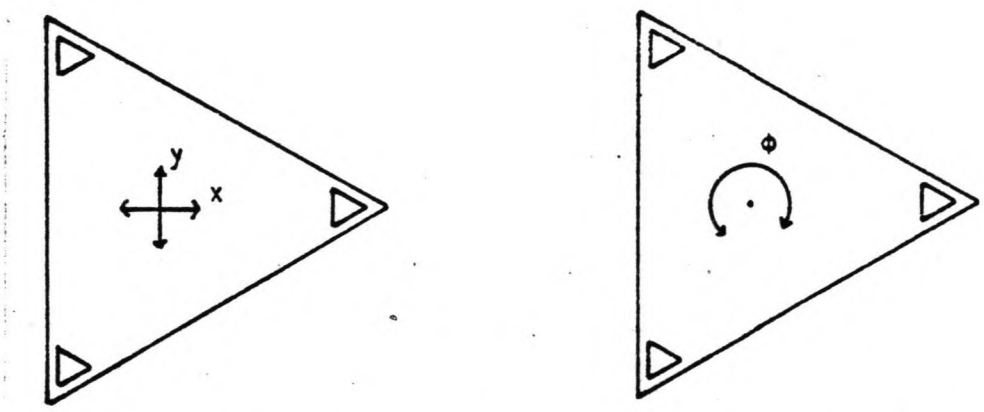

Figure 5.1: Degrees of freedom of the jack-up platform

The complete three-degrees-of-freedom system is handled in chapter 6 at the description of the frequency domain analysis method. This paragraph deals with the separate single-degree-of-freedom systems, which are all based on the dynamic model of one leg, described in the next section. The main properties of the separate motion modes of the complete platform are discussed in sections 5.4.3 and 5.4.4.

5.4.2 One leg

As already stated in paragraph 2.2, vertical translation and rotation of the deck about a vertical axis are neglible in the case of a multi-legged platform, if the amplitude of the lateral motions is small compared to the free leg length. The one leg model is introduced here with the purpose of providing a basis for the analysis of this type of platforms, and therefore it is assumed that the vertical translation and the rotation of the deck about a horizontal axis is negligible for the

one leg model as well. The one leg model resulting from this is shown in figure 5.2. The main parameters are:

M_D = total deck mass

n_l = number of legs of the platform

l = free leg length

m = leg mass per unit length

EI' = reduced bending stiffness of the leg, including shear stiffness of the leg

k_A = rotational leg-soil stiffness

k_B = rotational leg-hull stiffness

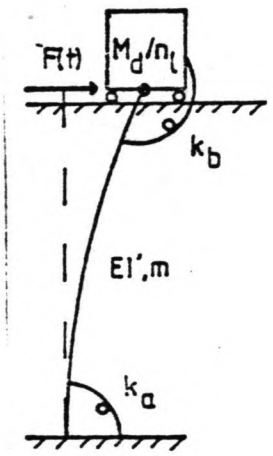

Figure 5.2: One leg model

In chapter 2, these parameters have already been combined to the mass parameter and the stiffness parameter, which are used in the single-degree-of-freedom system representing the dynamic one leg model (see figure 5.3):

$$M_l = \frac{M_{DYN}}{n_l} \qquad (5.01)$$

M_{DYN} = dynamic deck mass, including contributions from the legs, but no added mass

k_c = combined leg stiffness

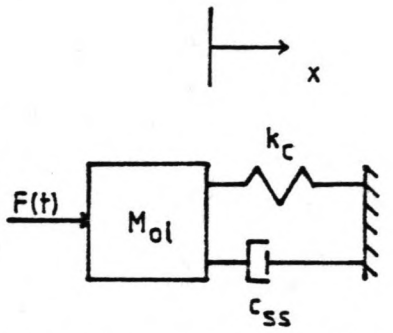

Figure 5.3: Dynamic model of one leg

According to the theory of single-degree-of-freedom systems, the critical damping, c_{CRIT}, is:

$$c_{CRIT} = 2\sqrt{k_c M_\ell} \qquad (5.02)$$

The structural and soil damping is given by:

$$c_{ss} = \frac{\zeta_{ss}}{100} c_{CRIT} \qquad (5.03)$$

where:

c_{ss} = structural and soil damping

ζ_{ss} = structural and soil damping percentage

The general equation of motion is:

$$M_\ell \ddot{x}(t) + c_{ss} \dot{x}(t) + k_c x(t) = F(t) \qquad (5.04)$$

where:

$x(t)$ = deck displacement

$\dot{x}(t)$ = deck velocity

$\ddot{x}(t)$ = deck acceleration

$F(t)$ = water load transfered to lower guide level

The natural period of the one leg model, T_ℓ, is given by:

$$T_l = \frac{2\pi}{\sqrt{k_c / M_l}} \qquad (5.05)$$

All physical parameters have been transfered to lower guide level, except for the water load and the hydrodynamic damping. Both are accounted for by means of the Morison equation, and therefore their transference will be handled simultaneously. For the equivalent tubular leg, which was introduced in section 4.2.2, Morison's equation is given by:

$$f(t,z) = C_1 \dot{r}(t,z)|\dot{r}(t,z)| + C_2' \ddot{r}(t,z) + C_2'' \ddot{u}(t,z) \qquad (5.06)$$

where:

$f(t,z)$ = water load per unit length

t = time

z = vertical coordinate

C_1 = modified drag coefficient

C_2', C_2'' = modified inertia coefficients

$\dot{r}(t,z)$ = relative velocity

$\ddot{r}(t,z)$ = relative acceleration

$\ddot{u}(t,z)$ = fluid acceleration

The elementary water load on a leg segment dz is equal to $f(t,z)dz$. Due to the assumed quasi-static behaviour of the leg, the contribution of this elementary water load to the overall water load at lower guide level, $F(t,z)$, as shown in figure 5.4, is given by:

$$F(t,z) = f(t,z)g(z)dz \qquad (5.07)$$

where

$$g(z) = \frac{z}{l} \qquad (5.08)$$

l = free leg length

The overall water load transfered to lower guide level, $F(t)$, can be found by means of integration with respect to the vertical coordinate, z:

$$F(t) = \int_0^l f(t,z)g(z)dz \qquad (5.09)$$

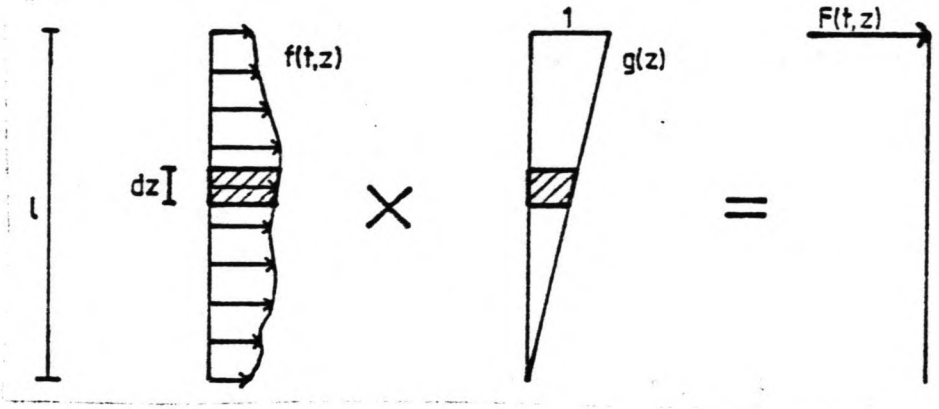

Figure 5.4: Transference of water load to lower guide level

This indicates that the contribution of the water loads , f(t,z), to the overall water load , F(t), increases going upwards from the sea bottom to the water surface.

In order to simplify the above integration, which incorporates the Morison equation, the leg motions are expressed in terms of the deck motions, by means of the dimensionless static deflection of the leg. Since the leg motions are assumed to be quasi-static, they can be expressed in terms of the deck motions by means of the dimensionless static leg deflection, h(z), as follows:

$$x(t,z) = h(z)x(t) \qquad (5.10)$$

where:

x(t,z) = leg motions

x(t) = deck motions

h(z) = dimensionless static leg deflection

This was already found in chapter 2. Now the structure motions, x(t,z) in the Morison equation are replaced by deck motions, x(t), or in other words, they are transfered to lower guide level as well. This means that the right hand side of the general equation of motion is also written in terms of deck motions:

$$F(t) = \int_0^d [C_1\{\dot{u}(t,z)-h(z)\dot{x}(t)\}|\dot{u}(t,z)-h(z)\dot{x}(t)| + C_2'\{\ddot{u}(t,z)-h(z)\ddot{x}(t)\} + C_2'\ddot{u}(t,z)]g(z)dz \qquad (5.11)$$

This overall water load also includes hydrodynamic damping.

5.4.3 Platform translations

In order to simplify the expressions used in this section, it is assumed that the water loads act in the direction of the x-axis. As different loading directions are only considereed in the frequency domain analysis, this item is handled in paragraph 6.5.

The dynamic model for the two translational modes of the platform is exactly the same as the one leg model. It can be regarded as a system of one leg models, which are connected at lower guide level by the rigid pontoon. Due to the quasi-static leg behaviour, this system reduces to a single-degree-of-freedom system, as shown in figure 5.5, with the following equation of motion:

$$M_{DYN}\ddot{x}(t) + c_{SS,TR}\dot{x}(t) + k_{TR}x(t) = F(t) \qquad (5.12)$$

where:

M_{DYN} = dynamic deck mass

$c_{SS,TR}$ = structural and soil damping of translation

k_{TR} = translational platform stiffness

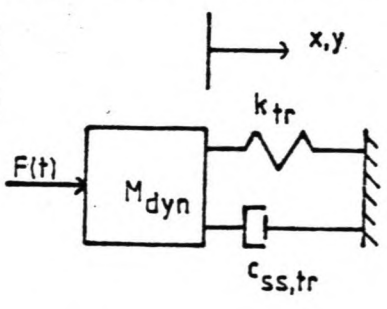

Figure 5.5: Dynamic model for platform translation

In chapter 2, the stiffness and damping properties for translation of the Russian jack-up platform, which is symmetrical,

were found by multiplying the one leg values by the number of legs:

$$k_{TR} = n_\ell k_c \tag{5.13}$$

$$c_{SS,TR} = n_\ell c \tag{5.14}$$

where:

n_ℓ = number of legs

k_c = combined leg stiffness

c_{SS} = structural and soil damping

As a result of this, The natural period of platform translations becomes:

$$T_{TR} = \frac{2\pi}{\sqrt{k_{TR}/M_{DYN}}}$$

$$= \frac{2\pi}{\sqrt{n_\ell k_c / n_\ell M_\ell}}$$

$$= \frac{2\pi}{\sqrt{k_c/M_\ell}}$$

$$T_{TR} = T_L \tag{5.15}$$

As to be expected, the natural period of the platform translations , T_{TR}, is equal to the natural period of the one leg model, T_L.

The water loads on the complete platform cannot be found by simply multiplying the water load on one leg with the number of legs. Due to the phase difference between wave loads on the legs, the water loads on each leg must be computed separately, before they are added:

$$F(t) = \sum_{i_\ell=1}^{m_\ell} F_{i_\ell}(t) \tag{5.16}$$

where:

$F(t)$ = water load on the complete platform

i_ℓ = leg number

n_l = total number of legs

$F_{i_l}(t)$ = water load on leg i_l

5.4.4 Platform rotation

The parameters of the single-degree-of-freedom system representing the rotational mode of the platform are different from those used for translation. The motions are not expressed in terms of displacement, but in terms of rotation about the vertical axis through the gravity centre of the platform, as shown in figure 5.6. The general equation of motion is given by:

$$J\ddot{\phi}(t,1) + c_{ss,ROT}\dot{\phi}(t,1) + k_{ROT}\phi(t,1) = T(t) \qquad (5.17)$$

where:

$\phi(t,1)$ = rotation of the deck

$\dot{\phi}(t,1)$ = angular velocity of the deck

$\ddot{\phi}(t,1)$ = angular acceleration of the deck

J = mass moment of inertia

$c_{ss,ROT}$ = structural and soil damping of rotation

k_{ROT} = rotational stiffness of the deck

$T(t)$ = moment due to water loads

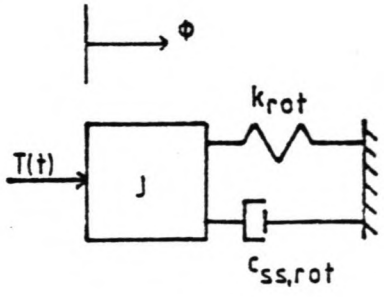

Figure 5.6: Dynamic model for platform rotation

The natural period of rotation, T_{ROT}, is given by:

$$T_{ROT} = \frac{2n}{\sqrt{k_{ROT}/J}} \qquad (5.18)$$

Since the stiffness properties as well as and the structural and soil damping properties of the legs are assumed to be constant for all directions, the legs can be represented by springs and dashpots as shown in figure 5.7, which is a top-view of the platform.

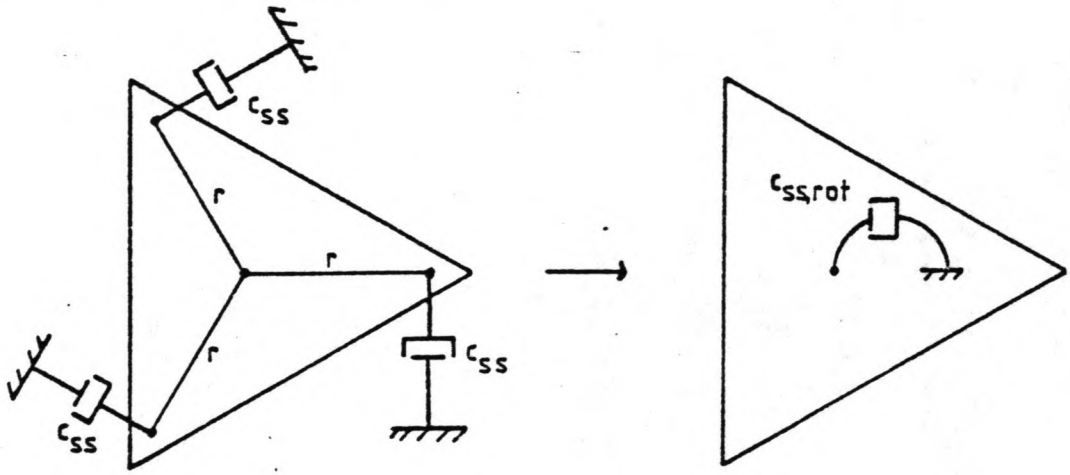

Figure 5.7: Structural and soil damping of platform rotation

From this figure it can be seen that a rotation of the deck causes a moment T:

$$T = \sum_{i_\ell=1}^{n_\ell} r_{i_\ell}^2 \, k_c \, \phi \qquad (5.19)$$

where:

i_ℓ = leg number

n_ℓ = total number of legs

r_{i_ℓ} = distance between the leg and the gravity centre of the platform

k_c = combined leg stiffness

The rotational stiffness of the platform is defined as:

$$k_{ROT} = \frac{T}{\phi} \tag{5.20}$$

Substitution of (5.19) into (5.20) yields:

$$k_{ROT} = \sum_{i_\ell=1}^{n_\ell} r_{i_\ell}^2 \, k_c \tag{5.21}$$

By considering the relationship between an external moment and the angular velocity of the deck, the structural and soil damping of rotation, $c_{ss,ROT}$, is found in a similar way:

$$c_{ss,ROT} = \sum_{i_\ell=1}^{n_\ell} r_{i_\ell}^2 \, c_{ss} \tag{5.22}$$

where:

$c_{ss,ROT}$ = structural and soil damping of rotation

c_{ss} = structural and soil damping of one leg

In the same way, the hydrodynamic damping of the platform is derived from the hydrodynamic damping of one leg. Consequently, the overall rotational damping can be found by first computing the overall damping of one leg. This procedure is used in the computer program.

It should be noted that the dimensions of the mass, damping and stiffness parameters of the rotation model are different from those used in the translation models.

The moment on the platform due to water loads is given by:

$$T(t) = \sum_{i_\ell=1}^{n_\ell} F_{i_\ell}(t) r_{i_\ell} \tag{5.23}$$

where:

$T(t)$ = moment on platform due to water loads

$F_{i_\ell}(t)$ = water load on one leg

Since expression for the water load on the leg incorporates the leg motions, these must be derived from the deck motions. In the case of translational motion modes, this can be done directly by means of the dimensionless static deflection,

h(z), which has already been included in the expression for the water loads on one leg. For the rotational platform mode, the platform rotations are transformed to leg motions in x- and y-direction, as shown in figure 5.8, by means of the following expressions:

$$x_{i_\ell}(t,1) = \phi(t,1)y_{i_\ell} \tag{5.24}$$

$$y_{i_\ell}(t,1) = \phi(t,1)x_{i_\ell} \tag{5.25}$$

where:

$x_{i_\ell}(t,1)$ = motion of leg i_ℓ at lower guide level in x-direction

$y_{i_\ell}(t,1)$ = motion of leg i_ℓ at lower guide level in y-direction

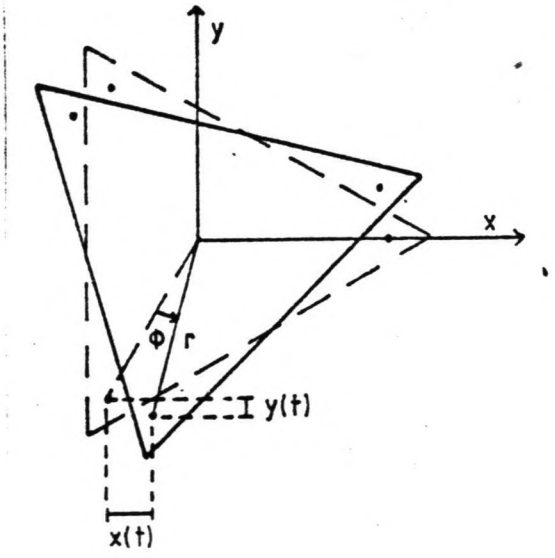

Figure 5.8: Conversion of platform rotation into leg displacements

This approximation is valid for small angles of rotation.

5.4.5 Leg sections

In the numerical model, all integrals with respect to the vertical coordinate, z, are replaced by a discrete summation. For this purpose, the free leg lenth is divided into a number of leg sections (see figure 5.9). All section parameters are computed by taking the average of the values at the boundaries of the leg section.

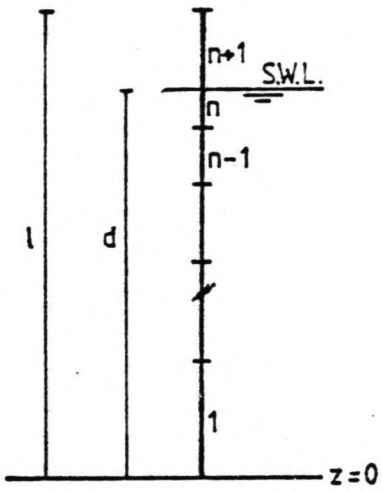

Figure 5.9: Numerical discretization of the leg

Since the leg sections near the sea bottom are relatively unsignificant for the dynamic behaviour of the platform, the size of the leg sections increases going downward from the sea surface.

It should be noted that the leg section between the sea surface and lower guide level has no impact on the platform behaviour, except for its mass. This has been accounted for.

6 FREQUENCY DOMAIN

6.1 INTRODUCTION

As stated before, the frequency domain analysis method is developed for the complete three-degrees-of-freedom system. This is done in order to allow the analysis of assymetric platform configurations. The numerical model is be capable of handling deterministic as well as stochastic wave loads. The stochastic wave model will be combined with current. Apart from numerical limitations, the frequency domain analysis method can handle any number of legs, including the one leg model, as the number of legs is an input parameter of the computer program.

Frequency domain analysis is based on the linearization of the drag term in Morison's equation, by means of a linearization coefficient. For the case of a deterministic wave model, this linearization coefficient is different from the one used for the stochastic wave model. Paragraph 6.2 deals with both expressions for the linearization coefficient.

Basically, the solution of the equation of motion of the complete three-degrees-of-freedom system is not different from the solution of a one-degree-of-freedom system. However, as the rewriting of the equation of motion, due to the linearization of the water load, is quite cumbersome, the solution for the one leg model will be presented first. This is done in paragraph 3 of this chapter.

Paragraph 6.4 deals with the computation procedure for the three-degrees-of-freedom-system. The mathematical background of the equation of motion is given in chapter 4 of the appendix.

At the completion of the dynamic model for the separate motion models, in chapter 5, all water loads were assumed to act in the x-direction. Since different loading directions and directional spreading of the waves are only considered for frequency domain analysis, these items are handled respectively in paragraphs 5 and 7 of this chapter. The frequency domain iteration for one loading direction is presented by means of a flowchart in paragraph 6.6.

During this study of jack-up dynamics, the computer program Jacquelin has been developed for frequency domain computations of the parameters discussed in this chapter. A complete listing of the input and output of this program is given in paragraph 6.8.

Again, it is pointed out that frequency domain theory is not valid for transient state computations, so all load and motion parameters apply to the steady state.

6.2 LINEARIZATION COEFFICIENT

6.2.1 General

A more complete derivation of the expression for the linearization coefficient is given in appendix 3. This paragraph deals with the starting points and the results. Current is only considered in the stochastic wave model.

The drag force per unit length on the equivalent tubular leg is given by:

$$f_D(t,z) = C_1 \dot{r}(t,z)|\dot{r}(t,z)| \qquad (6.01)$$

where:

$f_D(t,z)$ = drag force per unit length

t = time

z = vertical coordinate

C_1 = modified drag coefficient

$\dot{r}(t,z)$ = relative velocity

The relative velocity is split into two components:

$$\dot{r}(t,z) = v(z) + \dot{r}'(t,z) \qquad (6.02)$$

where:

$v(z)$ = current

$\dot{r}'(t,z)$ = relative velocity due to waves

As the determistic wave model is only used as a basis for the complete frequency domain analysis method, current is not accounted for in the computation of the deterministic linearization coefficient. The stochastic coefficients, however, include the influence of current.

6.2.2 Deterministic approach

For the deterministic case without current, the steady state relative velocity consists of a harmonic platform velocity and a harmonic fluid velocity. Since both components have the same period, the relative velocity can be written as:

$$\dot{r}(t,z) = \hat{\dot{r}}(z)\sin(\omega t') \qquad (6.03)$$

where:

$\hat{\dot{r}}(z)$ = amplitude of the relative velocity

$\omega t'$ = $\omega t + \psi$

ω = angular wave frequency

ψ = constant phase difference between structure and fluid motions

Now the drag force becomes:

$$f_D(t,z) = C_1 \dot{r}(z)^2 f_D(t) \qquad (6.04)$$

where:

$$f_D(t) = \sin(\omega t')|\sin(\omega t')| \qquad (6.05)$$

This expression is linearized to:

$$f_D(t,z) = C_1 a_D(z)\dot{r}(z)\sin(\omega t') \qquad (6.06)$$

where:

$a_D(z)$ = deterministic linearization coefficient

This linearization coefficient is found by developing the drag force in a Fourier progression. All cosine terms of this progression are zero, so only the sine components are left. Equation of first Fourier term of the drag force and the linearized drag force from (6.06) yields the deterministic linearization coefficient:

$$a_D(z) = \frac{8}{3\pi}\hat{\dot{r}}(z) \qquad (6.07)$$

6.2.3 Stochastic approach

In the case of the stochastic wave model, the excursion of the sea surface is assumed to be a Gaussian process in time, and thus the fluid velocity has a Gaussian distribution as well. The drag force is linearized to:

$$f_D(t,z) = C_1\{a_s(z)\dot{r}'(t,z)+b_s(z)\} \qquad (6.08)$$

where:

$\dot{r}'(t,z)$ = relative velocity due to waves

$a_s(z), b_s(z)$ = stochastic linearization coefficients

The linearization coefficients are found by minimizing the expectation value of the error, due to this linearization of the drag force. This yields:

$$a_s(z)E[\dot{r}'(t,z)^2] + b_s(z)E[\dot{r}'(t,z)] = E[\dot{r}'(t,z)\dot{r}(t,z)|\dot{r}(t,z)|] \qquad (6.09)$$

$$a_s(z)E[\dot{r}'(t,z)] + b_s(z) = E[\dot{r}(t,z)|\dot{r}(t,z)|] \qquad (6.10)$$

The result is:

$$a_s(z) = \frac{4\sigma_{i'}}{\sqrt{2\pi}}\exp\{\frac{-v(z)^2}{2\sigma_{i'}^2}\} + 4v(z)\,\mathrm{erf}\{\frac{v(z)}{\sigma_{i'}}\} \qquad (6.11)$$

$$b_s(z) = \frac{2\sigma_{i'}v(z)}{\sqrt{2\pi}}\exp\{\frac{-v(z)^2}{2\sigma_{i'}^2}\} + 2\{v(z)^2+\sigma_{i'}^2\}\,\mathrm{erf}\{\frac{v(z)}{\sigma_{i'}}\} \qquad (6.12)$$

where:

$$\mathrm{erf}(x) = \frac{1}{\sqrt{2\pi}}\int_0^x \exp\{\frac{-y^2}{2}\}dy$$

$\sigma_{i'}$ = standard deviation of the relative velocity due to waves

$v(z)$ = current

If there is no current, expressions (6.11) and (6.12) reduce to:

$$a_\varsigma(z) = \frac{4\sigma_{i'}}{\sqrt{2\pi}} \qquad (6.13)$$

$$b_\varsigma(z) = 0 \qquad (6.14)$$

6.3 ONE LEG MODEL

In this paragraph, the application of the linearization coefficients is demonstrated for the one leg model, as a preparation for the complete three-degree-of-freedom-system. The mathematic description to account for the phase differences between the water loads on the legs is already introduced here. The equation of motion for the one leg model is given by:

$$M_\ell \ddot{x}(t) + c_{ss}\,\dot{x}(t) + k_c\,x(t) = F(t) \qquad (6.15)$$

where:

$x(t)$ = deck displacement

$\dot{x}(t)$ = deck velocity

$\ddot{x}(t)$ = deck acceleration

M_ℓ = dynamic deck mass for one leg, including the mass contribution from the leg, but no added water mass

c_{ss} = structural and soil damping

k_c = combined leg stiffness

$F(t)$ = water load transfered to lower guide level

In section 5.4.2, an expression was found for the water load on the one leg model shown in figure 6.1.

Using a slightly different notation, this expression becomes:

$$F(t) = \int_0^d [C_1 \dot{r}(t,x,z)|\dot{r}(t,x,z)| + C_2'\ddot{r}(t,x,z) + C_2'\ddot{u}(t,x,z)]g(z)dz \qquad (6.16)$$

where:

C_1 = modified drag coefficient

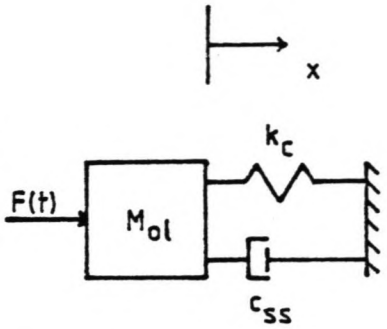

Figure 6.1: Dynamic one leg model

C_2', C_2'' = modified inertia coefficients

$\dot{r}(t,x,z)$ = relative velocity

$\ddot{r}(t,x,z)$ = relative acceleration

$\ddot{u}(t,x,z)$ = fluid acceleration

$$g(z) = \frac{z}{l} \qquad (6.17)$$

l = free leg length

The wave induced fluid velocity and thus the relative velocity are written as function of x, in order to allow the introduction of phase differences between the water loads on the legs in the analysis of the complete platform. The fluid velocity and fluid acceleration, due to sinusoidal wave i, are given by:

$$\dot{u}_i(t,x,z) = \hat{u}_i(z)\sin(\omega_i t - k_i x) \qquad (6.18)$$

$$\ddot{u}_i(t,x,z) = \hat{u}_i(z)\omega_i\cos(\omega_i t - k_i x) \qquad (6.19)$$

where:

$\dot{u}_i(t,x,z)$ = fluid velocity

$\ddot{u}_i(t,x,z)$ = fluid acceleration

$\hat{u}_i(z)$ = amplitude of fluid velocity

ω_i = angular wave frequency

k_i = wave number

Using trigonometry to rewrite these expressions and introducing the linearization coefficient in the drag force allows the water load, due to wave i, to be split as follows:

$$F_i(t) = F_i + \hat{F}_{si}\sin(\omega_i t) + \hat{F}_{ci}\cos(\omega_i t) + M_A\ddot{x}(1,t) + c_{HYD}\dot{x}(1,t) \quad (6.20)$$

where:

$$F_i = \int_0^d C_1 b(z)g(z)dz \quad (6.21)$$

$$\hat{F}_{si} = \int_0^d \{C_1 a(z)\cos(k_i x) + C_2\omega_i\sin(k_i x)\}\hat{u}_i(z)g(z)dz \quad (6.22)$$

$$\hat{F}_{ci} = \int_0^d \{-C_1 a(z)\sin(k_i x) + C_2\omega_i\cos(k_i x)\}\hat{u}_i(z)g(z)dz \quad (6.23)$$

$$M_A = \int_0^d C_2' h(z)g(z)dz \quad (6.24)$$

$$c_{HYD} = \int_0^d C_1 a(z)h(z)g(z)dz \quad (6.25)$$

M_A = added water mass

c_{HYD} = hydrodynamic damping

$C_2 = C_2' + C_2''$

The first term on the right of equation (6.20) is the constant part of the water load, while the second and the third term are the harmonic components of the water load.

The last two term respectively represent the acceleration force due to the added water mass and the damping force due to the hydrodynamic damping. They can be transfered to the left side of the equation of motion, which then becomes:

$$M_{EQ}\ddot{x}(t) + c_{EQ}\dot{x}(t) + k_c x(t) = F_i + \hat{F}_{si}\sin(\omega_i t) + F_{ci}\cos(\omega_i t) \qquad (6.26)$$

where:

$$M_{EQ} = M_l + M_A \qquad (6.27)$$

$$c_{EQ} = c_{SS} + c_{HYD} \qquad (6.28)$$

Now the left side of equation (6.26) contains all deck motions, while all fluid motions are on the right side. The solution of this equation is:

$$x(t) = x_i + \hat{x}_{si}\sin(\omega_i t) + \hat{x}_{ci}\cos(\omega_i t) \qquad (6.29)$$

where:

$$x_i = \frac{F_i}{k_c} \qquad (6.30)$$

$$\hat{x}_{si} = \frac{(k_c - M_{EQ}\omega_i^2)\hat{F}_{si} + c_{EQ}\omega_i\hat{F}_{ci}}{(k_c - M_{EQ}\omega_i^2)^2 + c_{EQ}^2\omega_i^2} \qquad (6.31)$$

$$\hat{x}_{ci} = \frac{-c_{EQ}\omega_i\hat{F}_{si} + (k_c - M_{EQ}\omega_i^2)\hat{F}_{ci}}{(k_c - M_{EQ}\omega_i^2)^2 + c_{EQ}^2\omega_i^2} \qquad (6.32)$$

These expressions complete the solution of the equation of motion. As can be seen, the water loads depend on the platform motions, and therefore the correct values of motions and loads can only be found by means of an iteration procedure, which is discussed in paragraph 6.6.

6.4 PLATFORM

The equation of motion of the complete platform and the solution of this equation are both based on the results from the previous paragraph. The three-degrees-of-freedom model is shown in figure 6.2.

The equation of motion of this system is given by:

$$M\ddot{X} + C\dot{X} + KX = F \qquad (6.33)$$

where:

$$X = \begin{bmatrix} x(t) \\ y(t) \\ \phi(t) \end{bmatrix}, \quad \dot{X} = \begin{bmatrix} \dot{x}(t) \\ \dot{y}(t) \\ \dot{\phi}(t) \end{bmatrix}, \quad \ddot{X} = \begin{bmatrix} \ddot{x}(t) \\ \ddot{y}(t) \\ \ddot{\phi}(t) \end{bmatrix}$$

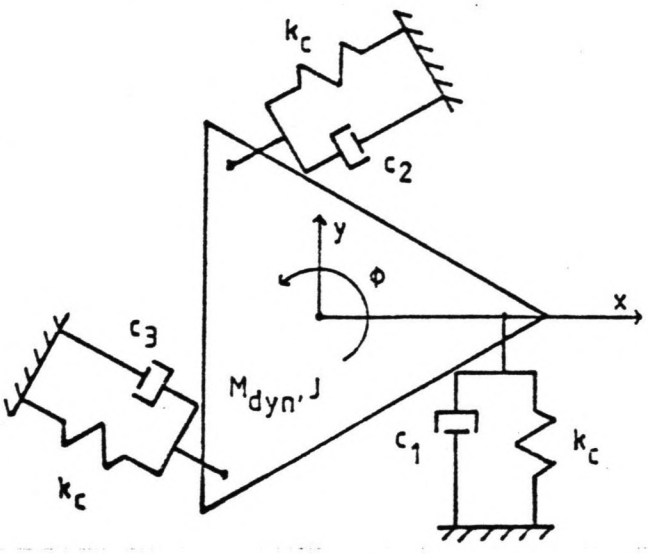

Figure 6.2: Dynamic platform model

$$M = \begin{bmatrix} M_{DYN} + \sum_{i_l=1}^{n_l} M_{A,i_l} & 0 & 0 \\ 0 & M_{DYN} + \sum_{i_l=1}^{n_l} M_{A,i_l} & 0 \\ 0 & 0 & J \end{bmatrix}$$

$$C = \begin{bmatrix} \sum_{i_\ell=1}^{n_\ell} c_{x,i_\ell} & 0 & -\sum_{i_\ell=1}^{n_\ell} c_{x,i_\ell} y_{i_\ell} \\ 0 & \sum_{i_\ell=1}^{n_\ell} c_{y,i_\ell} & \sum_{i_\ell=1}^{n_\ell} c_{y,i_\ell} x_{i_\ell} \\ -\sum_{i_\ell=1}^{n_\ell} c_{x,i_\ell} y_{i_\ell} & \sum_{i_\ell=1}^{n_\ell} c_{y,i_\ell} x_{i_\ell} & \sum_{i_\ell=1}^{n_\ell} [c_{x,i_\ell} y_{i_\ell}^2 + c_{y,i_\ell} x_{i_\ell}^2] \end{bmatrix}$$

$$K = \begin{bmatrix} \sum_{i_\ell=1}^{n_\ell} k_c & 0 & -\sum_{i_\ell=1}^{n_\ell} k_c y_{i_\ell} \\ 0 & \sum_{i_\ell=1}^{n_\ell} k_c & \sum_{i_\ell=1}^{n_\ell} k_c x_{i_\ell} \\ -\sum_{i_\ell=1}^{n_\ell} k_c y_{i_\ell} & \sum_{i_\ell=1}^{n_\ell} k_c x_{i_\ell} & \sum_{i_\ell=1}^{n_\ell} k_c [y_{i_\ell}^2 + x_{i_\ell}^2] \end{bmatrix}$$

c_{i_ℓ} = $c_{SS,i_\ell} + c_{HYD,i_\ell}$

M_{DYN} = dynamic deck mass

M_{A,i_ℓ} = added water mass per leg

J = mass moment of inertia of the platform

i_ℓ = leg number

n_ℓ = total number of legs

c_{SS,i_ℓ} = structural and soil damping of one leg

c_{HYD,i_ℓ} = hydrodynamic damping of one leg

k_c = combined leg stiffness

x_{i_ℓ} = x-coordinate of leg i_ℓ

y_{i_ℓ} = y-coordinate of leg i_ℓ

The load vector, F, is computed by using the expression found for the linearized water loads on the one leg model. Again, the linearized water load due to wave i consists of one constant term and two harmonic terms:

$$F = F_i + F_{si} \sin(\omega_i t) + F_{ci} \cos(\omega_i t) \qquad (6.34)$$

Expressed in terms of the water loads on the legs, the constant part of the load vector becomes:

$$F_i = \begin{bmatrix} \sum_{i_\ell=1}^{n_\ell} F_{x,i,i_\ell} \\ \sum_{i_\ell=1}^{n_\ell} F_{y,i,i_\ell} \\ \sum_{i_\ell=1}^{n_\ell} [F_{y,i,i_\ell} x_{i_\ell} - F_{x,i,i_\ell} y_{i_\ell}] \end{bmatrix}$$

where:

F_{x,i,i_ℓ} = constant load in x-direction on leg i_ℓ

F_{y,i,i_ℓ} = constant load in y-direction on leg i_ℓ

The expressions for the amplitudes of the sine and cosine components of the load vector, respectively F and F , are identical. Using the index of the sine component, the expression for these amplitudes is given by:

$$F_{si} = \begin{bmatrix} \sum_{i_\ell=1}^{n_\ell} \hat{F}_{x,si,i_\ell} \\ \sum_{i_\ell=1}^{n_\ell} \hat{F}_{y,si,i_\ell} \\ \sum_{i_\ell=1}^{n_\ell} [\hat{F}_{y,si,i_\ell} x_{i_\ell} - \hat{F}_{x,si,i_\ell} y_{i_\ell}] \end{bmatrix}$$

where:

$\hat{F}_{x,si,i_\ell}$ = sine component of the load in x-direction on leg 1_ℓ

$\hat{F}_{y,si,i_\ell}$ = sine component of the load in y-direction on leg i_ℓ

In vector notation, the solution of the equation of motion becomes:

$$X(t) = X_i + X_{si} \sin(\omega_i t) + X_{ci} \cos(\omega_i t) \qquad (6.35)$$

where:

$$X_i = \frac{F_i}{K} \tag{6.36}$$

$$X_{si} = \frac{(K-M\omega_i^2)F_{si} + C\omega_i F_{ci}}{(K-M\omega_i^2)^2 + C^2\omega_i^2} \tag{6.37}$$

$$X_{ci} = \frac{-C\omega_i F_{si} + (K-M\omega_i^2)F_{ci}}{(K-M\omega_i^2)^2 + C^2\omega_i^2} \tag{6.38}$$

6.5 LOADING DIRECTION

For loading directions different from the x-direction, a new coodinate system with the axes xx and yy is introduced. As shown in figure 6.3, the xx-direction is equal to the main direction of wave propagation, which was defined in paragraph 3.4. The two coordinate systems are linked by the angle of wave propagation, ϕ, of which the definition is shown in figure 6.3. The coordinate conversion is performred as follows:

$$xx = x\cos(\phi) + y\sin(\phi) \tag{6.39}$$

$$yy = x\sin(\phi) - y\cos(\phi) \tag{6.40}$$

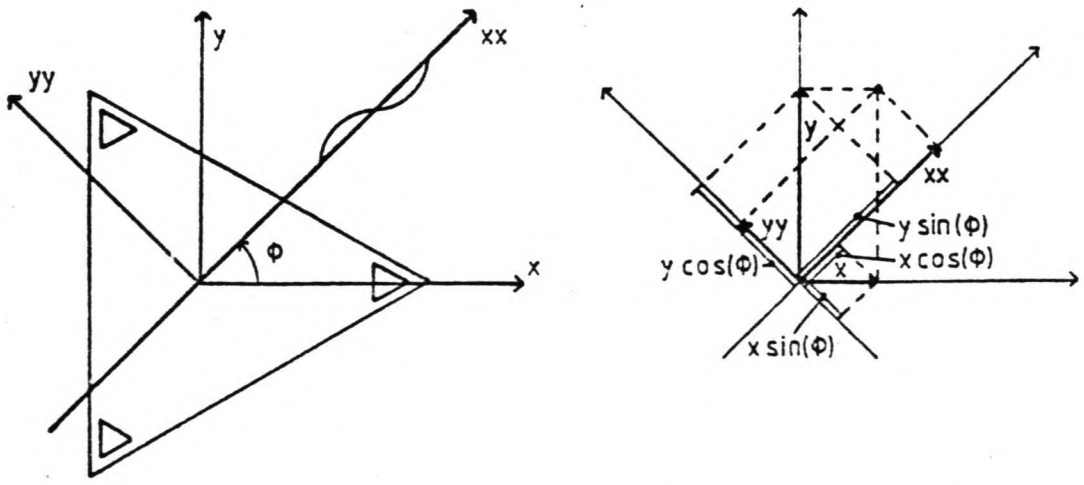

Figure 6.3: Conversion of coordinate system

The coordinate system xx,yy is the reference for all loads and motions. All results will be presented with respect to this coordinate system.

For the dynamic response analysis of the platform, the mass, stiffness and damping properties have to be related to the new reference as well. By definition, the dynamic deck mass is independent of the coordinate system. The gravity centre of the platform is the origin of both coordinate syustems, so the mass moment of inertia of the platform also remains unchanged.

Since it is assumed that the combined leg stiffness is constant for all directions, it can easily be seen that the stiffness properties of the platform are not affected by the coordinate change. The expression for the rotational stiffness of the platform, k_{ROT}, is valid for all loading directions:

$$k_{ROT} = \sum_{i_l=1}^{n_l} r_{i_l}^2 k_c \qquad (6.41)$$

where:

k_{ROT} = rotational stiffness of the platform

k_c = combined leg stiffness

r_{i_l} = distance between leg i_l and the gravity centre of the platform

This independence of the loading direction is also true for structural and soil damping, but not for hydrodynamic damping, which is computed using the direction-dependent drag coefficient. Therefore, the computed values of hydrodynamic damping refer to the loading direction considered, as is the case for load and motion values.

It should be noted that the added mass is also direction-dependent, since the added mass coefficient is direction-dependent. For this reason, the added mass and the natural periods of the platform are computed separately for each loading direction. Due to the symmetry of the legs, this effect does not occur at the Russian jack-up.

Being wind driven, the direction of waves probably coincide with the direction of the wind-driven current. This need not be the case for tidal current, which originates from a completely different source. If the directions of waves and current do not coincide, the resulting horizontal fluid velocity will have a direction varying in time. In the frequency domain this problem is handled by splitting the current into a component along the direction of wave propagation, xx, and a component

orthogonal to this direction, yy. The linearization procedure is carried out for both directions.

6.6 ITERATION PROCEDURE

6.6.1 General

Due to the fact that the water loads and the hydrodynamic damping are dependent of the platform motions, the steady state motions have to be computed by means of an iteration procedure, of which the general flowchart is shown in figure 6.4.

As stated in section 5.4.5, the integrals with respect to the vertical coordinate, z, are replaced by summations in the numerical model and for this purpose, the legs are divided into sections. Due to waves, the water depth is constantly changing. In the frequency domain, this effect cannot be included and the division of the legs into sections is only carried out once, at the start of the computations.

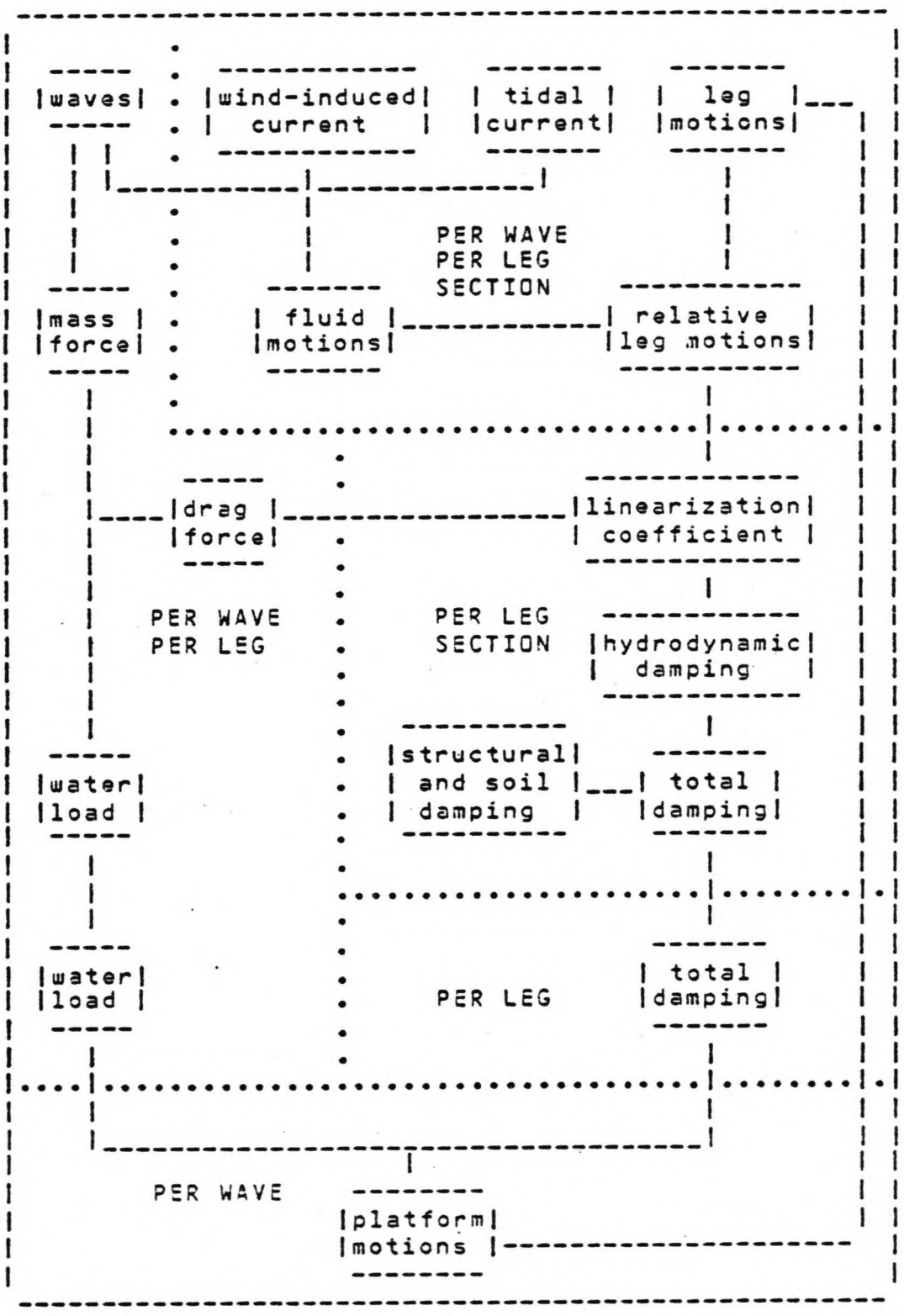

Figure 6.4: Frequency domain iteration flowchart

This iteration process is continued until the computed amplitude of the deck motions remains constant.

In the next sections, some details of the numerical analysis of several cases are highlighted.

6.6.2 Deterministic analysis

In the case of a regular wave, the deterministic linearization coefficient from section 6.2.2 is used, for which the amplitude of the relative velocity is needed. Per leg section this amplitude is found in the following way:

$$\hat{r}(z) = \sqrt{(\hat{u}_s(z)+h(z)\hat{\dot{x}}_s)^2 + (\hat{u}_c(z)+h(z)\hat{\dot{x}}_c)^2} \qquad (6.42)$$

where:

$\hat{r}(z)$ = relative velocity

$\hat{u}_s(z)$ = sine amplitude of fluid velocity

$\hat{u}_c(z)$ = cosine amplitude of fluid velocity

$\hat{\dot{x}}_s$ = sine amplitude of deck velocity

$\hat{\dot{x}}_c$ = cosine amplitude of deck velocity

$h(z)$ = dimensionless static leg displacement

After the iteration proces is completed, the amplitudes of the deck displacement and the water loads, respectively xx and F , are computed by combining the sine and cosine components:

$$\hat{x} = \sqrt{\hat{x}_s^2 + \hat{x}_c^2} \qquad (6.43)$$

$$\hat{F} = \sqrt{\hat{F}_{x,s}^2 + \hat{F}_{x,c}^2} \qquad (6.44)$$

6.6.3 Wave spectrum

As already outlined in chapter 3, the wave spectrum used for the stochastic description of the sea surface, is transformed to a number of sinusoidal waves. In frequency domain analysis, water loads and platform motions are computed for each of these waves, while the linearization coefficient and the hydrodynamic damping are computed for the complete spectrum. This is also shown in the iteration flowchart (see figure 6.4).

The stochastic linearization coefficient contains the standard deviation of the relative velocity, which is given by:

$$\sigma_{\dot{r}_i}(z) = \sum_{i=1}^{n} \hat{\dot{r}}_i(z)^2 / 2 \qquad (6.45)$$

where:

$\sigma_{\dot{r}_i}(z)$ = standard deviation of relative velocity

i = number of wave

n = total number of waves

$\hat{\dot{r}}_i(z)$ = relative velocity due to wave i

The expression for the relative velocity due to wave i is identical to the expression for the relative velocity in the case of a regular wave:

$$\hat{r}_i(z) = \sqrt{(\hat{u}_{si}(z)+h(z)\hat{\dot{x}}_{si})^2 (\hat{u}_{ci}(z)+h(z)\hat{\dot{x}}_{ci})^2} \qquad (6.46)$$

At the end of the iteration procedure, the amplitudes of the deck displacement and water load, respectively $\hat{x}_i$ and $\hat{F}_{xx,i}$, for each of the waves i representing a spectrum section, are given by:

$$\hat{x}_i = \sqrt{\hat{x}_{si}^2 + \hat{x}_{ci}^2} \qquad (6.47)$$

$$\hat{F}_{xx,i} = \sqrt{\hat{F}_{xx,si}^2 + \hat{F}_{xx,ci}^2} \qquad (6.48)$$

As a result of their stochastic nature, the overall deck motion and water load are represented by their standard deviations:

$$\sigma_{xx} = \sqrt{\sum_{i=1}^{n} \hat{x}_i^2 / 2} \qquad (6.49)$$

$$\sigma_{F_{xx}} = \sqrt{\sum_{i=1}^{n} \hat{F}_{xx,i}^2 / 2} \qquad (6.50)$$

where:

σ_{xx} = standard deviation of deck motion

$\sigma_{F_{xx}}$ = standard deviation of water load

6.6.4 Dynamic Amplification Factor

In order to obtain a dimensionless frequency characteristic of the platform in the case of a wave spectrum, the Dynamic Amplification Factor (D.A.F.) is introduced. The D.A.F. is defined as the ratio between the dynamic motion amplitude, $\hat{xx}_i$, due to a load with amplitude $\hat{F}_{xx,i}$, and the static deflection, due to a static load, $F\hat{x}_{x,i}$, of the same magnitude:

$$D.A.F. = \frac{\hat{xx}_i k}{F\hat{x}_{x,i}} \qquad (6.51)$$

where:

k = stiffness for the motion mode considered

For a single_degree-of-freedom system, the D.A.F. is computed by means of the following expression:

$$D.A.F. = \frac{1}{\sqrt{(1-(\frac{\omega}{\omega_n})^2)+4\zeta^2(\frac{\omega}{\omega_n})^2)}} \qquad (6.52)$$

where:

ω = angular frequency

ω_n = natural frequency

ζ = damping percentage

The D.A.F. has been plotted in figure 6.5 for several damping values.

Theoretically, the behaviour of the D.A.F. is as follows. If the excitation frequency is very low, the platform motions are quasi-static and the D.A.F. is equal to 1. For excitation frequencies near the natural frequency of the platform, the motions become severe and the D.A.F. is much greater than 1. If there is no damping, the D.A.F. has an asymptote at the natural frequency. For increasing values of the excitation frequency, the D.A.F. asymptotically reaches 0. This is due to the increasing influence of the platform inertia in the upper frequency range.

FIG. 6.5: DYNAMIC AMPLIFICATION FACTOR FOR SEVERAL DAMPING VALUES

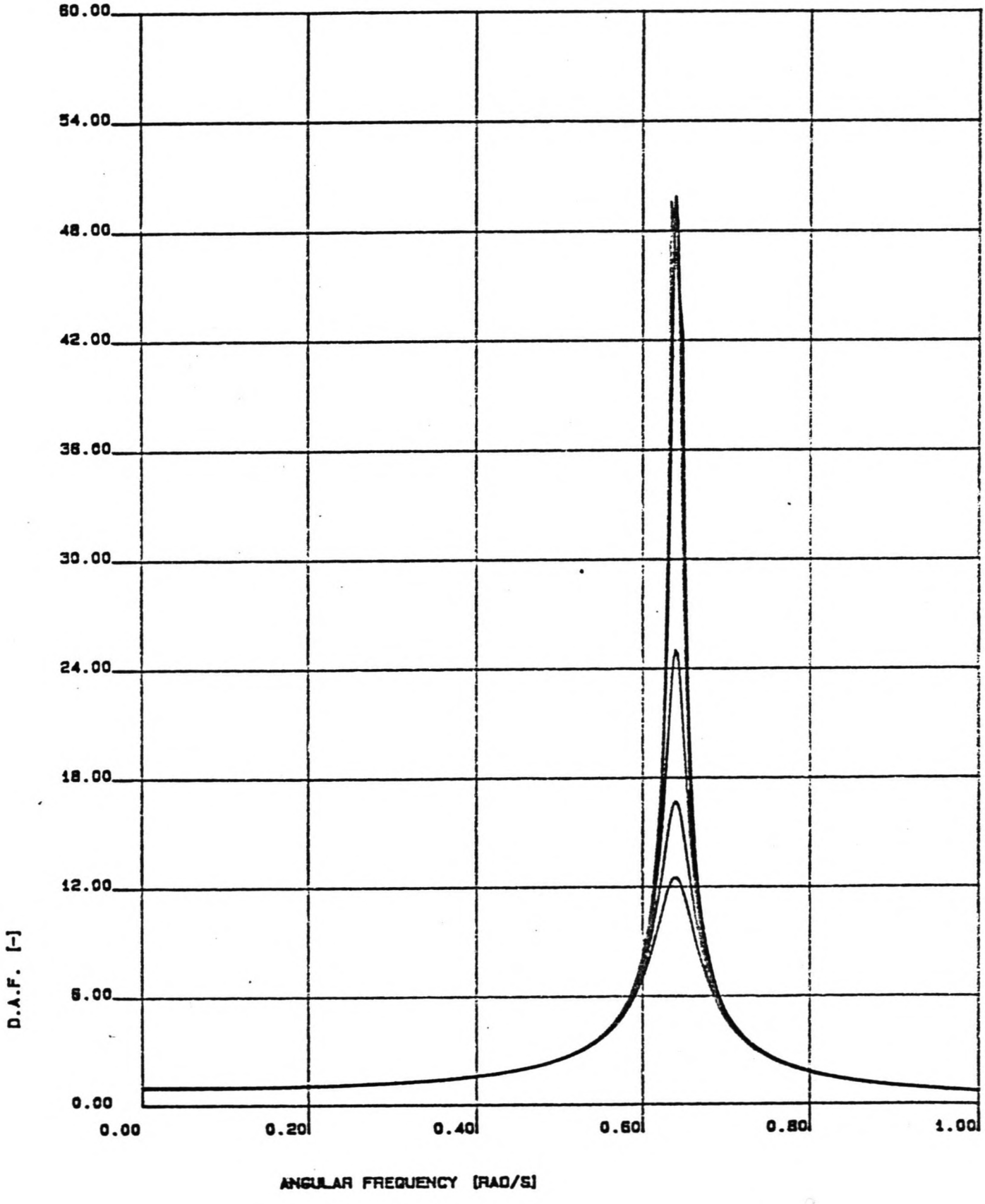

6.7 DIRECTIONAL WAVE SPREADING

As already mentioned in paragraph 3.4, the directional spreading of the wave energy is accounted for by means of a dimensionless wave spreading factor, $D(\phi)$:

$$D(\phi) = \frac{2}{\pi} \cos^2(\phi) \qquad (6.53)$$

where:

ϕ = wave direction with respect to the main wave direction

$D(\phi)$ = spreading factor

In frequency domain analysis, wave spreading is included by means of the following procedure. First, a complete motion computation is performed for a number of directions within the semicircle around the main wave direction. In this study, the directions are chosen at constant intervals of 15 degrees. The resulting 13 directions are shown in figure 6.6, together with the values of the spreading factor.

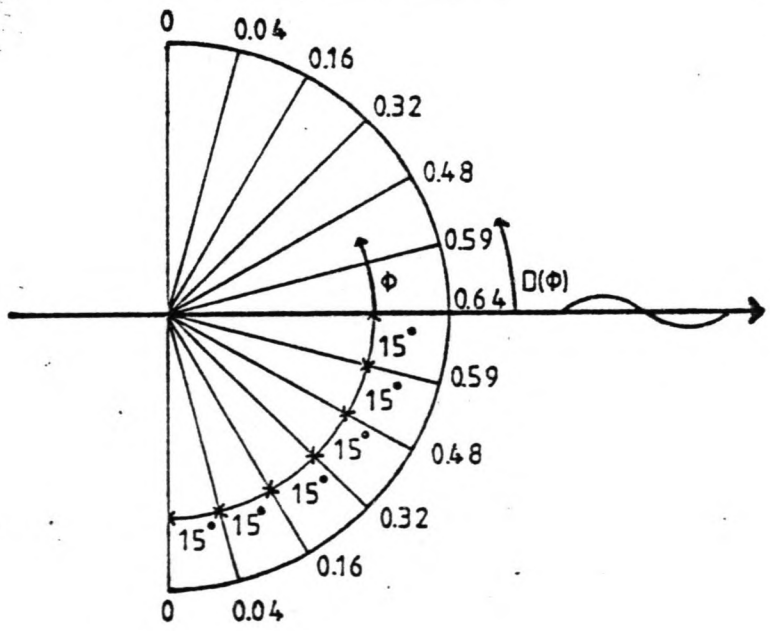

Figure 6.6: Wave spreading factor

For each of the directions, the complete iteration procedure

is performed, assuming that all waves propagate in the direction considered. Finally, the result of this operation consists of 13 values of each of the following parameters:

$xx(\phi)$ = mean deck displacement

$\sigma_{xx}(\phi)$ = standard deviation of deck motion

$F_{xx}(\phi)$ = mean water load

$\sigma_{F_{xx}}(\phi)$ = standard deviation of water load

$\xi_{HYD,xx}(\phi)$ = hydrodynamic damping percentage

It should be noted that each of the 13 values of one of the above parameters belongs to a different wave direction, and all of them refer to that direction.

The 13 values of a parameter are multiplied by the directional spreading factor, before an integration with respect to ϕ is carried out. For parameter $P(\phi)$, the value including the effect of directional wave spreading is now given by:

$$P' = \{ \int_{-\pi/2}^{+\pi/2} P(\phi)^n D(\phi) d\phi \}^{-n} \qquad (6.54)$$

where:

P' = parameter value including directional wave spreading

In this general expression, the power n is determined by the fact that $D(\phi)$ is related to the transport of wave energy, and therefore should be applied to energy- or variance-related parameters, before performing the above integration. This means that n = 2 for the standard deviations, in order to obtain variances, which are related linearly to energy. Due to the linear relationship between damping values and damping energy, the hydrodynamic damping values need not be squared and thus n = 1.

At first sight, it may seem strange to account for directional spreading in the case of mean values of deck motion and water load, since they are governed by current, which shows no directional spreading. Nevertheless, as a result of the non-linearity of the drag force in Morison's equation, the mean values are influenced by the waves and thus by the direction of wave propagation.

In a general way, this is a physical justification for the inclusion of wave spreading in the computation of mean displace-

ment and load values, in a general sence. However, the application the energy spreading factor, $D(\phi)$, in particular, is not justified by this, since the mean displacement and water load are not related to the transference of energy, as is the case for the other parameters listed above. Due to the lack of empirical information about this subject, it is assumed that $n = 1$ for the mean values.

6.8 COMPUTER PROGRAM JACQUELIN

6.8.1 General

The frequency domain theory discussed in this chapter has been implemented in the computer program Jacquelin (JACk-Up LINearization method). The program is written in Fortran 77 and has been tested on the Vax 11/750 from Digital. It computes the loads on and the motions of a jack-up platform in elevated condition, due to waves and current. Hydrodynamic damping percentages are also computed. The platform legs must be of the lattice type.

The computer program has a number of options, concerning platform configuration, deck elevation, sea states and currents. They are best described by the listing of input variables, as presented in the next section.

6.8.2 Input

All input variables of the computer program Jacquelin are listed in table 6.1.

gravity acceleration [m/s^2]			
pontoon mass [kg]	leg mass per unit length [kg/m]	mass moment of inertia of the pontoon [kgm^2]	
leg length [m]	free leg length [m]	equivalent leg diameter [m]	number of leg sections [-]
rotational leg-bottom stiffness [Nm/rad]	rotational leg-hull stiffness [Nm/rad]	reduced leg stiffness [Nm^2]	
structural and soil damping [%]			
number of legs [-]			
per leg:			
x-coordinate [m]	y-coordinate [m]		
24 values of			
equivalent drag coefficient [-]	equivalent mass coefficient [-]		
water density [kg/m^3]	water depth [m]		
switch : 0 = regular wave : 1 = JONSWAP spectrum			
number of spectrum sections [-]	lower boundary [rad/s]	upper boundary [rad/s]	peak enhancement factor [-]

(switch = 0, per regular wave:)			
number of regular waves [-]			
wave period [s]	wave height [m]	main direction [°]	
(switch = 1, per spectrum:)			
number of spectra [-]			
peak period [s]	significant wave height [m]	main direction [°]	
tidal current [m/s]	direction of tide [°]	wind speed at 10 m above sea level [m/s]	wind direction [°]
termination criterion [-]			

Table 6.1: Input for computer program Jacquelin

Most of the options are well described by table 6.1. In addition, the following should be noted:

a. The origin of the coordinate system, used for the positioning of the legs, is defined as the gravity centre of the legs. Consequently, an eccentric grayty centre can be included by changing the coordinates of the legs.

b. Spectrum sections with wave heights less than 1 mm are neglected for the computation of the platform response and the number of spectrum sections is reduced accordingly. This is done in order to save computer time.

c. All loading directions must be in the range of 0^{o} to 345^{o} , with steps of 15^{o} . The 24 values of the drag and mass coefficients also apply to tnese directions.

d. The directions of wave propagation, tidal current and wind-driven current are independent.

e. The termination criterion is a relative criterion. In other words, the iteration procedure is monitored by means of the relative differences between two iteration loops. To be more specific, this monitoring consists of comparing the standard deviation of the deck displacement in the last two iteration loops.

6.8.3 Output

The output of the computer program Jacquelin consists of all input parameters, the regular wave or spectrum parameters and the actual output parameters listed in table 6.3. Apart from the input, the following parameters are computed per spectrum:

a. Test wave height for the purpose of checking the numerical representation of the wave spectrum.

b. Number of spectrum sections with wave heights greater than 1 mm.

c. Natural period of platform translation.

d. Natural period of platform rotation.

e. Mean value of water load.

f. Standard deviation of water load.

g. Mean value of deck displacement.

h. Standard deviation of deck displacement.

i. Hydrodynamic damping percentage.

The water loads, deck displacements and hydrodynamic damping are computed for all three motion modes, with and without the effect of directional wave spreading.

The computer program is capable of generating plots of the frequency characteristics of the water loads and the platform motions and of the dynamic amplification factor for translations and rotations per loading directions. It should be noted that these plots include the effect of non-linear interaction between the frequency intervals, which is accounted for by means of the linearization coefficient. The influence of hydrodynamic damping is included as well.

7 TIME DOMAIN

7.1 INTRODUCTION

In time domain analysis, the platform response is simulated numerically with a computer. Since the time consumption of numerical simulations is very large, the following restrictions are made for the time domain analysis method:

a. Only one translational mode of the platform is considered.

b. Directional spreading of the waves is neglected.

The method consists of solving the equation of motion for a number of time steps. This procedure is applicable to the stochastic model as well as the deterministic model and is briefly discussed in the next paragraph.

In the case of a stochastic model, the motion and load values resulting from a time series can be transformed to statistic distribution functions and probabilities of exceedance, which is of particular importance for the purpose of jack-up design. The statistical procedures are discussed in paragraph 7.3.

During this study of jack-up dynamics, the computer program Jacques has been developed for time domain analysis of the parameters discussed in this chapter. A listing of the input and output of this program is given in paragraph 7.4.

7.2 GENERAL PROCEDURE

The time domain analysis procedure will be outlined for the spectral representation of the sea state. In paragraph 5.4, the equation of motion for platform translations was written as:

$$M_{DYN}\,\ddot{x}(t) + c_{SS,TR}\,\dot{x}(t) + k_{TR}\,x(t) = F(t) \qquad (7.01)$$

where:

M_{DYN} = dynamic deck mass

$c_{SS,TR}$ = structural and soil damping of translation

k_{TR} = translational stiffness of the platform

$x(t)$ = deck displacement

$\dot{x}(t)$ = deck velocity

$\ddot{x}(t)$ = deck acceleration

$F(t)$ = water load on the complete platform

For time domain computations it is more convenient to write the equation of motion as:

$$\ddot{x}(t) = \frac{F(t)-c_{SS,TR}\,\dot{x}(t)-k_{TR}\,x(t)}{M_{DYN}} \qquad (7.02)$$

The water load on the complete platform is found by summation of the water loads per leg:

$$F(t) = \sum_{i_\ell=1}^{n_\ell} F_{i_\ell}(t) \qquad (7.03)$$

where:

i_ℓ = leg number

n_ℓ = total number of legs

$F_{i_\ell}(t)$ = water load on leg i_ℓ

The water load per leg is given by the Morison equation:

$$F_{i_\ell}(t) = \int_0^d [C_1\{\dot{u}_{i_\ell}(t,z)-h(z)\dot{x}(t)\}|\dot{u}_{i_\ell}(t,z)-h(z)\dot{x}(t)| + C_2'\{\ddot{u}_{i_\ell}(t,z)-h(z)\ddot{x}(t)\} + C_2''\ddot{u}_{i_\ell}(t,z)]g(z)dz \qquad (7.04)$$

where:

C_1 = modified drag coefficient

C_2', C_2'' = modified mass coefficients

$\dot{u}_{i_\ell}(t,z)$ = fluid velocity at leg i_ℓ

$\ddot{u}_{i_\ell}(t,z)$ = fluid acceleration at leg i_ℓ

$h(z)$ = dimensionless leg deflection

For the purpose of simulating the platform response the required simulation time is divided into a number of time steps, Δt. For each time step, i_t, a number of computations is performed. The numerical scheme of one time step will be discussed below.

As already mentioned in chapter 3, the wave spectrum is transformed to a wave train by dividing it into a number of sections, n, and superimposing the resulting sinusoidal waves with a random phase angle. For each time step, i_t, the fluid velocities and accelerations are found by a similar superposition of the individual fluid velocities and accelerations:

$$\dot{u}_{i_\ell, i_t}(z) = \sum_{i=1}^{n} \dot{u}_{i, i_\ell, i_t}(z) \qquad (7.05)$$

$$\ddot{u}_{i_\ell, i_t}(z) = \ddot{u}_{i, i_\ell, i_t}(z) \qquad (7.06)$$

where:

$\dot{u}_{i, i_\ell, i_t}(z)$ = fluid velocity at leg i_ℓ due to wave i

$\dot{u}_{i_\ell, i_t}(z)$ = fluid velocity at leg i_ℓ

$\ddot{u}_{i, i_\ell, i_t}(z)$ = fluid acceleration at leg i_ℓ due to wave i

$\ddot{u}_{i_\ell, i_t}(z)$ = fluid acceleration at leg i_ℓ

The resulting fluid velocities and accelerations at each leg are substituted into the Morison equation, together with the deck displacement and velocity computed in the previous time step, i_t-1:

$$\begin{aligned} F_{i_\ell, i_t} = \int_0^d [& C_1 \{\dot{u}_{i_\ell, i_t}(z) - h(z)\dot{x}_{i_t-1}\} \\ & * |\dot{u}_{i_\ell, i_t}(z) - h(z)\dot{x}_{i_t-1}| \\ & + C_i' \{\ddot{u}_{i_\ell, i_t}(z) - h(z)\ddot{x}_{i_t-1}\} \\ & + C_i'' \ddot{u}_{i_\ell, i_t}(z)] g(z) dz \end{aligned} \qquad (7.07)$$

This is done for all legs and addition of the results yields the overall water load:

$$F_{i_t} = \sum_{i_\ell=1}^{n_\ell} F_{i_\ell, i_t} \qquad (7.08)$$

Substitution of this water load and substitution of the deck veloctity and acceleration from the previous time step into the rewritten equation of motion yields:

$$\ddot{x}_{i_t} = \frac{F_{i_t} - c_{SS,TR}\,\dot{x}_{i_{t-1}} - k_{TR}\,x_{i_{t-1}}}{M_{DYN}} \qquad (7.09)$$

The deck velocity and displacement are found by means of the following expressions:

$$\dot{x}_{i_t} = \dot{x}_{i_{t-1}} + \ddot{x}_{i_t} * \Delta t \qquad (7.10)$$

$$x_{i_t} = x_{i_{t-1}} + \dot{x}_{i_t} * \Delta t \qquad (7.11)$$

This completes the basic computations made at each time step.

In order to get an accurate approximation of physical reality, the time steps should be small compared to the wave periods and the natural periods of the platform. Several time steps have been tested and it was found that there are no significant changes of results for more than 20 time steps per regular wave period or 20 steps per zero-crossing period of a wave spectrum. Therefore this is the ratio used for all simulations.

7.3 STATISTICAL ANALYSIS

In the case of a stochastic wave model, it is impossible to define a maximum wave height. Instead of this, during one sea state, each wave height has a probability of occurence, described by the distribution function, and a probability of exceedance. The second parameter will depend on the duration time of the sea state.

For the purpose of structural design it is of great importance to define the probability of exceedance of certain stress and strain levels. Therefore it is needed to know the distribution of these parameters and thus the distribution of the water loads and the platform motions.

Since the distribution function of the excursion of the water surface is assumed to be Gaussian, it is possible to predict the distribution function of the water loads for certain flow regimes. For this prediction it is assumed that the relationship between the surface excursion and the fluid motions is linear, or in other words, that short wave theory is a realistic description of hydrodynamics at sea. Apart from minor errors, this assumption is correct.

In the case of mass forces being dominant, the relationship between water loads and surface excursion is linear, and thus the water loads will have a Gaussian distribution, as shown in figure 7.1.

FIG. 7.1: GAUSSIAN DISTRIBUTION

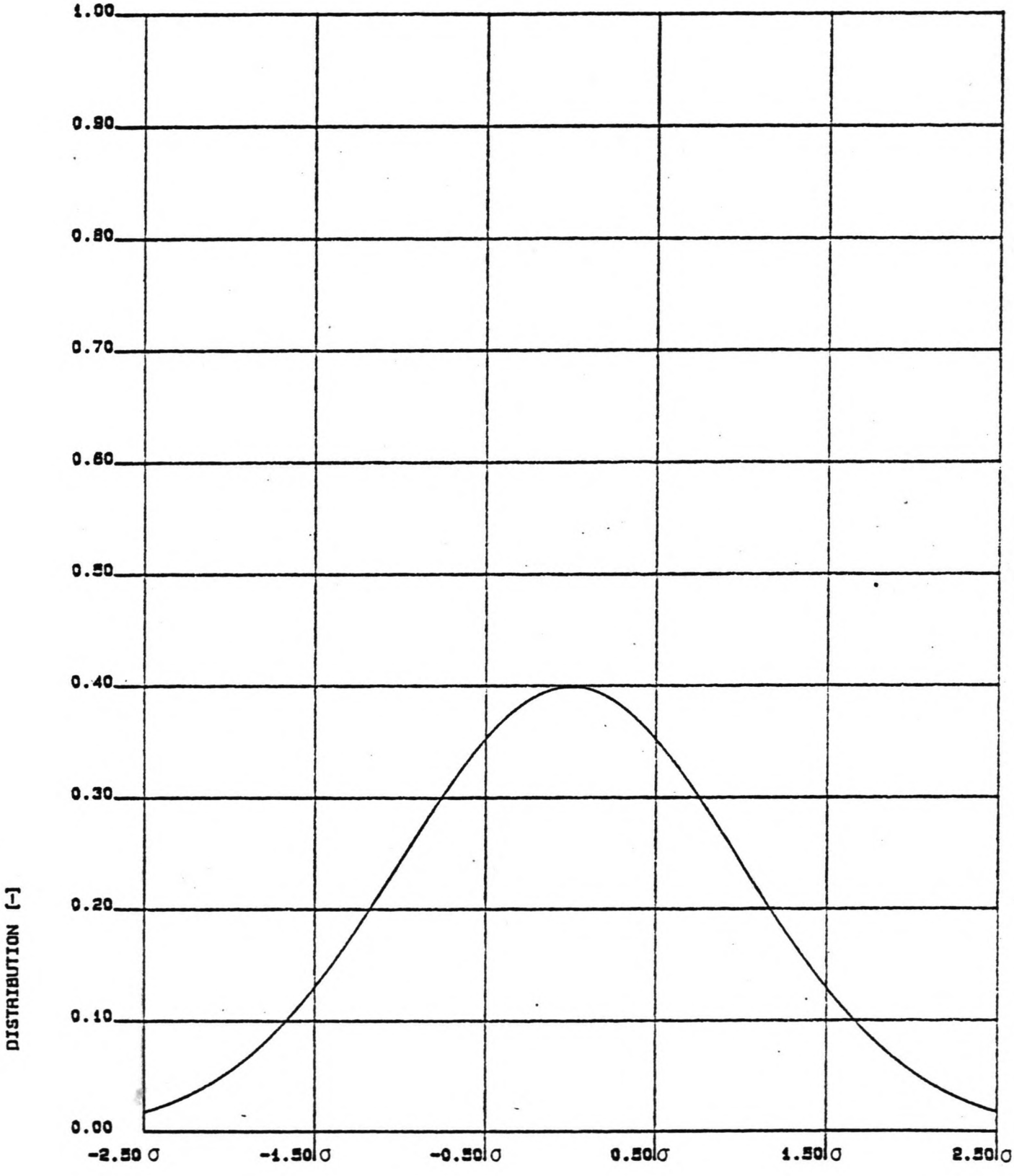

If the drag forces are dominant, the water loads are propotional to the squared surface excursion. From statistics it is known that a variable, proportional to a Gaussian variable, will have an exponential distribution function. Therefore, this is the distribution to be expected for the drag forces.

The general expression for the exponential distribution is:

$$p(X) = \frac{a}{2\sigma_x} \exp\{-a\frac{|X-\mu_x|}{\sigma_x}\} \qquad (7.12)$$

where:

$p(X)$ = probability of occurence

a = shape factor

σ_x = standard deviation

μ_x = mean value

This distribution has been plotted in figure 7.2 for values of the shape factor, a, ranging from 1.0 to 2.0 with steps of 0.1.

If drag and mass forces are of the same order of magnitude, the distribution of the water loads cannot be described by a theoretical expression.

Due to the influence of the non-linear hydrodynamic damping, the transfer function between water loads and platform motions is non-linear as well, and therefore it is not possible to predict the statistical distribution of the platform motions.

The results of a numerical simulation can be subdue to statistical analysis very easily. In the time domain computer program, the distribution functions and the probabilities of exceedance are computed for the following parameters:

a. Excursion of the water surface

b. Mass force

c. Drag force

d. Total water load

e. Deck displacement

The mean value and the standard deviation of each parameter are computed from a time series by means of the following ex-

FIG. 7.2: EXPONENTIAL DISTRIBUTION

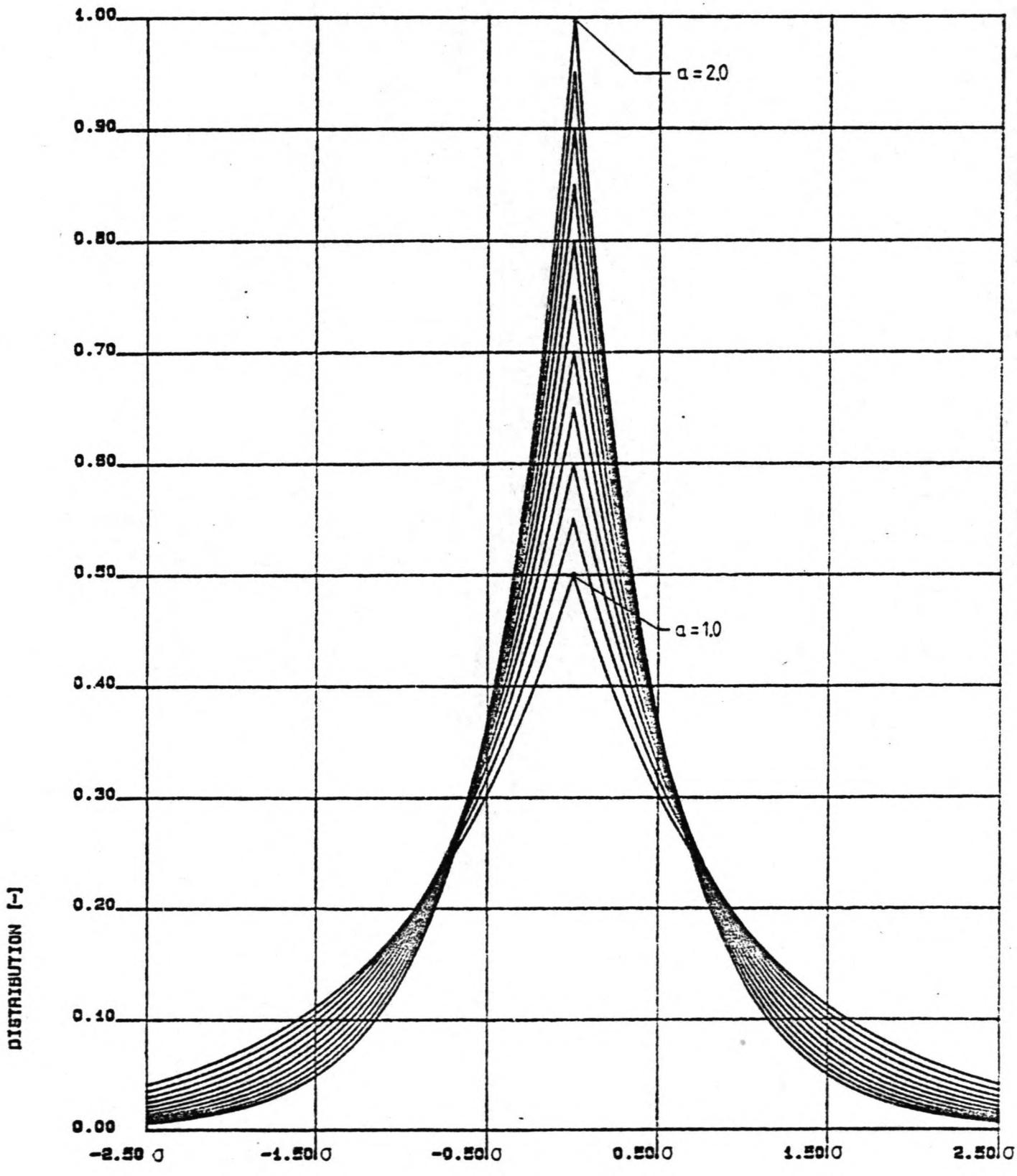

pressions:

$$\mu_p = \frac{\sum_{i_t=1}^{n_t} p_{i_t}}{n_t} \qquad (7.13)$$

$$\sigma_p = \sqrt{\frac{\sum_{i_t=1}^{n_t} (p_{i_t} - \mu_p)^2}{n_t}} \qquad (7.14)$$

where:

n_t = total number of time steps

i_t = time step considered

p_{i_t} = parameter considered

μ_p = mean value

σ_p = standard deviation

7.4 COMPUTER PROGRAM JACQUES

7.4.1 General

The time domain theory discussed in this chapter has been implemented in the computer program Jacques (JACk-Up Simulation). The program is written in Fortran 77 and has been tested on the Vax 11/750 from Digital. It computes the loads on and the motions of a jack-up platform in elevated condition, due to waves. The platform legs must be of the lattice type.

The computer program has a number of options, concerning platform configuration, deck elevation and sea states. They are best described by the listing of input variables, as presented in the next section.

7.4.2 Input

All input variables of the computer program Jacques are listed in table 7.1.

gravity acceleration [m/s^2]			
pontoon mass [kg]	leg mass per unit length [kg/m]	mass moment of inertia of the pontoon [kgm^2]	
leg length [m]	free leg length [m]	equivalent leg diameter [m]	number of leg sections [-]
rotational leg-bottom stiffness [Nm/rad]	rotational leg-hull stiffness [Nm/rad]	reduced leg stiffness [Nm^2]	
structural and soil damping [%]			
number of legs [-]			
per leg:			
x-coordinate [m]	y-coordinate [m]		
24 values of			
equivalent drag coefficient [-]	equivalent mass coefficient [-]		
water density [kg/m^3]	water depth [m]		
switch : 0 = regular wave : 1 = JONSWAP spectrum			
number of spectrum sections [-]	lower boundary [rad/s]	upper boundary [rad/s]	peak enhancement factor [-]

(switch = 0, regular wave:)			
	wave period [s]	wave height [m]	main direction [°]
(switch = 1, spectrum:)			
	peak period [s]	significant wave height [m]	main direction [°]
simulation time [s]	number of time steps per zero-crossing period [-]	estimated transient time (in zero-crossing periods) [-]	

Table 7.1: Input for computer program Jacques

Most of the options are well described by table 7.1. In addition, the following should be noted:

a. The origin of the coordinate system, used for the positioning of the legs, is defined as the gravity centre of the legs. Consequently, an eccentric grat y centre can be included by changing the coordinates of the legs.

b. Spectrum sections with wave heights less than 1 mm are ignored for the computation of the platform response and the number of spectrum sections is reduced accordingly.

c. All loading directions must be in the range of 0^{o} to 345^{o} , with steps of 15^{o} . The 24 values of the drag and mass coefficients also apply to these directions.

d. In order to obtain the statistical figures applying to the steady state motion only, it is possible to neglect an estimated transiant time for the statistic computations. The estimated transient time is measured in zero crossing periods. This option is built in to allow the comparision with the frequency results, which apply to the steady state motions of the platform.

e. The effect of the changing water depth due to the waves is included in the computation of the profiles of the relative velocity and the relative ac-

celeration. This means that complete structure velocity profiles and fluid velocity and acceleration profiles are computed at each time step.

7.4.3 Output

The output of the computer program Jacques consists of all input parameters, the regular wave or spectrum parameters and the actual output parameters listed in table 6.3. Apart from the input, the following parameters are computed per spectrum:

a. Test wave height.

b. Number of spectrum sections with wave heights greater than 1 mm.

c. Natural period of platform translation.

d. Standard deviation of water load.

e. Maximum amplitude of water load.

f. Standard deviation of deck displacement.

g. Maximum amplitude of deck displacement.

The water loads, deck displacements and hydrodynamic damping are computed for the translational mode, while the effect of directional wave spreading is neglected.

The computer program is capable of generating plots of the distribution function and the probabilities of exceedance of the following parameters:

a. Excursion of water surface

b. Drag force

c. Mass force

d. Total water load

e. Deck displacement

All plotted parameters are presented in a dimensionless form.

8 RESULTS AND CONCLUSIONS

8.1 INTRODUCTION

In this chapter, the results from the dynamic response analysis of the Russian jack-up platform, the Kolskaya, located at the Forties field on the North Sea, will be discussed.

The results from time domain analysis of the three-legged platform loaded by a JONSWAP spectrum are presented in the next paragraph. This case will serve as a basis for several comparisons made in this chapter and will be called the reference case for convenience.

The influence of structural and soil damping on the overall water loads and motions as well as on their distributions is examined in paragraph 8.3.

The one leg model is handled in paragraph 4 of this chapter, while the results of deterministic analysis are discussed in paragraph 5.

In paragraph 6 of this chapter, a comparison is made between the results from frequency domain analysis and time domain analysis. The frequency domain results for a stochastic sea state are also used for plots of the D.A.F. and the frequency characteristics of loads and motions.

Paragraph 8.7 deals with the hydrodynamic damping percentages computed in the frequency domain.

Several conclusions are drawn during the discussion of the results. A resume of these conclusions is given in paragraph 8.8.

It should be noted that the transient state response of the platform, occuring during the 'transition' of one stationary sea state to another, will not be examined. This is done for the following reasons:

a. The transient response of the platform will be influenced by the properties of both adjacent sea states. As it is desirable to link certain load and motion values to one specific sea state, from the viewpoint of jack-up design, it is logical to examine the loads and motions during one stationary sea state and to neglect the transient state.

b. Transient state response cannot be computed by means of frequency domain analysis, so there is no basis for checking time domain results.

In time domain analysis, the start of a time series will always have a transient nature. By estimating the transient time and neglecting the results from this period, the remaining results will reflect the steady state. It was found that a time interval of 20 average zero-crossing periods at the beginning of a simulation is sufficient to cover the transient time. This is the estimation of the transient time used for all simulations. Consequentially, the estimated transient time depends on the properties of the waves, as is the case for the time step used (see paragraph 7.2).

8.2 REFERENCE CASE

8.2.1 Properties

The reference case for the discussion of the results obtained by means of the computer programs Jacques and Jacquelin is the three legged jack-up platform Kolskaya loaded by a JONSWAP wave spectrum. The basic parameters of this reference case are listed in table 8.1, while the values used for the numerical discretization of the model are listed in table 8.2.

Pontoon mass	= 10610	tons
Mass moment of inertia	= $4.3*10^6$	$tonm^2$
Leg mass per unit length	= 8	tons/m
Total leg length	= 140	m
Free leg length	= 120	m
Equivalent leg diameter	= 10.50	m
Leg-soil stiffness	= 0	kNm/rad
Leg hull stiffness	= $8*10^7$	kNm/rad
Reduced leg stiffness	= $1.93*10^9$	kNm^2
Structural and soil damping	= 0	%
Water depth	= 95	m
Water density	= 1024	kg/m^3
Peak enhancement factor	= 3.3	
Lower spectrum boundary	= 0	rad/s
Upper spectrum boundary	= 2	rad/s
Main wave direction	= 0	degrees
Total simulation time	= 3600	s
Estimated transient time (in zero-crossing periods)	= 20	

Table 8.1: Properties of reference case

The platform with the properties from table 8.1 has the following natural periods for translation, T_{TR}, and for rotation, T_{ROT}:

T_{TR} = 9.81 s

T_{ROT} = 7.10 s

Again it is pointed out that time domain analysis is carried out for one translational degree of freedom with neglection of directional wave spreading

Number of leg sections	= 15
Number of spectrum sections	= 70
Number of time step per zero-crossing period	= 20

Table 8.2: Numerical descretization values

8.2.2 Results

The results of three 1 hour simulations are listed in table 8.3. Looking at the standard deviation of the water loads and of the deck displacement, it can be seen that the loads increase with the increasing significant wave height, as to be expected, but that there is hardly any difference between the standard deviations of displacement of the last two cases. This indicates the presence of a relatively large dynamic amplification at the second spectrum. Considering the natural period of 9.81, it seems that the dynamic amplification is governed by the energy peak of the spectrum rather than by its average zero-crossing period. This is in agreement with the sharp-peaked nature of the Jonswap spectrum used in this study, but need not be the case for other types of wave spectra. The item will be dealt with during the discussion of the frequency domain results.

peak period	sign. wave height	zero-cross. period	water load s.d.	water load max.	deck displ. s.d.	deck displ. max.
[s]	[m]	[m]	[kN]	[kN]	[m]	[m]
8.0	6.0	6.68	66.7	473.4	0.101	0.248
10.0	10.0	8.15	174.1	1139.0	0.397	1.031
12.0	14.0	9.65	405.7	3789.3	0.409	1.253

Table 8.3: Results of the reference case

The maximum water load and deck displacement, on the other

hand, are governed by the amount of overall spectral energy, represented by the significant wave height, rather than by dynamic amplification. This can be explained by realizing that the large waves causing these loads and motions will have periods much greater than the natural period and thus will be well outside the frequency range affected by dynamic amplification.

In table 8.4, the comparison of drag and mass forces clearly shows the dominance of the drag forces, as to be expected for legs of the lattice type. There is a trend of increasing drag force dominance for increasing wave periods. This is due to the fact that the flow regime approaches stationary flow for increasing wave periods. For stationary flow, the fluid accelerations, and thus the mass forces, are zero.

peak period	sign. wave height	standard deviation of drag force	standard deviation of mass force	ratio of mass and drag force
[s]	[m]	[kN]	[kN]	[%]
8.0	6.0	65.0	12.9	19.8
10.0	10.0	175.2	15.8	9.0
12.0	14.0	408.5	17.0	4.2

Table 8.4: Ratio of drag and mass force

The histograms of the water loads and the deck displacements in the reference case are plotted in figures 8.1 to 8.6. Figures 8.1 to 8.3 show the histograms of the water loads. As already mentioned in paragraph 7.3, the distribution of the water loads should approximate an exponential distribution, if the drag forces are dominant.

The exponential distribution best fitting the water load histograms is found to be:

$$p(X) = \frac{1.5}{2\sigma_x} \exp\{-1.5 \frac{|X-\mu_x|}{\sigma_x}\} \qquad (8.01)$$

where:

$p(X)$ = probability of occurence

σ_x = standard deviation

μ_x = mean value

FIG. 8.1: HISTOGRAM OF THE TOTAL WATER LOAD ON THE PLATFORM

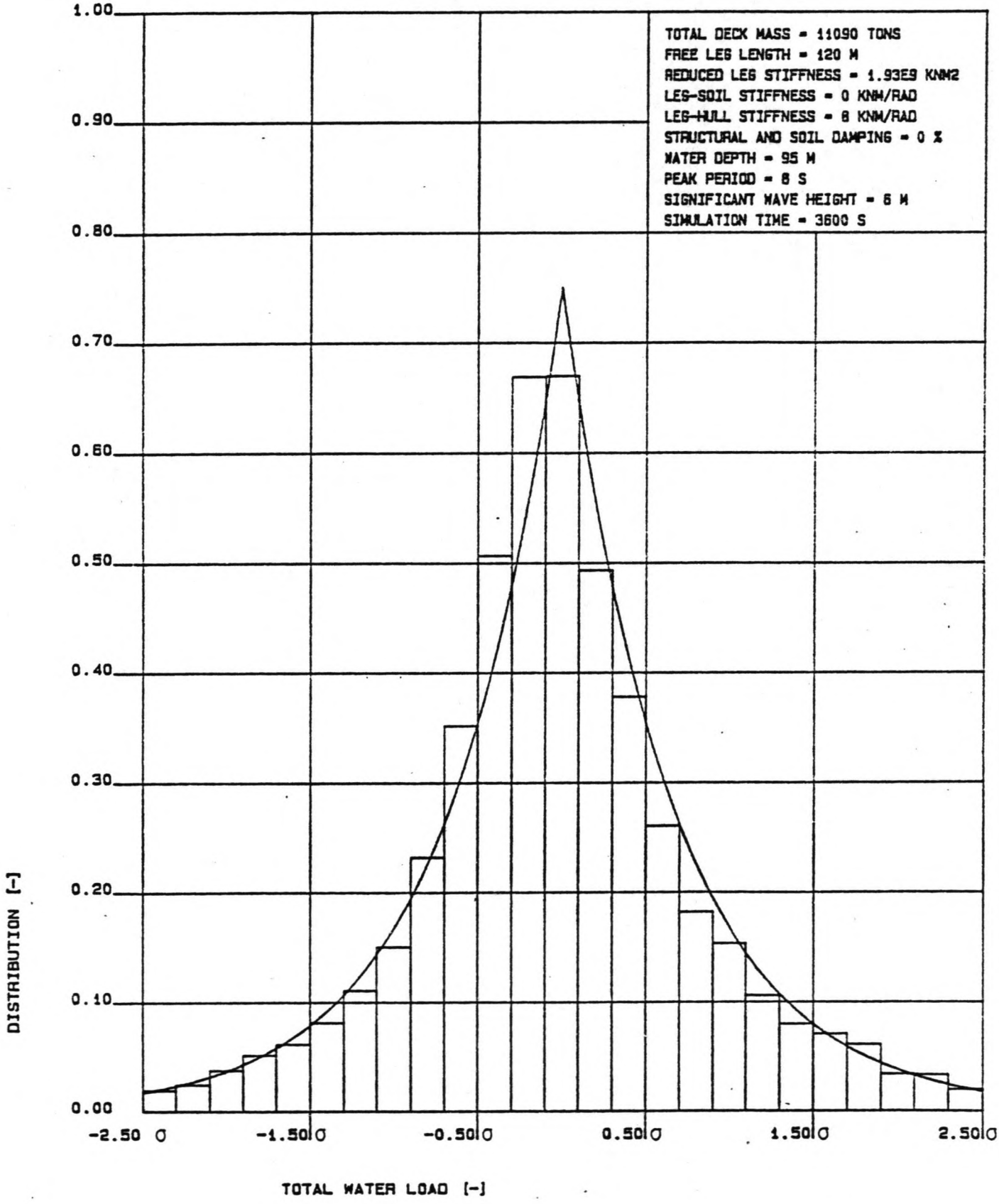

FIG. 8.2: HISTOGRAM OF THE TOTAL WATER LOAD ON THE PLATFORM

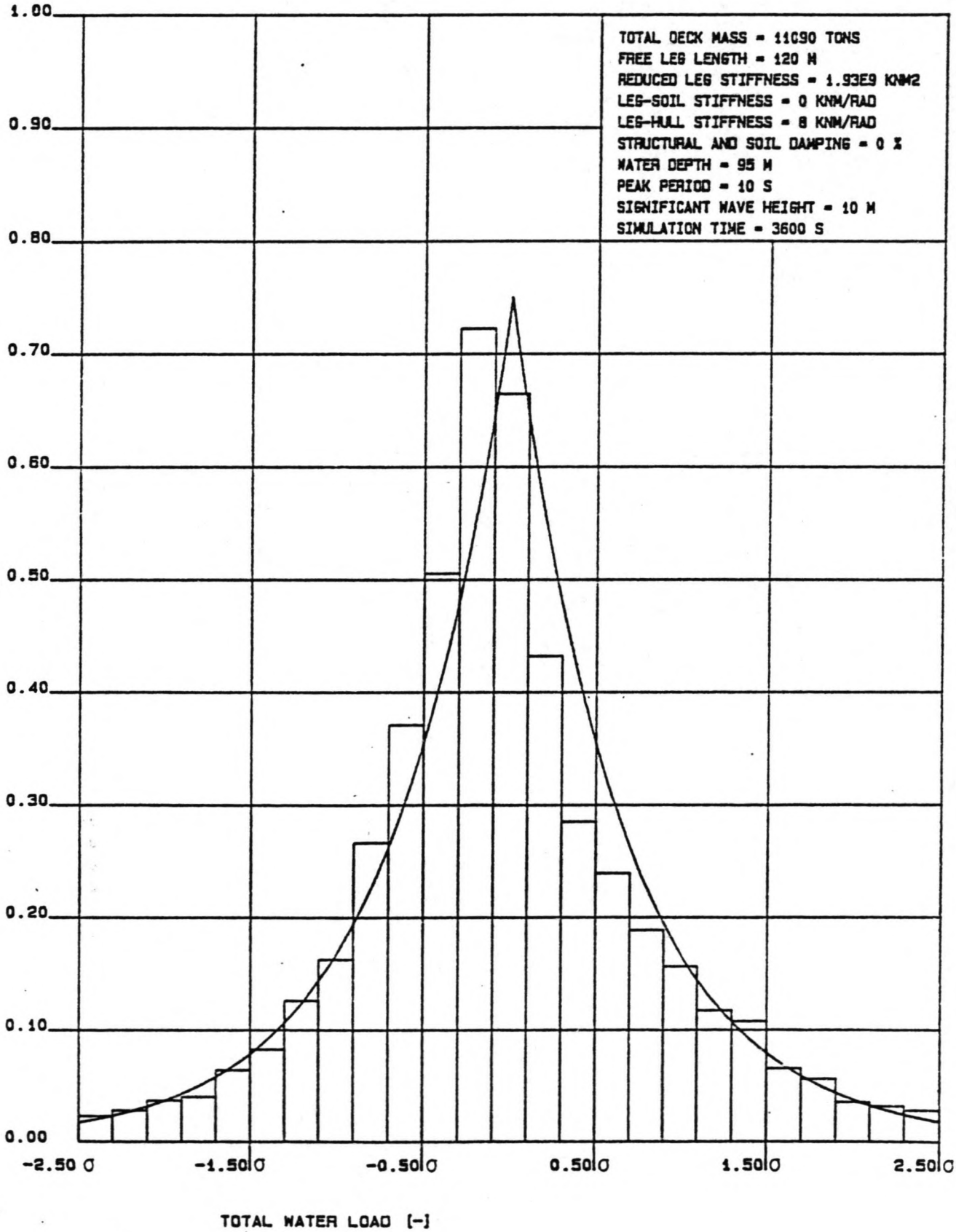

FIG. 8.3: HISTOGRAM OF THE TOTAL WATER LOAD ON THE PLATFORM

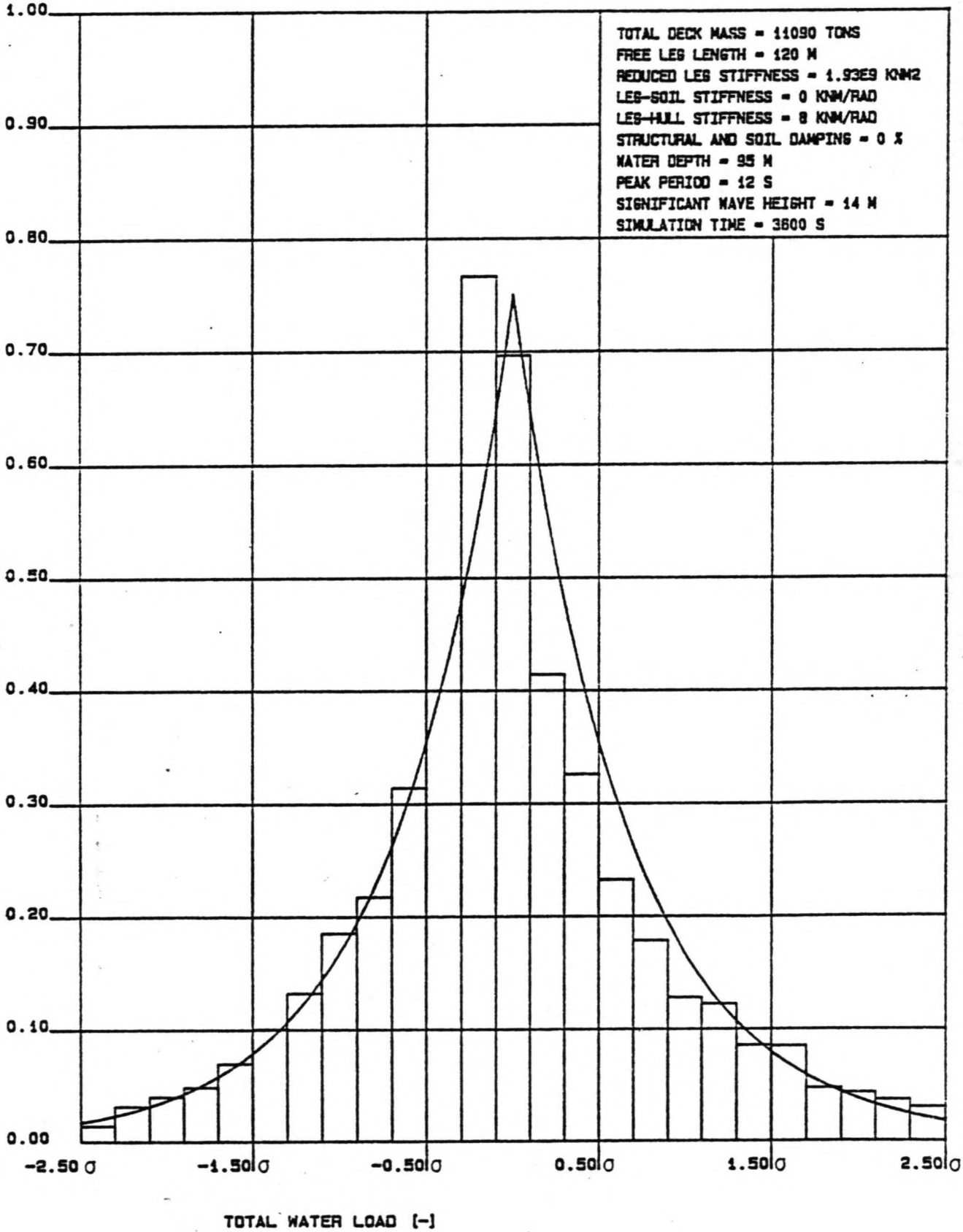

This distribution has been plotted in the load histograms and it can be seen that there is a very good fit. This is as to be expected, since the water load is drag force dominated.

Comparison of figures 8.1 to 8.3 reveals a weak trend of increasing asymmetry for an increasing significant wave height. This can be explained by considering the effect of the changing water depth during one wave period, as described in section 4.2.1. The maximum wave load in the positive direction, occuring 'under' the wave crest, will be greater than the maximum load in the negative direction, occuring 'under' the wave trough. This effect will increase for an increasing significant wave height, causing the asymmetry of the load histograms.

Figures 8.4 to 8.6 show the deck displacement histograms of the reference case. Although no mathematical distribution curve was predicted for the deck displacement, the histograms show a strong resemblance to the Gaussian curve, which has also been plotted in figures 8.4 to 8.6. It is not quite understood how the exponential distribution of the water load yieds a Gaussian distribution of the deck displacement. One possible theory will be presented below in a general, qualitative way.

The deck displacement at one point in time, t, is not only determined by the water load at time t, but by the loading history of a time interval previous to t, called Δt. If this loading history is thought to be split into a number of momentary water loads, each of this momentary loads will contribute to the deck displacement at time t. The relative importance of these contributions is governed by the following two items:

a. The time interval between the momentary load and the deck displacement considered. Going backwards in time from t, the influence of the momentary loads on the deck displacement at time t will decrease.

b. The periods of the waves causing the momentary loads. The frequency characteristics of the structure will determine the transfer of loads to motions.

If the correlation between the various momentary water loads in the interval is low, the deck displacement at time t will be a summation of low correlated displacement components. From statistics it is known that a summation of a large number of stochastically independent distributions yields a Gaussian distribution. If the components of the deck displacement at time t, caused by the momentary loads in the time interval Δt, could be assumed to be stochastically independent, this would explain the approximate Gaussian distribution observed for the

FIG. 8.4: HISTOGRAM OF THE DECK DISPLACEMENT OF THE PLATFORM

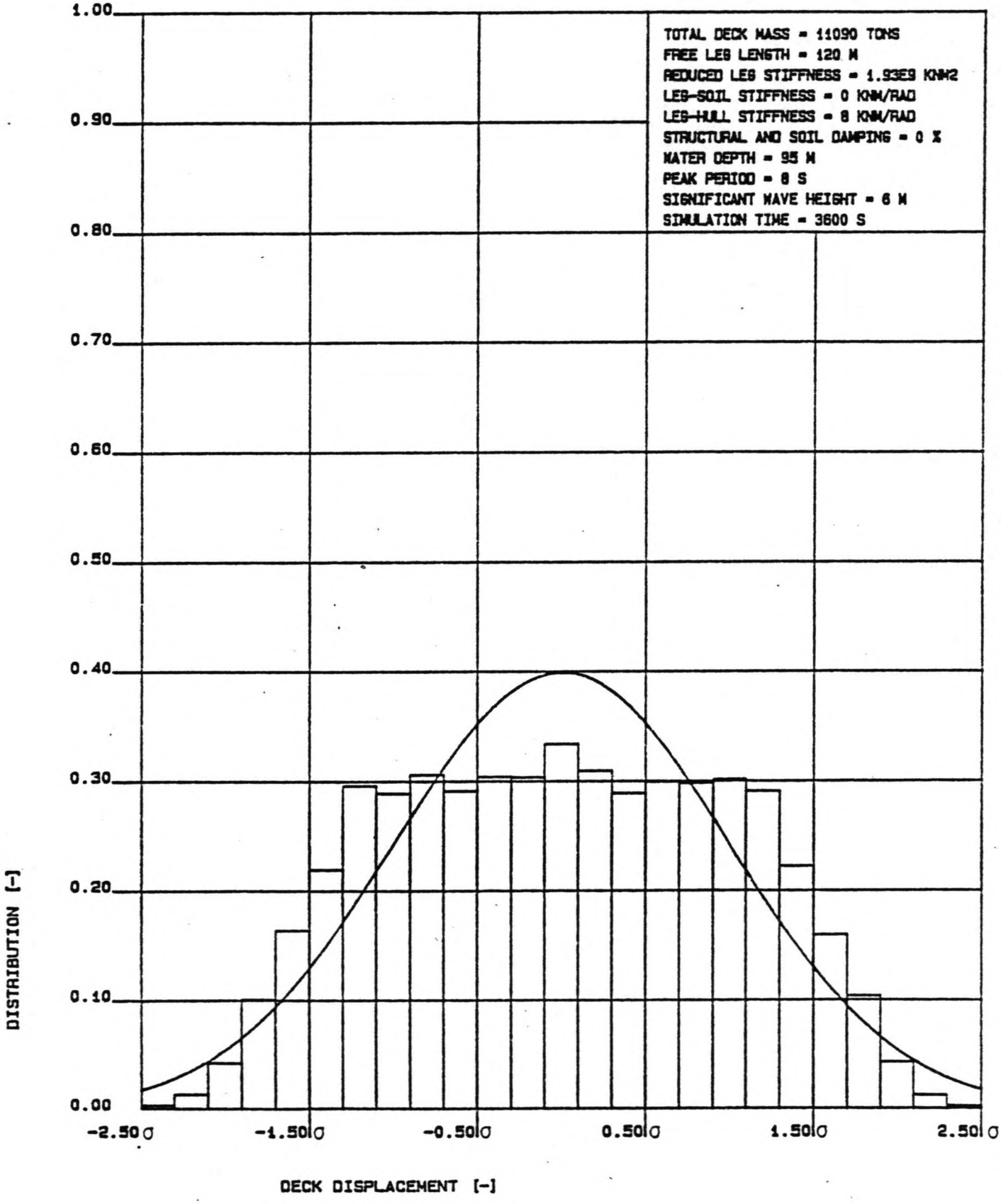

FIG. 8.5: HISTOGRAM OF THE DECK DISPLACEMENT OF THE PLATFORM

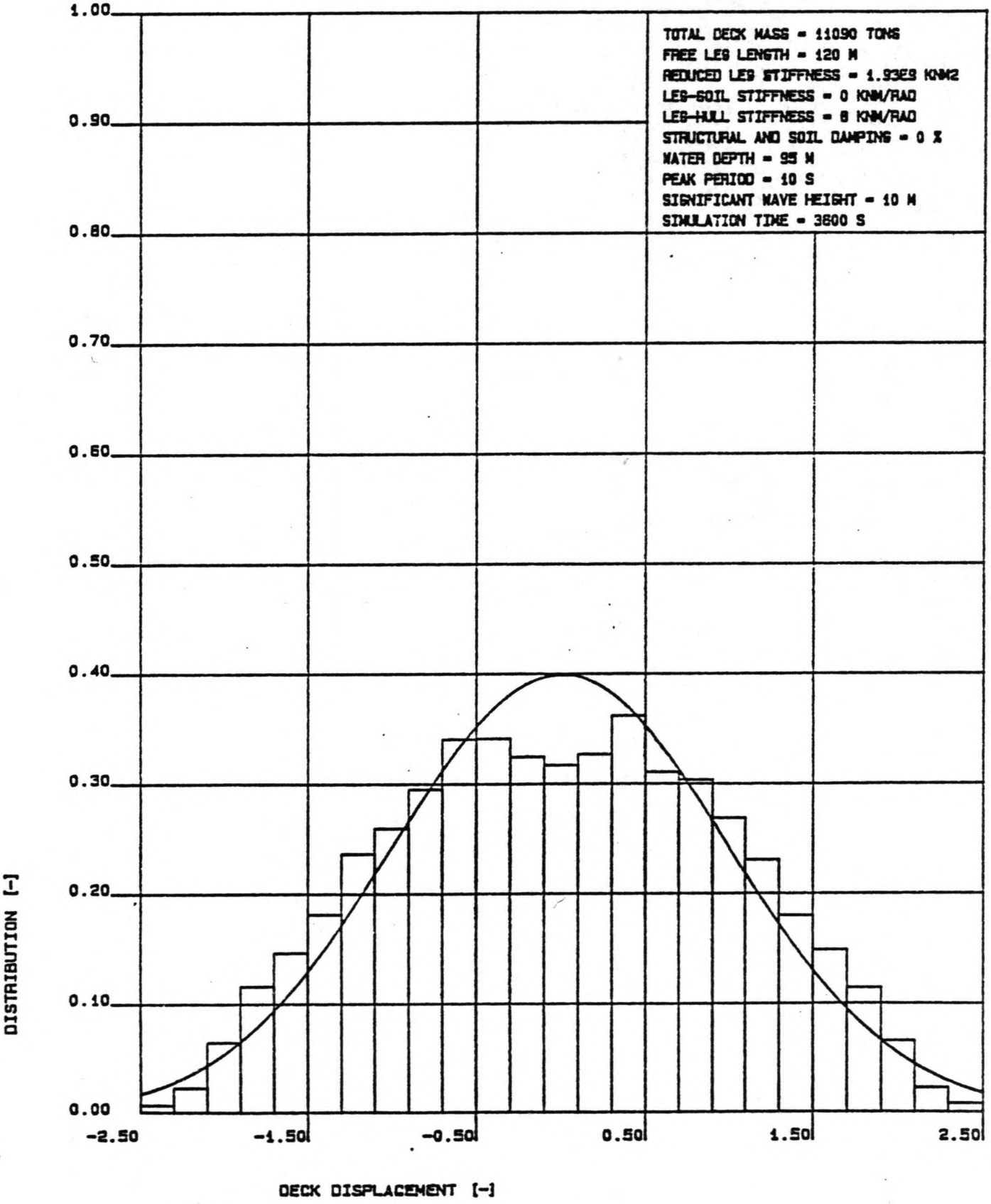

FIG. 8.6: HISTOGRAM OF THE DECK DISPLACEMENT OF THE PLATFORM

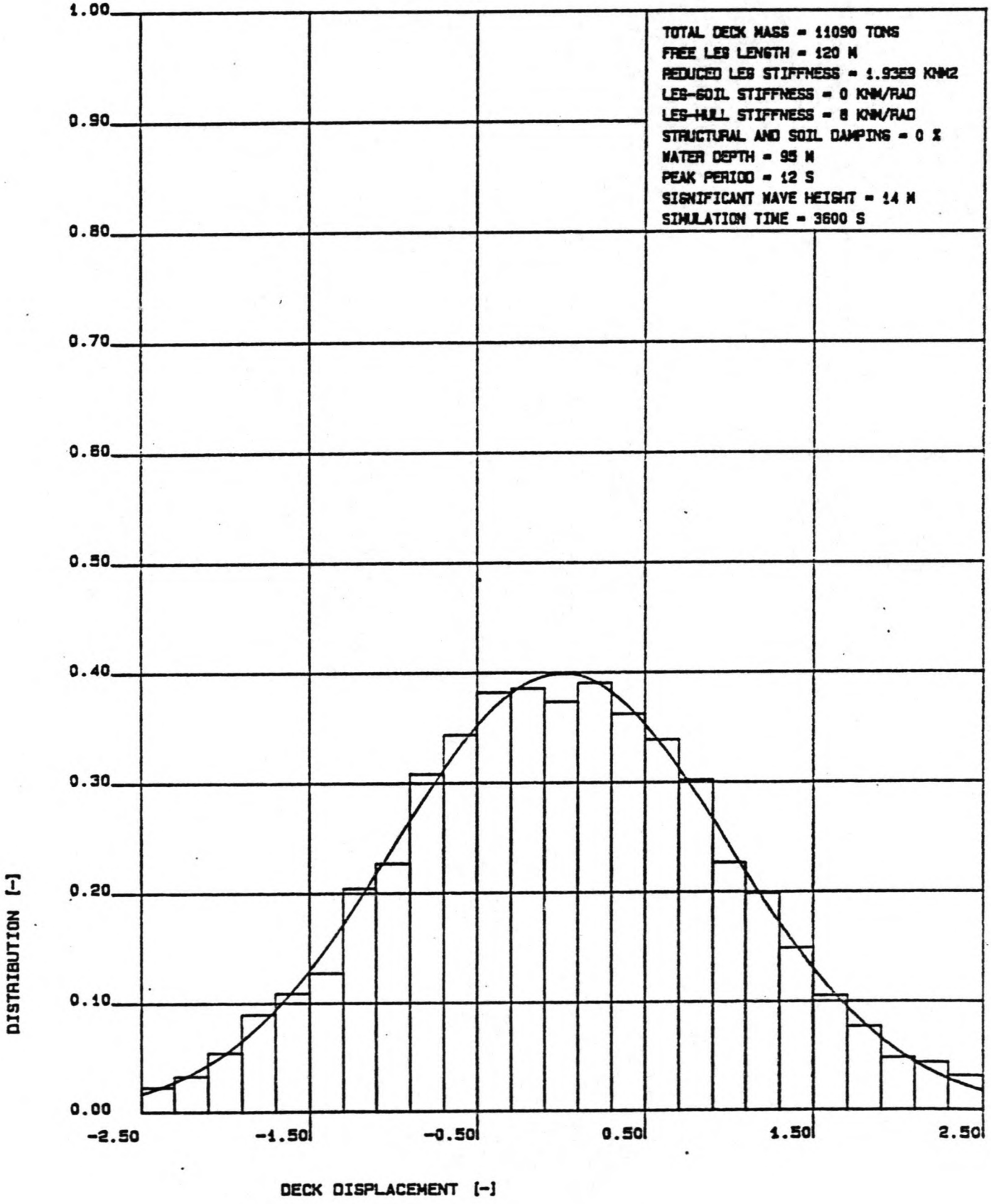

deck displacement.

This theory yields two direct consequences:

a. For a deterministic sea state, the wave loads at all points in time are fully correlated and their distribution is uniform, with a rectangular profile. As a result of this, their contributions to the deck displacement are fully correlated as well, and thus the distribution of the deck displacement will not be Gaussian. Instead of this, for a linear transfer between loads and motions, this distribution will also be uniform. For a stochastic sea state, this extreme case will be approached if the platform response has a narrow-banded frequency characteristic. The correlation of the deck displacement components contributions will not be small enough to yield a Gaussian distribution and the deck displacement histogram will move towards the uniform distribution function found for a deterministic wave load. A narrow-banded response can be induced by a narrow-banded load spectrum or a wide-banded load spectrum filtered by a sharp-peaked transfer function.

b. An increasing length of the time interval influencing the deck displacement at time t allows this interval to contain more low correlated momentary loads and thus yields a more accurate reproduction of the Gaussian curve for the deck displacement. If the time interval is too short to contain virtually uncorrelated momentary loads, the deck displacement at time t is governed by the momentary load at time t. In the case of a linear transfer between the water load and the deck displacement, a exponential load distribution will yield an exponential distribution of the deck displacement.

It should be noted that the validity of this theory depends on the correlation of the momentary loads in a certain time interval, but not on the actual distribution of these momentary loads. This means that a Gaussian distribution of the deck displacement is predicted for drag force dominance as well as mass force dominance.

The best fit of the Gaussian curve is found for the 12 s spectrum. The other two histograms show a trend towards the rectangular distribution mentioned above, which could indicate a narrow-banded response for the 8 s and 10 s wave spectra. An effort to confirm this will be made at the discussion of the frequency characteristics obtained from frequency domain analysis.

8.3 STRUCTURAL AND SOIL DAMPING

In the reference case, the structural and soil damping percentage is equal to 0. In this paragraph the influence of structural and soil damping will be examined for the 12 s wave spectrum. The damping percentages considered are 0, 1 and 2 %. Higher structural and soil damping values are not included, since the physical relevance of these values is debatable. Apart from this, they do not enlarge the fundamental understanding of the effects involved.

Table 8.5 shows the influence of structural and soil damping. Theoretically, the water loads are virtually independent of this damping, since a load reduction due to an increase of damping can only be caused by a reduction of the platform motion component of the relative velocity and this component will be relatively small compared to the fluid velocity. This theory is confirmed by the results listed in table 8.5.

struct. and soil damping	peak period	sign. wave height	water load		deck displ.	
			s.d.	max.	s.d.	max.
[%]	[s]	[m]	[kN]	[kN]	[m]	[m]
0.0	12.0	14.0	405.7	3789.3	0.409	1.253
1.0	12.0	14.0	400.9	3698.2	0.346	1.166
2.0	12.0	14.0	398.3	3637.5	0.309	1.108

Table 8.5: Influence of structural and soil damping

From the theory of dynamics it is known that the influence of damping on the response of a system is restricted to the excitation periods near the natural period. The relatively moderate motion reductions from table 8.5 indicate that this influence of damping is not very strong in the case of the 12 s wave spectrum, in particular for the maximum deck displacement. Again, it is concluded that the dynamic amplification is governed by the spectral energy peak rather than the zero-crossing period and that the large waves causing the maximum deck displacement are outside the amplification range.

Figures 8.7 and 8.8 show the load histograms for 1 and 2 % damping. The good fit of the exponential distribution confirms the independency of the damping stated above. Again, the histograms are slightly asymetrical due to the effect of changing waterdepth on the water loads.

FIG. 8.7: HISTOGRAM OF THE TOTAL WATER LOAD ON THE PLATFORM

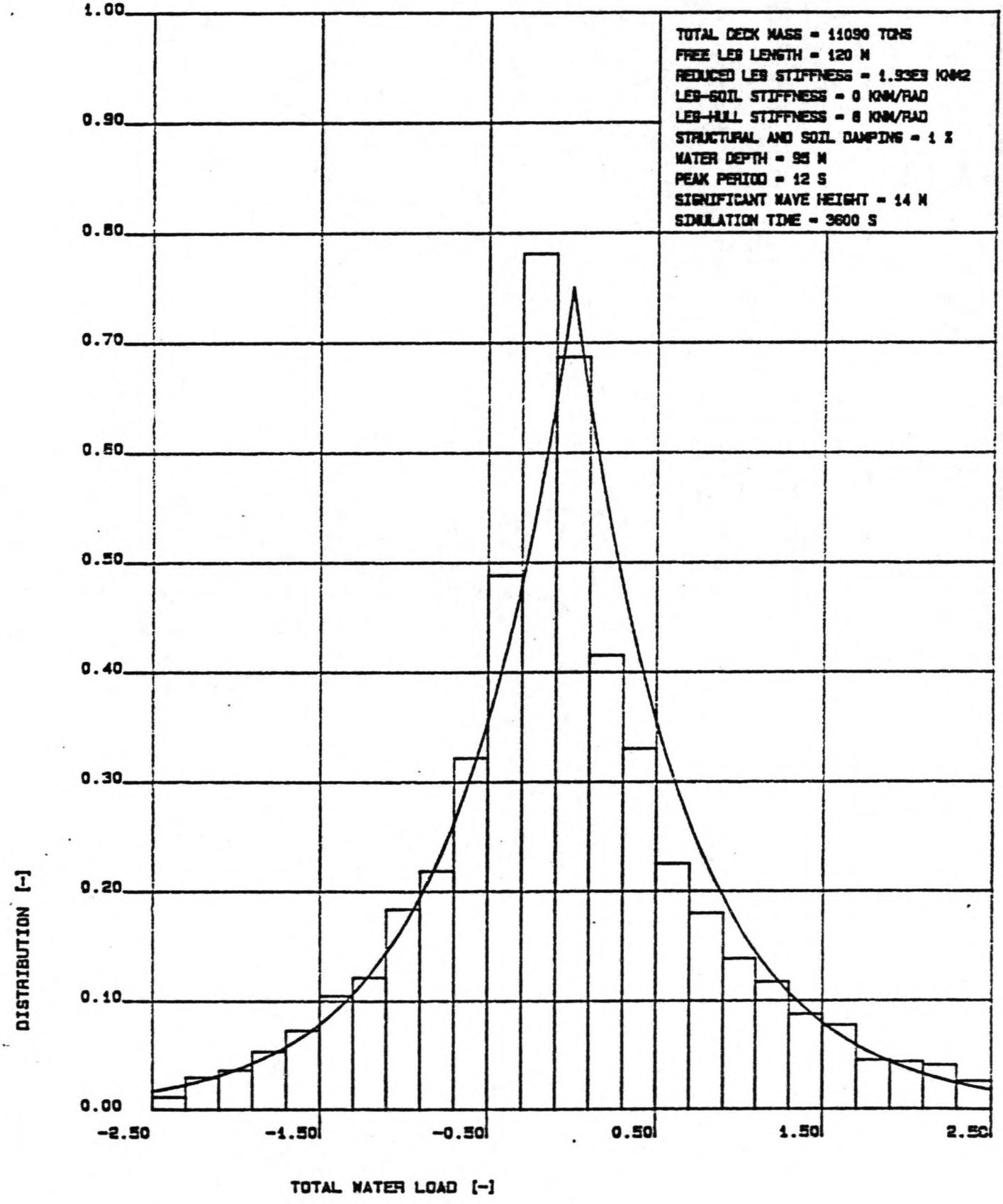

FIG. 8.8: HISTOGRAM OF THE TOTAL WATER LOAD ON THE PLATFORM

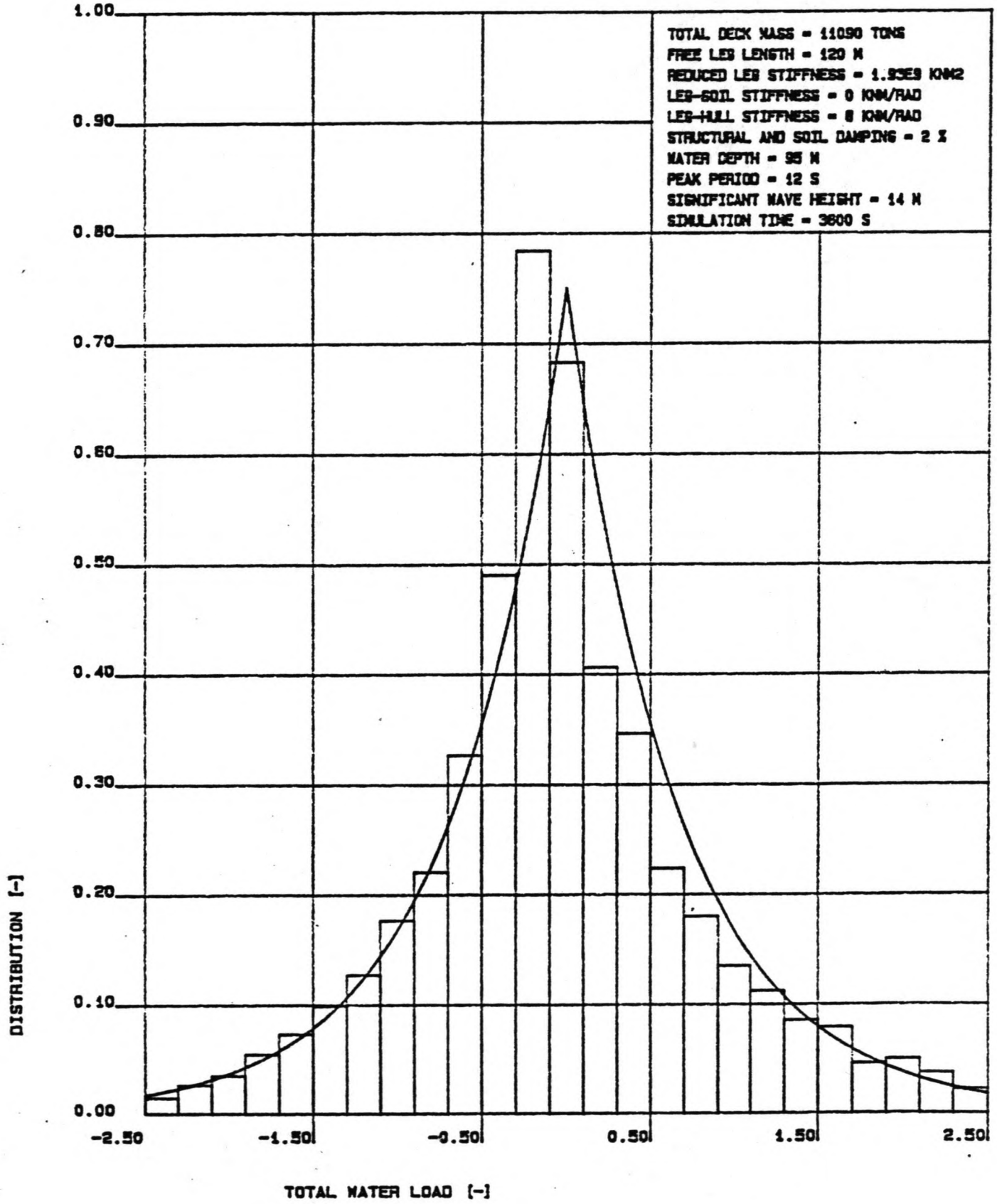

With respect to the deck displacement, the following remark is made. For increasing damping percentages, the momentary contributions to the deck displacement, t, will damp out faster, and thus the length of the influencing time interval, Δt, will decrease. According to the theory from the previous paragraph, this decrease should yield deck displacement histograms with an increasing deviation from the Gaussian curve.

In figures 8.9 and 8.10, showing the deck displacement histograms for 1 and 2 % structural and soil damping, a slight deviation is observed indeed. It should be noted that these histograms seem to move towards an exponential distribution, which would indicate a nearly-linear transfer or water loads to deck displacement, if the theory presented above is correct.

FIG. 8.9: HISTOGRAM OF THE DECK DISPLACEMENT OF THE PLATFORM

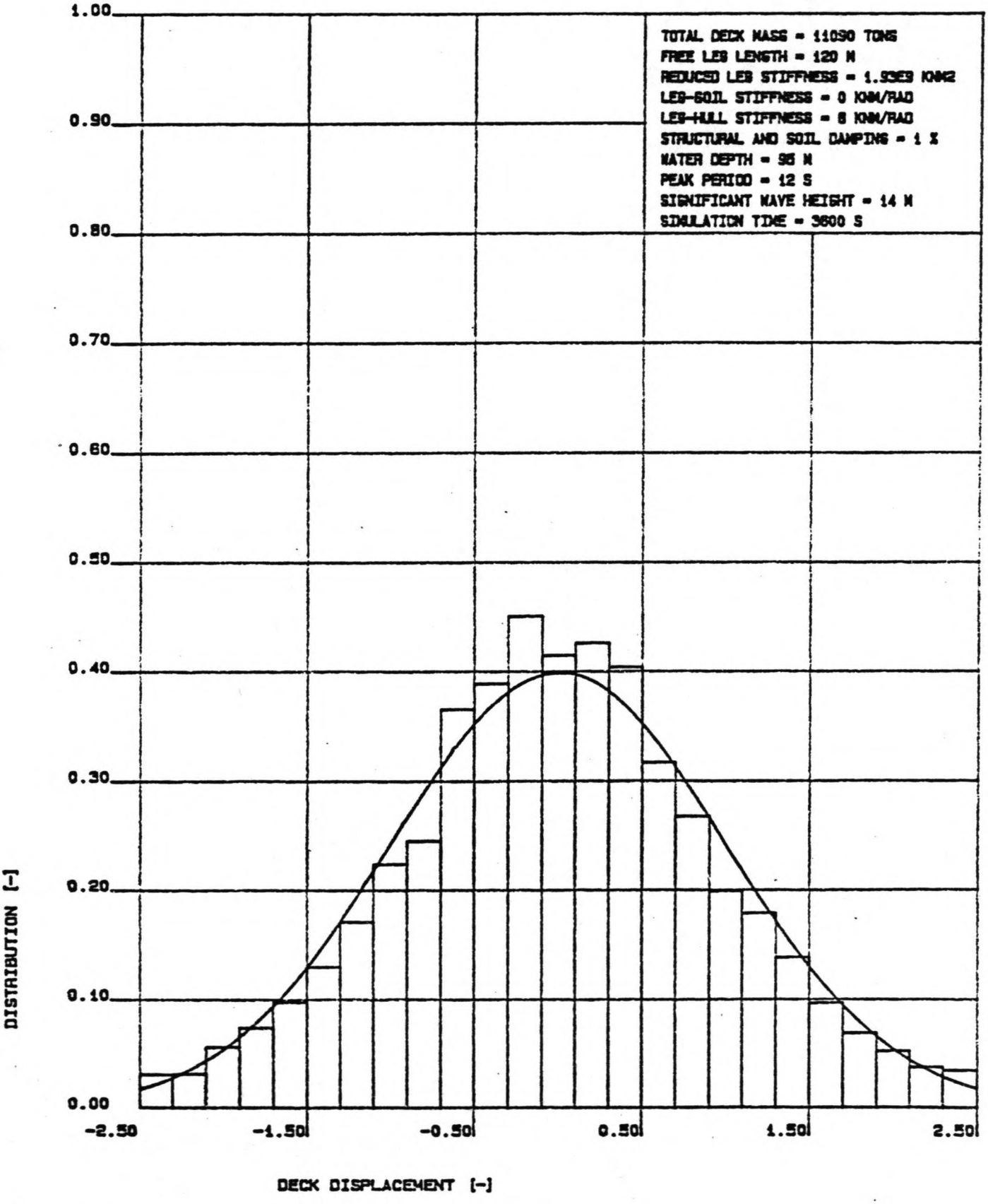

FIG. 8.10: HISTOGRAM OF THE DECK DISPLACEMENT OF THE PLATFORM

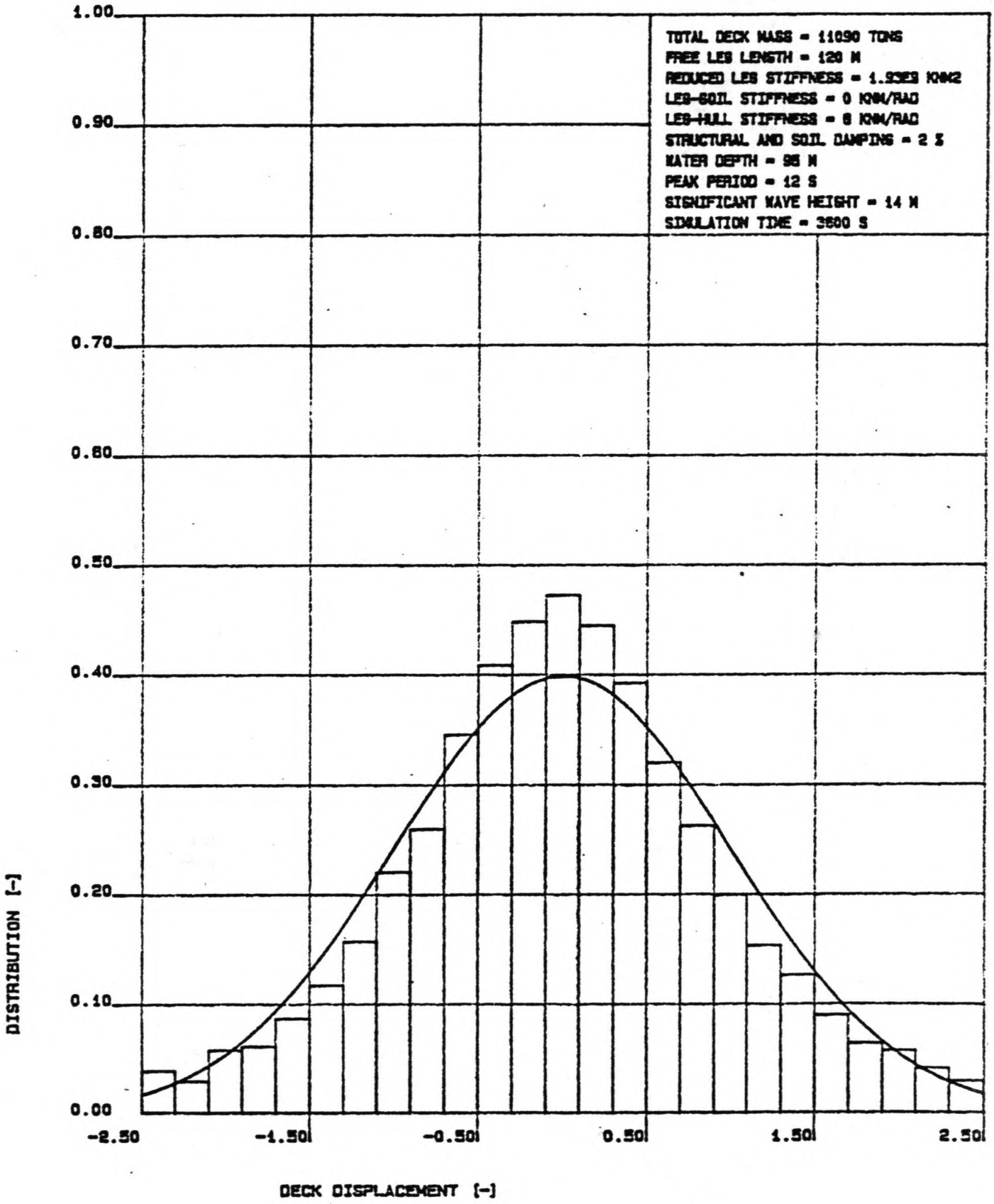

8.4 ONE LEG MODEL

In this paragraph, the reference case will be compared to a one leg model with a total deck mass equal to one third of the total deck mass of the three-legged platform, in order to obtain identical dynamic characteristics for both models. This allows the examination of the load reduction in the multi-legged case due to phase differences between the legs.

If these phase differences are neglected, the water load on the three-legged platform will exactly be three times the load on the one leg model and the response of both models will be identical, but in reality, the phase differences between the legs cause a load reduction and consequentially the platform response will always be less than the one leg response.

Table 8.6 shows the results for the one leg model. As in the reference case, the motions are relatively severe for the 10 s wave spectrum. This could be expected since both models have the same dynamic characteristics.

peak period	sign. wave height	zero-cross. period	water load s.d.	water load max.	deck displ. s.d.	deck displ. max.
[s]	[m]	[m]	[kN]	[kN]	[m]	[m]
One leg						
8.0	6.0	6.68	38.6	302.3	0.165	0.415
10.0	10.0	8.15	89.0	613.7	0.655	1.626
12.0	14.0	9.65	182.2	1618.7	0.642	1.927
Platform						
8.0	6.0	6.68	66.7	473.4	0.101	0.248
10.0	10.0	8.15	174.1	1139.0	0.397	1.031
12.0	14.0	9.65	405.7	3789.3	0.409	1.253

Table 8.6: Results for the one leg model

It can be seen that, according to the theory presented above, the motions of the one leg model are more severe, while the loads are significantly greater than one third of the water load on the three-legged platform. This indicates important load and motion reductions due to the phase differences between the legs.

In table 8.7, the standard deviations of the loads and motions

of both cases are compared. The following comarisons are made:

a. The deck displacement of the platform versus the deck displacement of the platform.

b. The water load on the platform versus three times the water load on the one leg model.

As can be seen, the reduction of loads as well as motions in the range from 25 % to 40 %, which is quite significant. The load reduction decreases for increasing peak periods and the reduction of the deck displacement shows the same trend, except for the 10 s spectrum. This is probably due to the fact that the wave periods 'affected' by dynamic amplification, which was found to govern the motions for the 10 s spectrum, are also 'affected' by the phase differences between the legs. Therefore a reduction of the water loads caused by this spectrum has an enhanced effect on the deck displacement.

peak period	sign. wave height	zero-cross. period	reduction due to phase differences between the legs	
			water load	deck displ.
[s]	[m]	[m]	[%]	[%]
8.0	6.0	6.68	42.4	38.8
10.0	10.0	8.15	34.8	39.4
12.0	14.0	9.65	25.8	26.3

Table 8.7: Reduction of loads and motions due to phase differences between the legs

In the reference wave direction, which is parallel to the x-axis of the platform fixed coordinate system, the wave crests hit the first two legs simultaneously, while they have to travel 57.8 metres in this direction to reach the third. For a regular wave, the maximum load reduction occurs if the wave length is equal to 2 * 57.8 = 115.6 m. According to short wave theory, the corresponding wave period is 8.61 s. These figures will depend on the loading direction.

If this is compared to the parameters of the wave spectra, it can be concluded that reductions due to phase differences are related to the peak period rather than the zero-crossing period. This is the same conclusion drawn for the dynamic amplification.

The above conclusion supports the explanation for the high reduction of the deck displacement in the case of the 10 s wave spectrum, since the peak period of this spectrum is relatively near the period of the regular wave subdue to maximum load reduction.

The examination of the phase differences between the legs yields the important conclusion that the motions and loads due to a certain sea state can be influenced by the choice of the platform geometry.

The histograms of the loads and motion have been plotted in figures 8.11 to 8.16. The differences with the plots made for the reference case are only marginal, as to be expected, since the dynamic properties do not differ fundamentally. For increasing peak periods there seems to be a tendency towards more peaked load distributions for the one leg model, but no explanation could be found for this. All other trends coincide with those observed for the three-legged platform.

FIG. 8.11: HISTOGRAM OF WATER LOAD ON THE ONE LEG MODEL

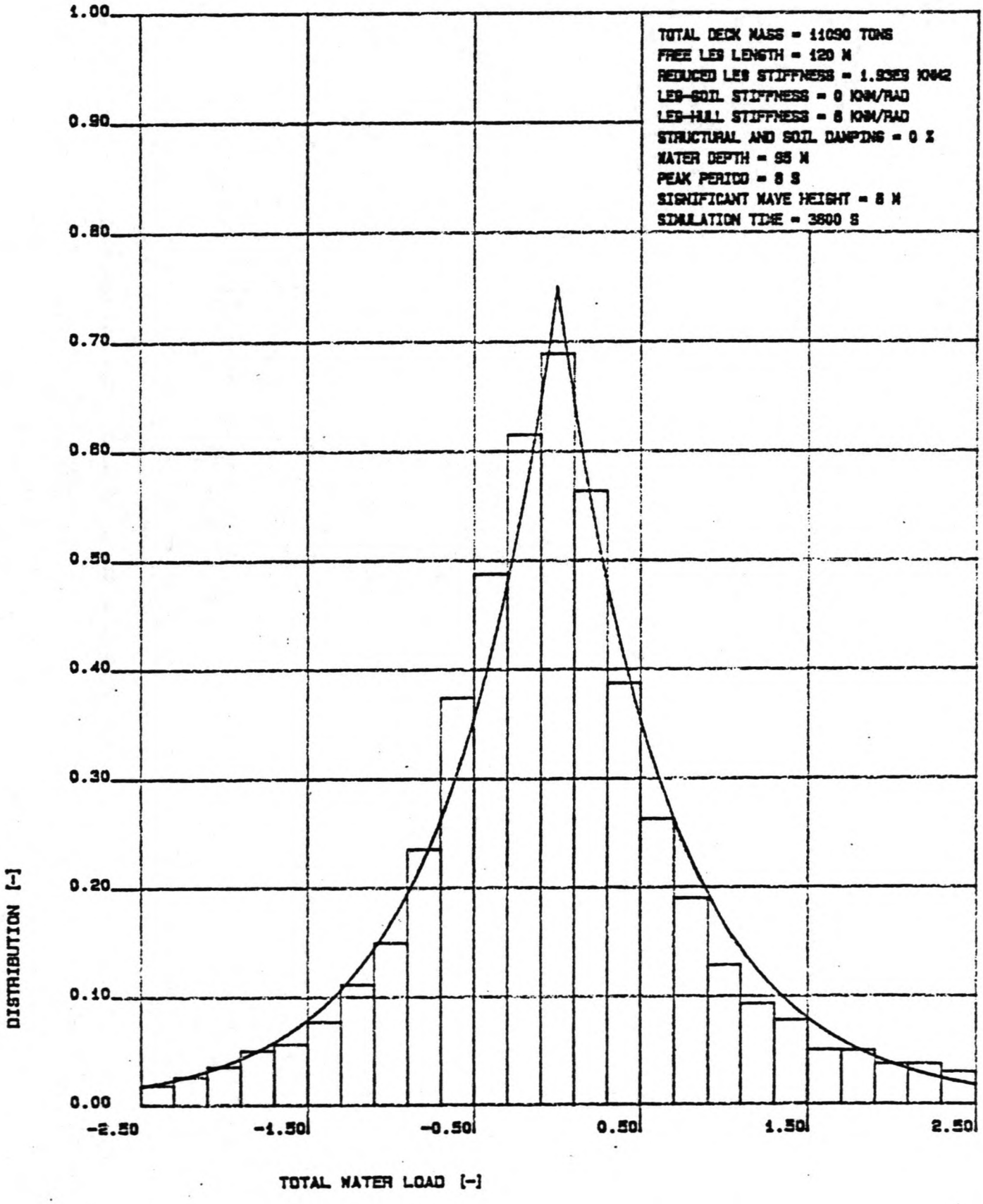

FIG. 8.12: HISTOGRAM OF THE WATER LOAD ON THE ONE LEG MODEL

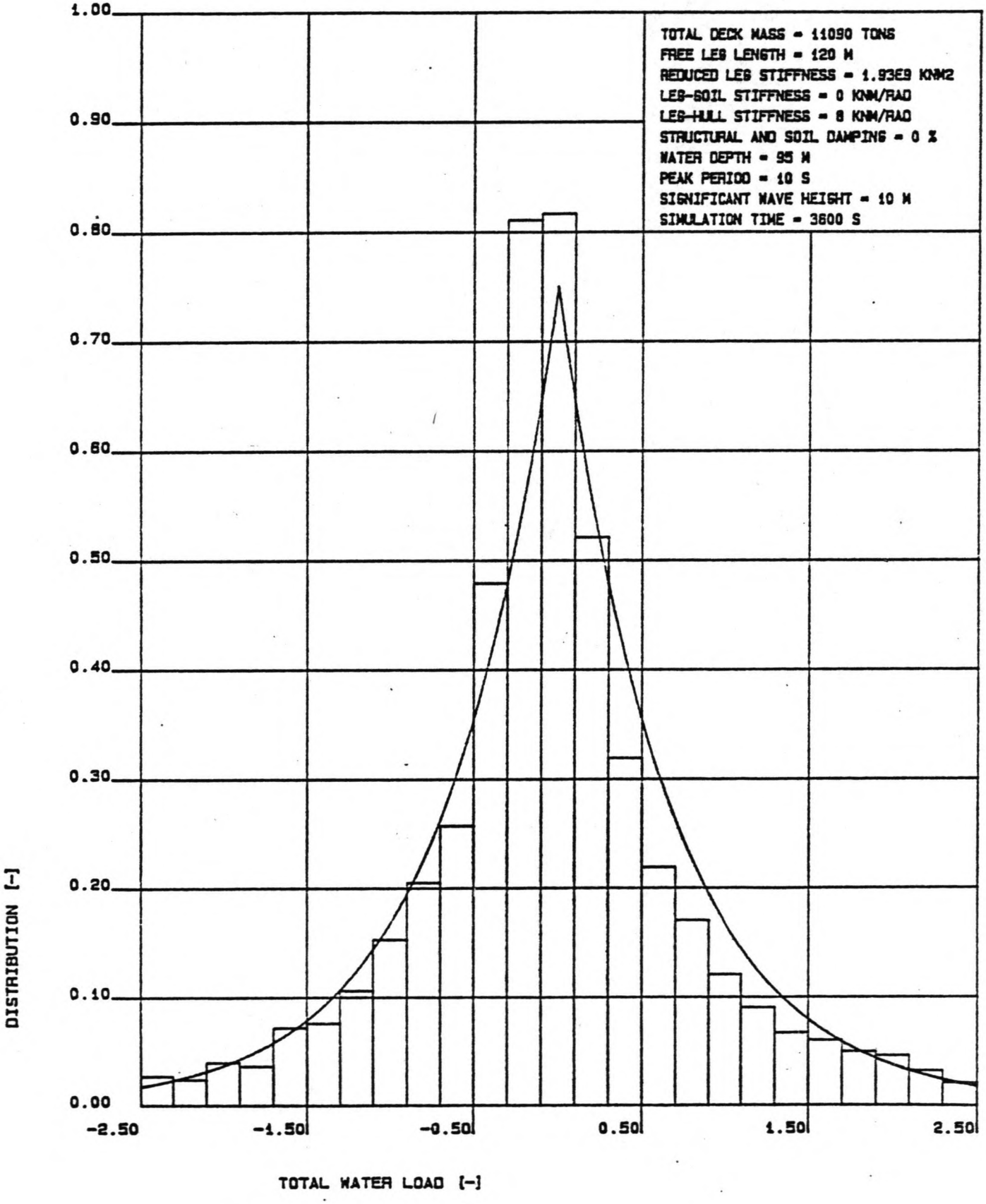

FIG. 8.13: HISTOGRAM OF THE WATER LOAD ON THE ONE LEG MODEL

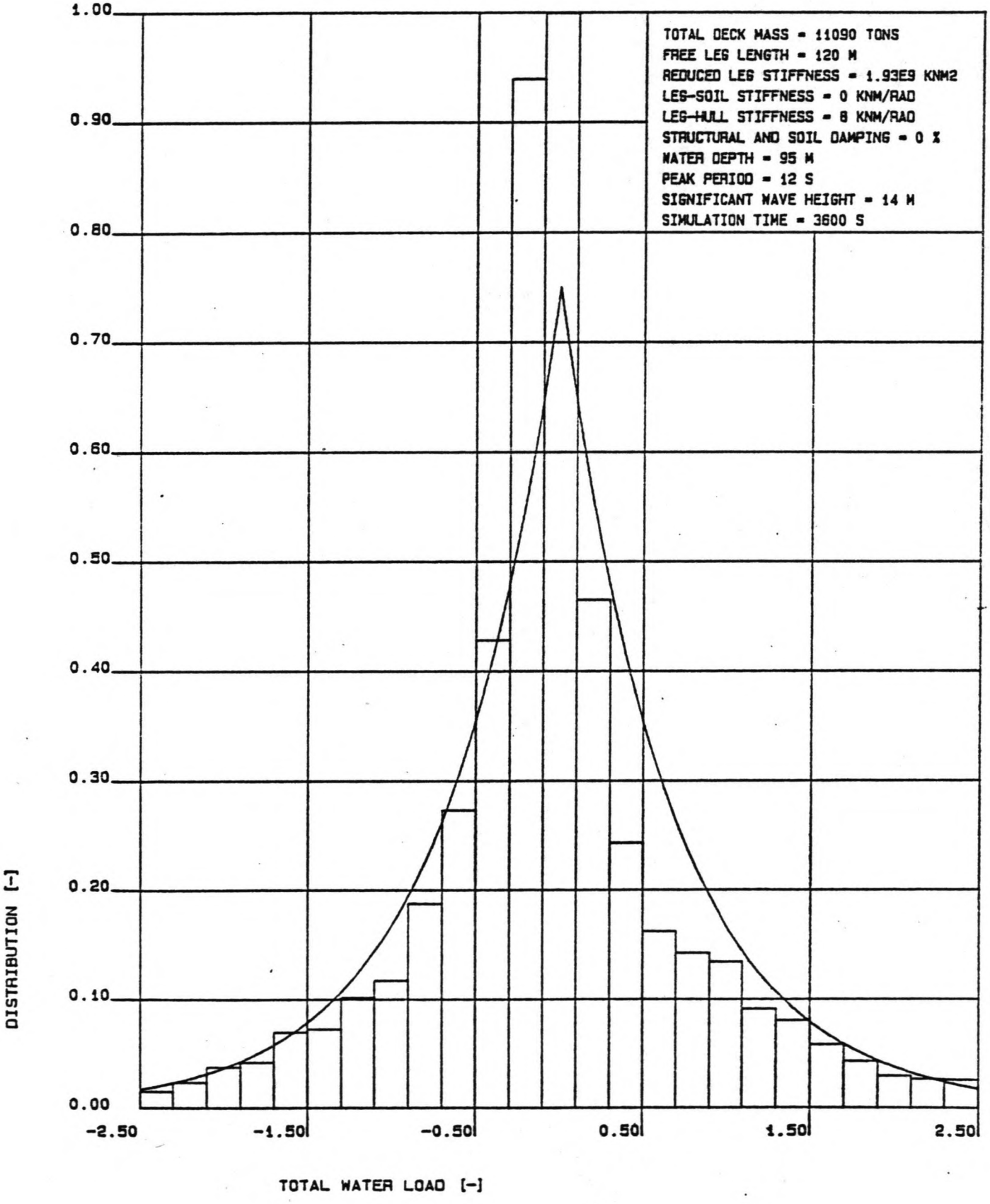

FIG. 8.14: HISTOGRAM OF THE DEK DISPLACEMENT OF THE ONE LEG MODEL

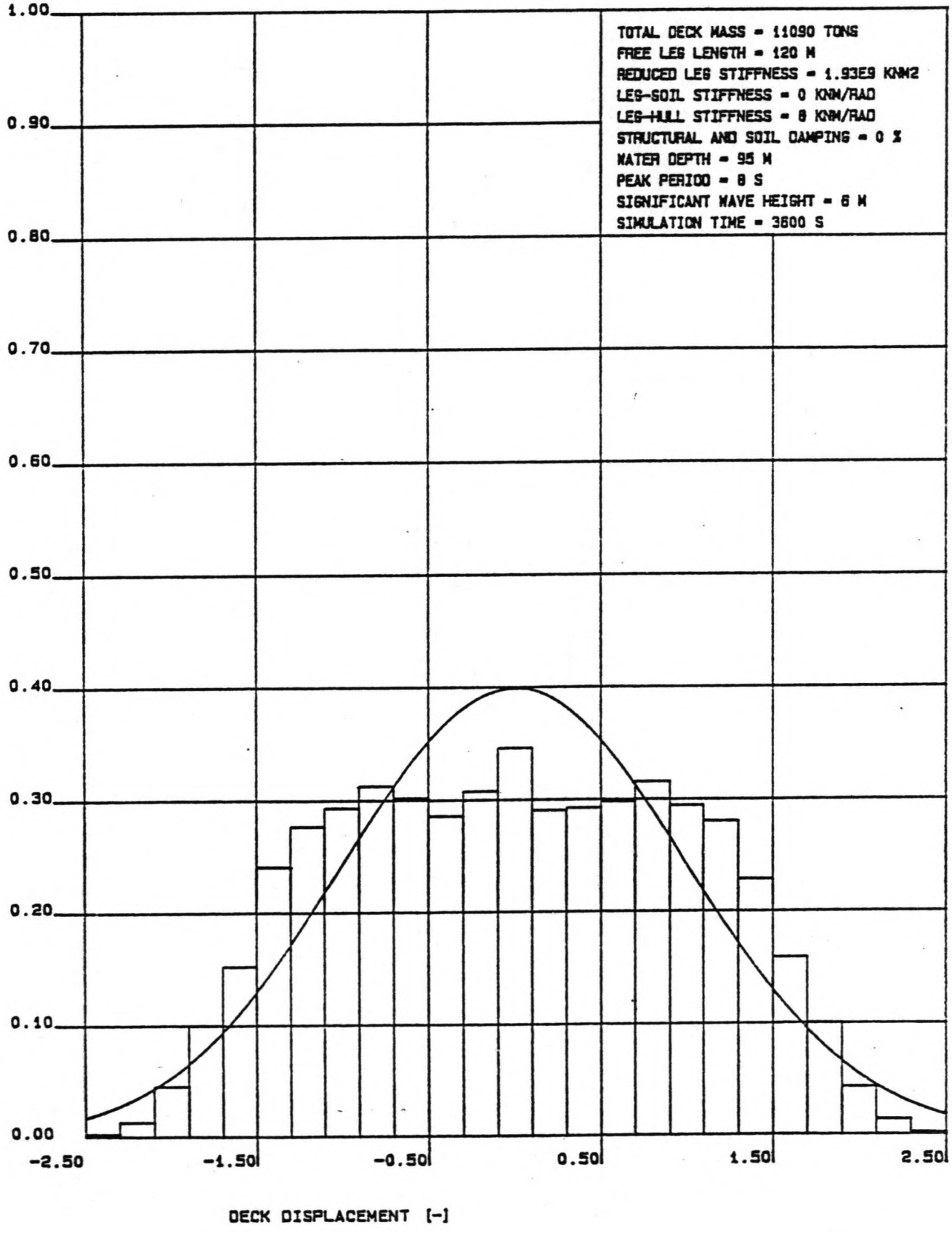

FIG. 8.15: HISTOGRAM OF THE DECK DISPLACEMENT OF THE ONE LEG MODEL

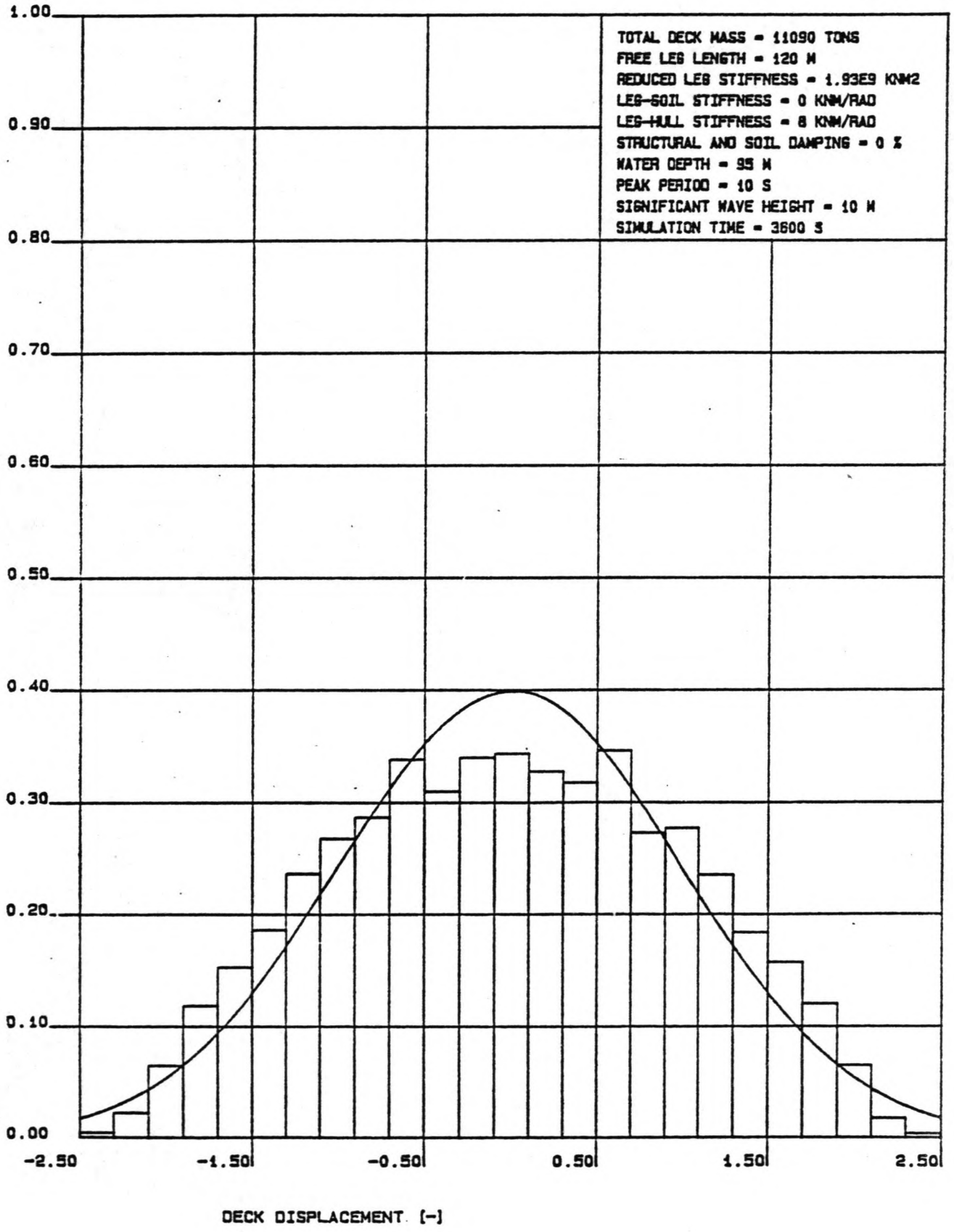

FIG. 8.18: HISTOGRAM OF THE DECK DISPLACEMENT OF THE ONE LEG MODEL

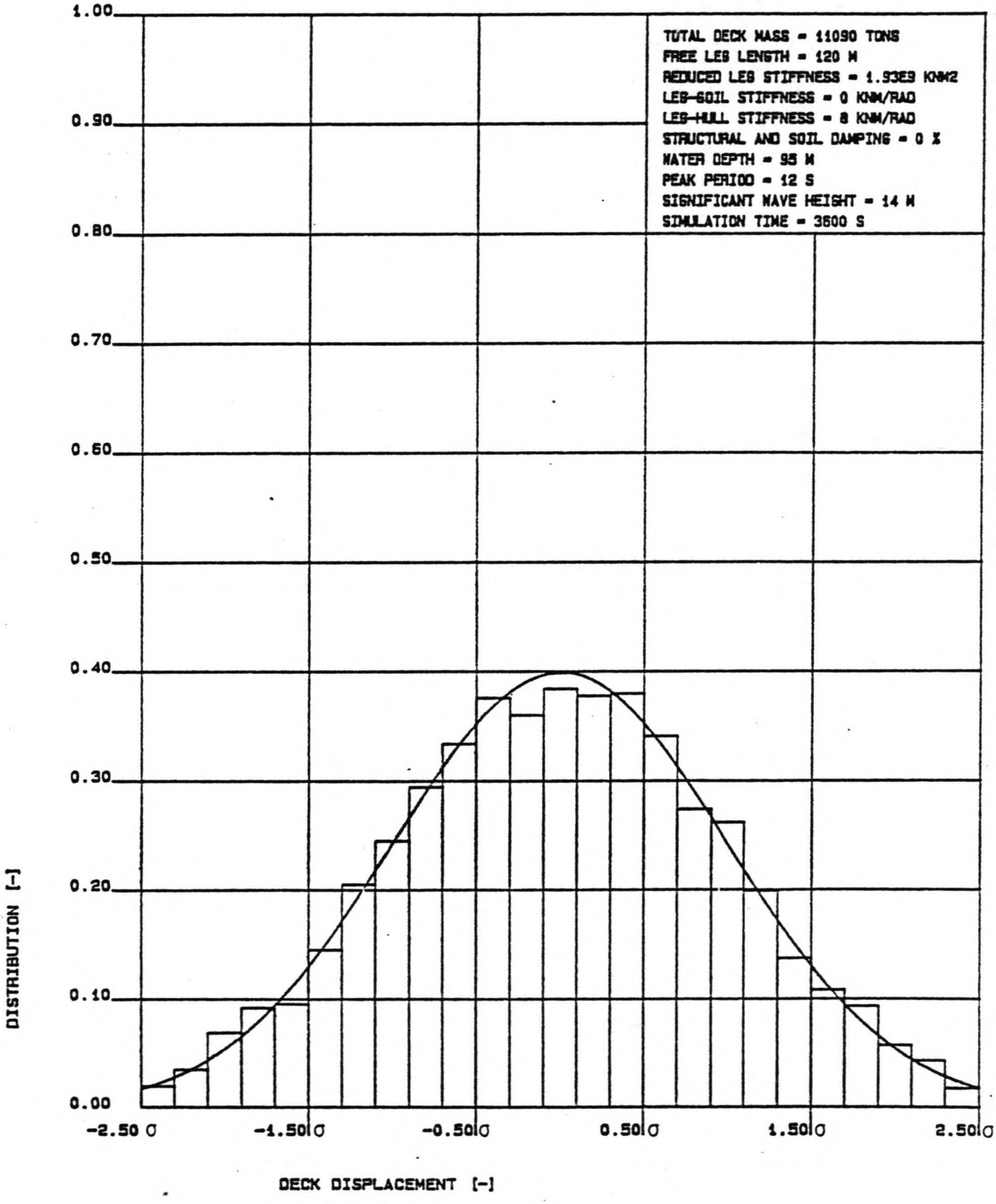

8.5 DETERMINISTIC ANALYSIS

In this paragraph, the results from deterministic analysis will be presented. This type of analysis is applied to the three-legged platform Kolskaya and the one leg model, both as described in the previous paragraphs.

In the discussion of these results special attention will be given to comparing them with the results from stochastic analysis presented in the previous paragraphs.

Since the steady state motion of the platform due to a regular, sinusoidal wave will be sinusoidal as well, with constant period and amplitude, the time domain simulation time need not be taken as long as for a wave spectrum in order to obtain reliable steady state results. Therefore the total simulation time for deterministic analysis is taken as 1000 s.

Three of the wave periods examined are chosen near the natural period of the platform, while the fourth regular wave has the maximum relevant period stated by D.N.V. and is called the design wave.

The wave height is related to the wave period by means of the D.N.V. 100 year wave steepness criterion from chapter 3.

wave period	wave height	water load		deck displ.		
		s.d.	max.	s.d.	max.	s.d./max.
[s]	[m]	[kN]	[kN]	[m]	[m]	[-]
One leg						
9.0	15.22	348.9	619.1	1.084	1.571	0.690
10.0	17.62	242.2	426.7	2.968	4.276	0.694
11.0	19.95	519.3	919.1	1.359	1.914	0.710
18.0	32.00	1447.6	2423.4	1.216	2.013	0.604
Platform						
9.0	15.22	591.4	1096.0	0.591	0.856	0.690
10.0	17.62	476.3	848.4	1.793	2.562	0.700
11.0	19.95	1114.9	1423.3	0.977	1.389	0.703
18.0	32.00	4075.7	6552.5	1.129	1.826	0.618

Table 8.8: Results of regular wave analysis

From the results listed in table 8.8, first the ratio of the standard deviation and the maximum value of the deck displacement is considered. For an harmonic motion with constant period and amplitude the theoretical value of this ratio is given by:

$$\frac{\text{s.d.}}{\text{max.}} = \frac{1}{2}\sqrt{2} = 0.707 \qquad (8.02)$$

A deviation from this ratio in table 8.8 indicates that the results do not apply solely to the steady state, but are influenced by the preceeding transient state. This means that the transient time is estimated too short.

Since the standard deviation is computed from the results of all time steps, the steady state standard deviations will hardly be influenced by the relatively short transient time, which is included in the computations due to an underestimation of the total transient time. As a result of this, a divergence from the theoretical ratio stated above will be caused by an error in the maximum value.

As can be seen in table 8.8, the only significant deviation is found for the design wave, for which the estimation of the transient time is obviously too short. From the fact that the ratio is too small it can be concluded that the stated maximum deck displacement is an overestimation of the actual steady state motion amplitude.

Although the maximum wave loads are found for the design wave, as to be expected, the maximum motions are found for the 10 s regular wave, which is nearest to the natural period of the platform. This means that the response of the structure is governed by the dynamic amplification near the natural period, as opposed to the response due to wave spectra, which is governed by the amount of spectral energy, rather than by amplification effects.

Another conclusion is that the loads and motions due to a regular wave are much greater than those due to a stochastic sea state. In a stochastic sea state, the waves resulting from various spectrum sections will compensate each other partially and thus the loads and motions cannot as severe as for one regular wave, in which case counteracting waves are present. In fact, this conclusion points out the severe overestimation by deterministic analysis of the physical reality concerning water loads and deck displacements.

The ratio of the standard deviation and the maximum value of the deck displacement for a stochastic sea state is much less than the ratio for a regular wave. This is merely a confirma-

tion of the stochastic nature of the platform response in the case of a stochastic sea state, allowing relatively large motion peaks. For longer simulation times, the ratio will even reduce more. It is pointed out that this does not apply to deterministig analysis, for which the theoretical ratio remains unchanged for longer simulations.

It should be noted that the water loads in deterministic analysis are found to be clearly drag force dominated. The ratio of mass and drag forces does not exceed 7.4 %.

Table 8.9 shows the reduction of loads and motions due to the phase differences between the legs of the three-legged platform Kolskaya. Again, the maximum reduction occurs for the wave with the period nearest to the 8.61 s computed in the previous chapter and decreases for increasing wave periods.

As for the wave spectra, the loads and motions are subdue to the same amount of reduction, except for the 10 s wave, which is 'affected' significantly by dynamic amplification causing an enhanced reduction of the deck displacement.

Generally speaking, the conclusions concerning the load and motion reductions due to phase differences between the legs are identical for regular and stochastic sea states.

wave period	wave height	reduction due to phase differences between the legs	
		water load	deck displ.
[s]	[m]	[%]	[%]
9.0	15.22	43.5	45.5
10.0	17.62	34.4	39.6
11.0	19.95	28.4	28.1
18.0	32.00	6.2	7.2

Table 8.9: Reduction of loads and motions due to phase differences between the legs

8.6 FREQUENCY DOMAIN

8.6.1 General

In the previous paragraphs, the results from time domain analysis applying to the steady state motions have been presented. This paragraph deals with the comparison of these results with those obtained from frequency domain analysis of the same two models. All parameters are equal to those stated for the reference case and the one leg model, apart from those specifically applying to time domain analysis.

As stated before, frequency domain analysis does not yield maximum values of loads and motions for a stochastic sea state, but only standard deviations. For this reason, the comparison of time domain and frequency domain is restricted to the standard deviations of these parameters and the maximum values found in the time domain will not be mentioned here.

In order to allow a clear comparison of deterministic and stochastic sea conditions, this restriction is made for deterministic analysis as well. It should be noted that the load and motion values stated for this type of analysis do not represent the amplitudes, but the standard deviations.

The frequency domain results for a stochastic sea state are also used for plots of the D.A.F. and the frequency characteristics of loads and motions.

The frequency domain computer program Jacquelin includes the computation of the effect of directional wave spreading and the result of this will be discussed in this paragraph.

8.6.2 Deterministic analysis

The results from deterministic analysis of both models are listed in table 8.10. The frequency domain and the time domain are respectively denoted as f.d. and t.d.. The differences between both methods are generally less than 20 %, except for the 10 s wave, which is near the natural period, and the water loads in particular. The overestimation of the water load by frequency domain analysis is more than 25 % for the platform and almost 80 % for the one leg model. The cause of these large overestimations could not be traced, but one possible explanation is given below.

wave period	wave height	standard deviation of water load			standard deviation of deck displ.		
		f.d.	t.d.	diff.	f.d.	t.d.	diff.
[s]	[m]	[kN]	[kN]	[%]	[m]	[m]	[%]
One leg							
9.0	15.22	330.8	348.9	- 5.2	0.971	1.084	-10.4
10.0	17.62	433.8	242.2	+79.1	3.880	2.968	+30.7
11.0	19.95	604.9	519.3	+16.5	1.613	1.359	+18.7
18.0	32.00	1471.7	1447.6	+ 1.7	1.133	1.216	- 2.7
Platform							
9.0	15.22	568.6	591.4	- 3.9	0.554	0.591	- 6.3
10.0	17.62	596.5	476.3	+25.2	1.971	1.793	+ 9.9
11.0	19.95	1249.4	1114.9	+12.1	1.114	0.977	+14.0
18.0	32.00	4191.3	4075.7	+ 2.8	1.123	1.129	- 0.5

Table 8.10: Results for a deterministic sea state

For the theoretical case of an undamped single-degree-of-freedom system subdue to an harmonic load with a period equal to the natural period of the system, it is known that the displacement and the load are in phase. From this theory it can be derived that the minimum phase difference between loads and motions in table 8.10 is found for the 10 s wave.

Since the platform motion are relatively large for the 10 s wave, an error in the frequency domain representation of this phase difference yields a relatively large error in the relative velocity and thus in the water load. For the other waves, this effect will not be as strong, as the platform motions are less severe.

Apart from this explanation of the large load differences, it should be noted that the time domain water load includes the damping force, which is not the case for the frequency domain. Since the direction of this damping force is always opposite to the loading direction, this will cause an overestimation by frequency domain analysis of the overall water load on the plaform.

8.6.3 Stochastic analysis

Table 8.11 shows the loads and motions due to a stochastic sea state. The comparison of frequency domain and time domain water loads yields less extreme, but still significant differences up to 30 %..

The deck displacement shows much more inconsistency. There is a large frequency domain overestimation, rapidly decreasing for increasing peak periods. The reason for this is not quite understood. Since this trend does not seem to be correlated to the trend observed for the water loads, the displacement differences could be caused by dynamic amplification effects, but this would probably yield a maximum error for the 10 s wave spectrum, rather than the 8 s spectrum.

As opposed to time domain analysis, the maximum motions from the frequency domain are found for the wave spectrum subdue to maximum dynamic amplification, instead of the spectrum with the maximum overall wave energy.

Since time domain analysis is believed to provide an accurate representation of physical reality, the observed inconsistencies are probably due to the frequency domain linearization of the drag force. As opposed to the drag force dominated cases examined here, the errors should become much less for mass force dominance.

peak period	sign. wave height	standard deviation of water load			standard deviation of deck displ.		
		f.d.	t.d.	diff.	f.d.	t.d.	diff.
[s]	[m]	[kN]	[kN]	[%]	[m]	[m]	[%]
One leg							
8.0	6.0	45.7	38.6	+18.4	0.286	0.165	+73.3
10.0	10.0	83.1	89.0	- 6.6	0.928	0.655	+41.7
12.0	14.0	128.5	182.2	-29.5	0.673	0.642	+ 4.8
Platform							
8.0	6.0	79.1	66.7	+18.6	0.177	0.101	+75.2
10.0	10.0	151.6	174.1	-12.9	0.563	0.397	+41.8
12.0	14.0	279.2	405.7	-31.2	0.422	0.409	+ 3.2

Table 8.11: Results for a stochastic sea state

Despite the observed differences between frequency domain and time domain, again the general conclusion can be drawn that deterministic analysis yields an overestimation of load and motion values.

The conclusion that dynamic amplification is related to the peak period of the wave spectrum, rather than by the average zero-crossing period is confirmed by the frequency domain computations.

8.6.4 Load and motion spectra

In the previous paragraphs, only the translational motion mode of the platform has been considered. Since the frequency domain computer program Jacquelin includes the analysis of the rotational mode, the spectral presentation of the results in this paragraph will also include this rotational mode as well.

However, the main wave direction of 0 degrees used until now is a symmetrical loading direction of the Kolskaya, as pointed out in chapter 6, and thus no rotational excitation occurs, theoretically. Indeed none of the cases with this loading direction, examined by means of the computer program Jacquelin, showed any wave-induced moments and rotations.

The dynamic computations underlying the spectral plots presented in this chapter are made for a main wave direction of 30 degrees, using the same wave spectra as in the previous paragraphs.

As is the case for the translational water loads, the phase differences between the legs will influence the water loads for the rotational mode of the platform. For the wave direction of 30 degrees shown in figure 8.17 the maximum wave-induced moments will occur if the loads on legs 1 and 3 are in phase, while the load on leg 3 is in counterphase with the load on the other two legs. This is the case for a wave with awave length equal to the distance beteen leg 1 and 3.

For the Kolskaya, the distance between leg 1 and 3 is 53.69 m. A sinusoidal wave with this wave length has the following frequency:

$$\omega = 1.07 \text{ rad/s}$$

At this frequency, the maximum enhancement of the wave-induced moments, due to the platform geometry, occurs. It should be noted that this frequency is dependent of the wave direction.

Figure 8.18 shows the translational load spectra. Their shape is quite similar to that of the Jonswap wave spectra, with a

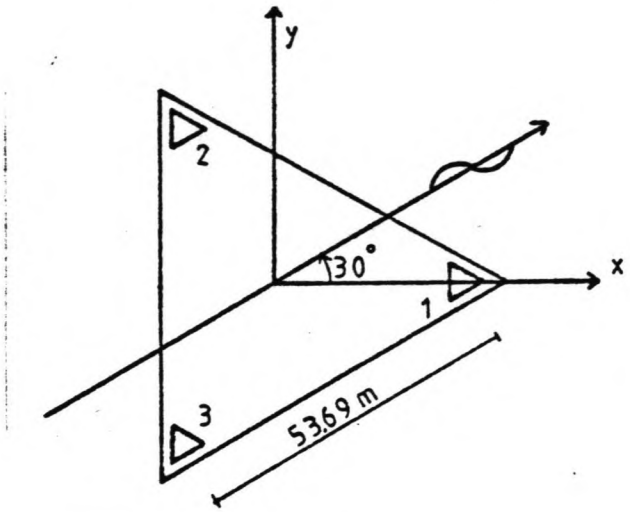

Figure 8.17: Situation for a wave direction of 30 degrees

clear coincidence of the peak periods. However, an increase of the overall wave energy causes a more than proportional increase of the variance of the water loads. This is due to the fact that the water loads are dominated by the drag force, which is proportional to the squared surface excursion.

The load spectra for rotation, plotted in figure 8.19, do not show such a resemblance to the Jonswap wave spectra. At all three load spectra, there still is a peak near the peak period of the wave spectra, but a second peak is observed. It is caused by the platform geometry, as pointed out above. The wave frequency of this peak is a little less than the 1.07 rad/s computed, which is due to the fact that the geometrical enhancement is 'counteracted' by a decrease of the spectral density of the wave spectrum, for increasing frequencies.

The geometrical peak in the load spectra increases for increasing significant wave heights, due to the fact that the spectral density of the wave spectra near the geometrical peak increases.

Again, the conclusion can be drawn that the motions and loads due to a certain sea state can be influenced by the the platform geometry.

Figure 8.20 shows the motion spectra for translation in the wave direction. If the band width of the load spectra in figure 8.18 is considered, it is clear that the motions computed

FIG. 8.18: LOAD SPECTRA IN THE WAVE DIRECTION

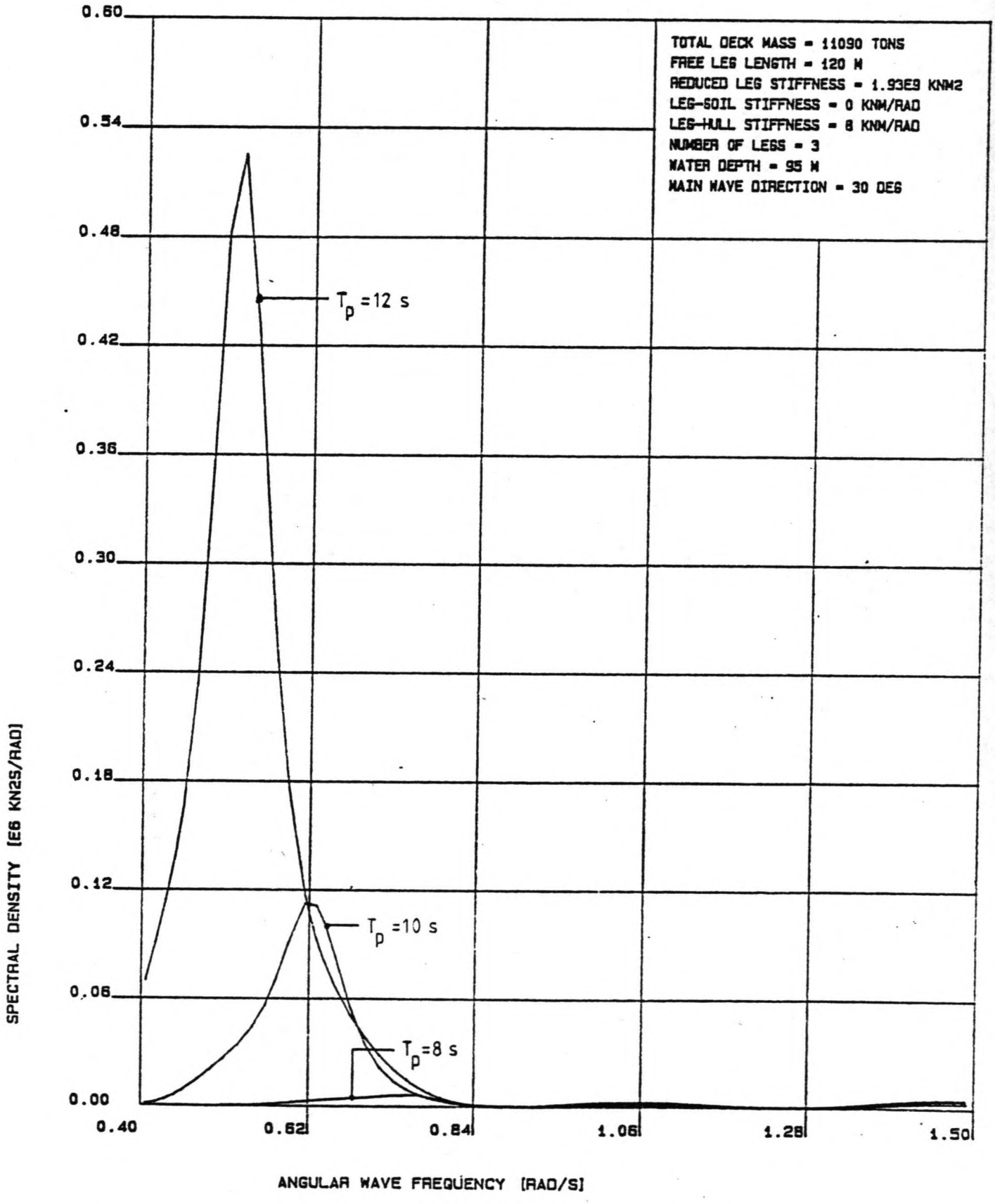

FIG. 8.19: LOAD SPECTRA FOR ROTATION

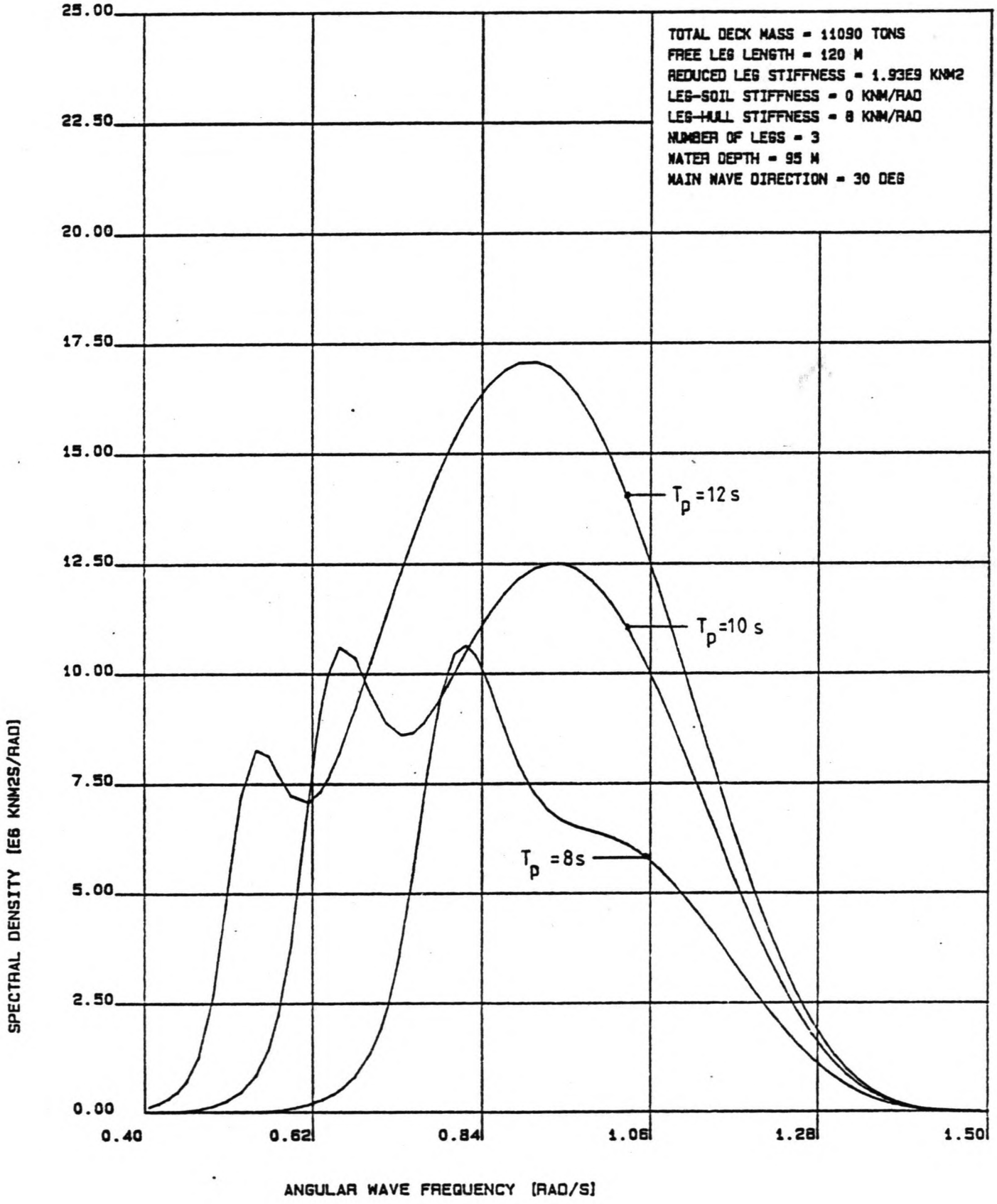

in the frequency domain are governed by dynamic amplification effects, as already concluded earlier in this paragraph. The motion spectra show a sharp peak at the natural period of translation. The maximum motions are caused by the 10 s wave spectrum, with its peak period near the natural period.

At the presentation of the theory explaining the Gaussian distribution of the deck displacement in paragraph 8.2, it was suggested that a narrow banded motion spectrum would cause deviation from the Gaussian curve. Indeed it is observed that the largest deviation occurs for the 8 s wave spectrum, causing the most narrow-banded response. The best fit of the Gaussian distribution is found for the most wide-banded response spectrum , induced by the 12 s wave spectrum. This is in line with the theory presented.

The motion spectra for rotation, shown in figure 8.21, supports the conclusions concerning the importance of dynamic amplification. There is a sharp peak at the natural period of platform rotation.

The dynamic amplification factors for both motion modes, plotted in figures 8.22 and 8.23, show the sharp peaks causing the relatively narrow banded response already observed. The dynamic amplification of rotation shows an increasing peak for a decreasing significant wave height, due to the decreasing hydrodynamic damping.

At the D.A.F for translation this trend is disturbed by the fact that the peak of the 10 s wave spectrum is very near the natural period of the platorm, causing the maximum dynamic amplification. The 8 s spectrum shows a second translational peak at the natural period of platform rotation. For a loading direction of 30 degrees, both motion modes are not completely independent. Due to this, the relatively large rotations for the 8 s spectrum cause a secondary peak in the graph of the D.A.F. for translation.

It should be noted that the interaction between the motion modes, and thus secondary amplification peaks can become much more important for platforms with more assymetry than the Kolskaya. An increase of this interaction can be caused by:

a. An eccentric gravity centre of the pontoon.

b. Different stiffness parameters per leg.

c. Different drag and mass coefficients per leg.

The frequency domain computer program Jacquelin is capable of handling an eccentric gravity centre as well as different drag and mass coefficient per leg and can easily be modified for

FIG. 8.20: MOTION SPECTRA IN THE WAVE DIRECTION

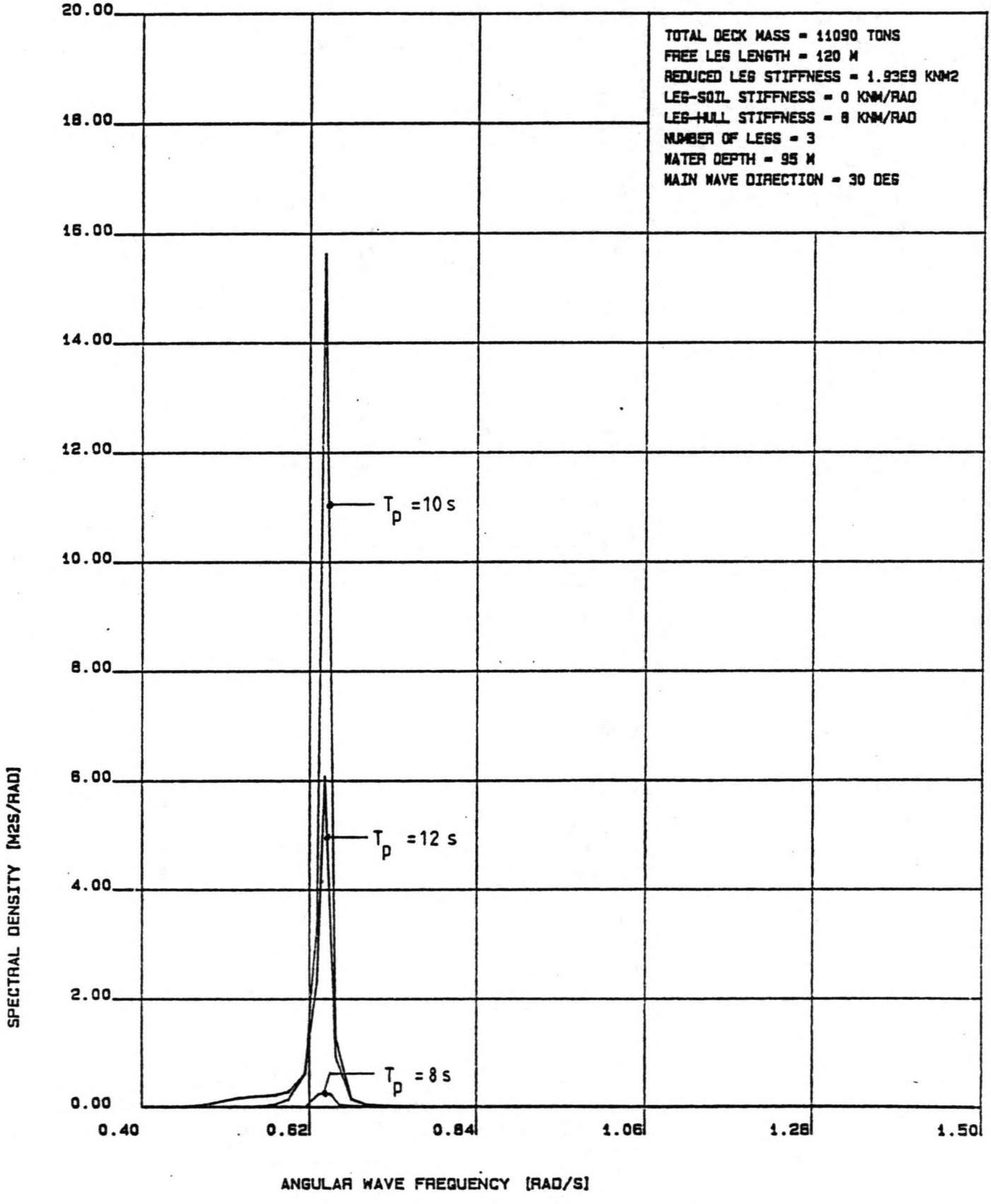

FIG. 8.21: MOTION SPECTRA FOR ROTATION

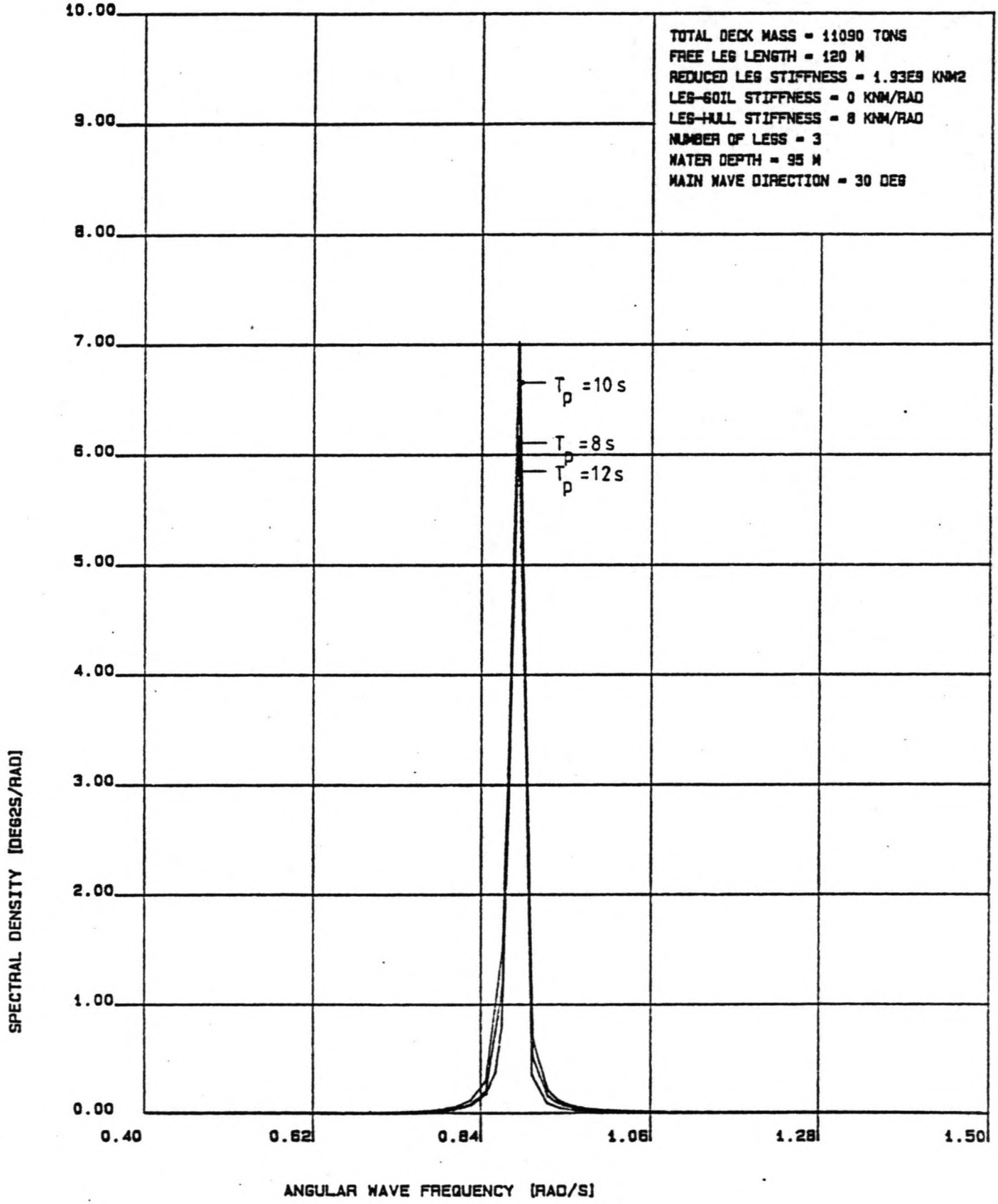

FIG. 8.22: DYNAMIC AMPLIFICATION FACTOR IN THE WAVE DIRECTION

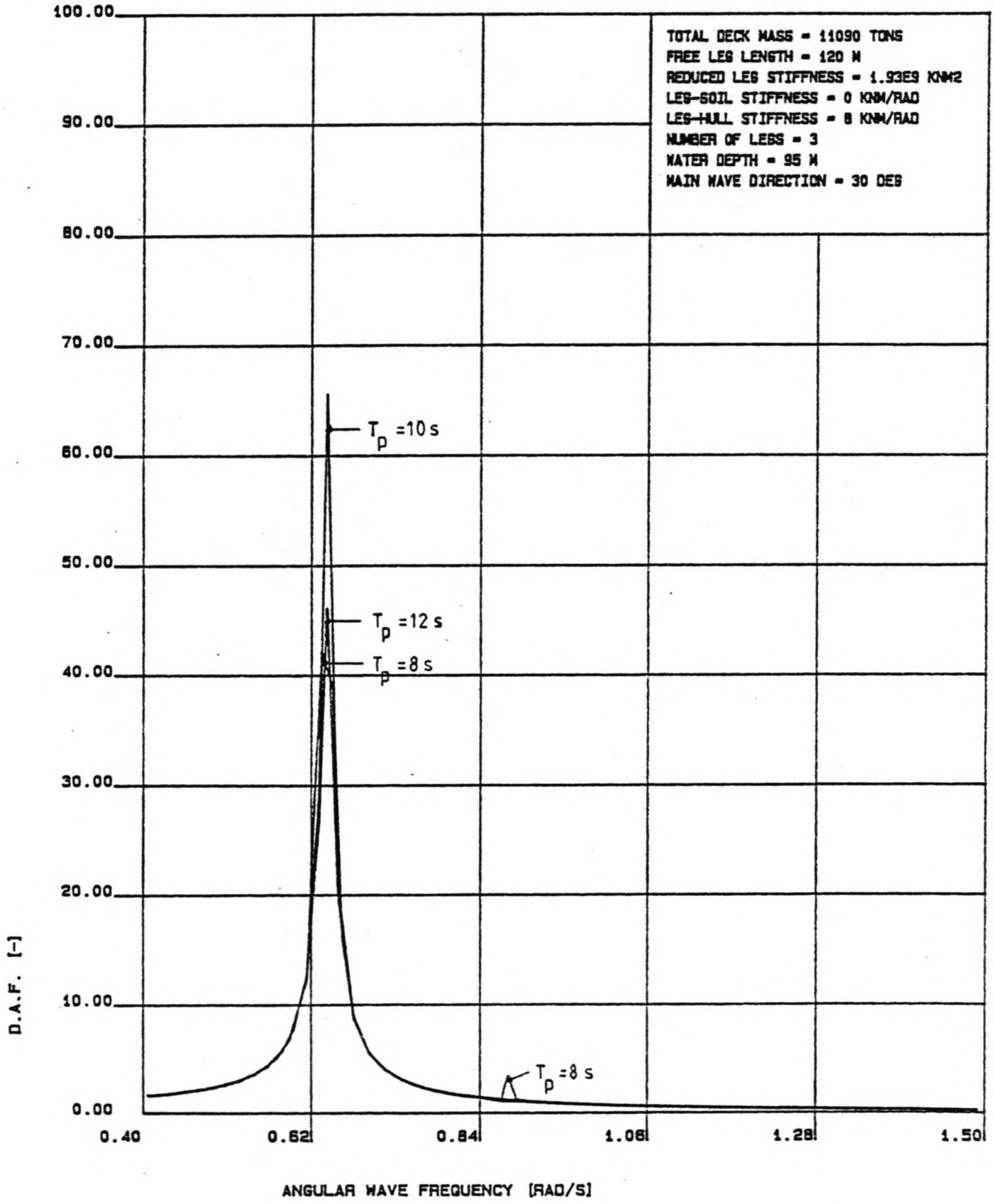

FIG. 8.23: DYNAMIC AMPLIFICATION FACTOR FOR ROTATION

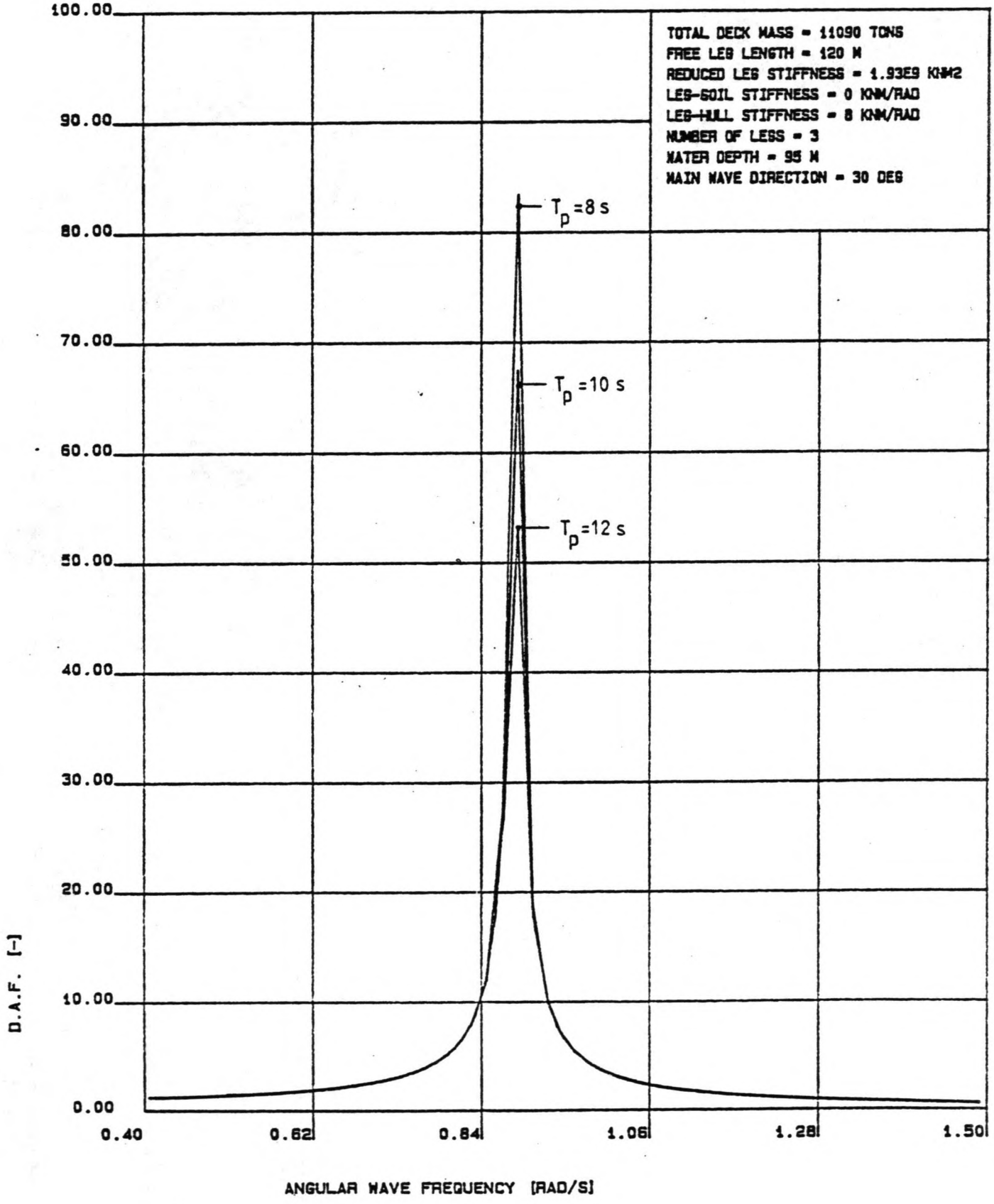

the use of different stiffness parameters per leg.

8.6.5 Directional wave spreading

The directional spreading of the waves is accounted for by means of the cosine square distribution, as outlined in chapter 6. The lack of empirical data confirming the correctness of this distribution has already been mentioned, but nevertheless it is interesting to consider the computed load and motion reductions, which are listed in table 8.12.

peak period	sign. wave height	standard deviation of water load			standard deviation of deck displ.		
				red.			red.
[s]	[m]	[kN]	[kN]	[%]	[m]	[m]	[%]
8.0	6.0	79.1	54.4	31.2	0.177	0.152	14.1
8.5	7.0	92.9	67.0	27.9	0.247	0.213	13.8
9.0	8.0	109.8	82.8	24.6	0.353	0.306	13.3
9.5	9.0	128.9	100.8	21.8	0.493	0.430	12.8
10.0	10.0	151.6	121.9	19.6	0.563	0.492	12.6
10.5	11.0	179.1	146.8	18.0	0.537	0.469	12.7
11.0	12.0	209.9	174.5	16.9	0.479	0.417	12.9
11.5	13.0	243.0	204.1	16.0	0.438	0.381	13.0
12.0	14.0	279.2	236.3	15.4	0.422	0.367	13.0

Table 8.12: Load and motion reduction due to directional wave spreading

The directional wave spreading factor has been applied to the variance of the water load and the deck displacement. Since the factor describes the directional spreading of energy transport, there seems to be more justification fort its use with the variance of motion, which is related very clearly to energy properties, than with the variance of loads.

This doubt concerning the method used for the reduction of the loads seems to be confirmed by the inconsistency between the reduction percentages of the loads and the motions. While the motion reduction is almost constant for all wave spectra, the load reduction shows a decrease for increasing peak periods. Since no physical explanation could be found for this, there is some suspicion about the application of the wave spreading factor to the water loads.

It should be noted that directional wave spreading will not

always cause reductions. Platforms with strong asymmetry could even show increasing loads and motions for certain main wave directions.

8.7 HYDRODYNAMIC DAMPING

As stated before, hydrodynamic damping perdentages are only computed in the frequency domain. The results for regular wave analysis are listed in table 8.13.

The last column of this table shows the hydrodynamic damping for waves with a range of periods, but all with the same wave height. It can be seen that there is a dip in the hydrodynamic damping at the natural period. This is explained by the fact that the phase difference between the fluid motions and the platform motions is minimal at the natural period, causing minimal damping forces.

wave period	wave height	hydrodynamic damping		
		one leg	platform	
				wave height = 12.79 m
[s]	[m]	[%]	[%]	[%]
8.0	12.79	1.735	1.826	1.826
9.0	15.22	1.981	2.198	1.850
10.0	17.62	2.618	2.210	1.779
11.0	19.95	3.257	3.123	2.053
12.0	22.18	3.594	3.530	2.061
13.0	24.28	3.928	3.890	2.066
14.0	26.27	4.238	4.213	2.064
15.0	28.12	4.538	4.521	2.067
16.0	29.84	4.820	4.807	2.069
17.0	31.44	5.084	5.074	2.072
18.0	32.00	5.182	5.175	2.075

Table 8.13: Hydrodynamic damping for deterministic sea state

For increasing wave heights, the hydrodynamic damping increases, due to the increasing platform motions, which generate increasing damping forces.

Comparing the damping values found for one leg and found for the complete platform it can be concluded that there is hardly

any difference and that the hydrodynamic damping percentages for regular waves are in the range of 1 to 5 %.

The same trend of increasing damping values for increasing wave heigths of regular waves is observed for stochastic sea states, for which the results are listed in table 8.14. Due to a similar mechanism of decreasing platform motions, the hydrodynamic damping decreases for increasing values of structural and soil. However, this decrease is not very significant, which is probably caused by the fact that the increasing overall damping induces greater phase differences between fluid motions and platform motions, with the result of increased hydrodynamic damping forces. Both effects seem to compensate each other by and large.

It is concluded that the influence of physically realistic structural and soil damping values on the platform motions is only marginal, in the case of a stochastic sea state. This conclusion is supported by the results found in the time domain.

wave period	wave height	hydrodynamic damping					
		one leg			platform		
		css=0	css=1	css=2	css=0	css=1	css=2
[s]	[m]	[%]	[%]	[%]	[%]	[%]	[%]
8.0	6.0	0.432	0.400	0.397	0.428	0.415	0.414
8.5	7.0	0.518	0.475	0.470	0.512	0.495	0.493
9.0	8.0	0.615	0.552	0.544	0.602	0.577	0.574
9.5	9.0	0.725	0.639	0.627	0.695	0.661	0.657
10.0	10.0	0.827	0.741	0.726	0.786	0.752	0.747
10.5	11.0	0.907	0.843	0.829	0.870	0.846	0.840
11.0	12.0	0.979	0.936	0.924	0.952	0.936	0.930
11.5	13.0	1.051	1.021	1.012	1.033	1.021	1.017
12.0	14.0	1.129	1.105	1.097	1.116	1.107	1.103

Table 8.14: Hydrodynamic damping for stochastic sea state

The damping values for a stochastic sea state are much lower than those found by means of deterministic analysis, in the order of 0 to 1 % only. Since this representation of the sea surface is much more realistic than a deterministic representation, its hydrodynamic damping values will be more realistic as well. From this the conclusion can be drawn that the deterministic analysis method yields an overestimation of the hy-

drodynamic damping. This is in line with earlier conclusions concerning the water loads and deck displacements.

8.8 CONCLUSIONS

In this paragraph, a resume is given of the main conclusions of this study of the dynamic behaviour of a jack-up platform with lattice legs, in elevated condition.

The following general conclusions can be drawn:

a. The water loads on a jack-up with lattice legs are drag force dominated.

b. The phase differences between the legs of a multi-legged platform cause considerable load reductions for platform translation in comparison with the one-legged case. The reduction of the deck displacement proportional to the load reduction, except for wave periods near the natural period, for which the motion reduction is enhanced by dynamic amplification effects. The reduction depend on the loading direction.

c. The load spectrum for the rotational mode shows a geometrical peak, apart from peak of the wave spectrum. This peak is dependent of the loading direction.

d. The motions and loads due to a certain sea state can be influenced by the choice of the platform geometry. This is a more general conclusion concerning the phase differences between the legs.

e. Deterministic analysis yields significantly greater values for the loads and motions as well as hydrodynamic damping than stochastic analysis. This is due to the simplification of the physical reality by regular wave analysis, causing an overestimation of these parameters.

f. There are major inconsistencies between the results of the frequency domain and the time domain, particularly those from stochastic analysis. Since time domain analysis is believed to provide a reliable representation of the physical processes involved, it seems that this inconsistencies are caused by the frequency domain linearization of the drag force. This assumption is supported by the drag force dominance in the cases examined. For mass force dominance, the errors should be much less.

The following conclusions specifically apply to stochastic analysis:

g. For a stochastic sea state represented by a Jonswap spectrum, the dynamic amplification is governed by the peak period of the wave spectrum, rather than by its average zero-crossing period. This effect is related to the sharp-peaked nature of the Jonswap spectrum and need not occur for other types of wave spectra.

h. Structural and soil damping values which can be expected to be physically relevant, less than 4 %, do not influence the platform motions substantially, in case of a stochastic sea state.

i. In the case of drag force dominance, the statistical distribution of the water loads can be represented by an exponential distribution function. A shape factor equal to 1.5 generally gives good results. For increasing significant periods of the wave spectrum, the load distribution becomes slightly asymmetrical, due to the increasing differences between the fluid velocity profiles 'under' a wave crest and 'under' a wave trough.

j. For low damping percentages, the deck displacement follows a Gaussian distribution. A divergence from the Gaussian curve towards a uniform distribution is linked to a narrow-banded response spectrum. In case of a linear transfer between loads and motions, increasing damping values cause a divergence from the Gaussian distribution towards the load distribution curve. This conclusion is valid for drag force as well as mass force dominated cases and for a any number of platform legs.

During the modelling of the relevant mechanisms and processes, perfomed in the previous chapters, the following items were found to be of particular interest for further investigation:

a. The reliability of the Morison equation in general and the correct determination of drag and mass coefficients.

b. The rotational stiffness of the leg-soil connection.

c. The significance of lift forces.

The examination of all three items will have to be carried out on an empirical basis.

REFERENCES

1. Anonymous (1984)
"Dynamics of Jack-up Platforms"
Det Norske Veritas, Hovik, Norway

2. Anonymous (1985)
"Environmental Parameters on the United Kingdom Continental Shelf"
Department of Energy, London

3. Anonymous (1983)
"Strength Analysis of Main Structures of Self Elevating Units"
Det Norske Veritas, Hovik, Norway

4. Battjes, J. A. (1985)
"Korte Golven"
Lecture notes b76, Department of Civil Engineering, Delft University of Technology

5. Battjes, J. A. (1984)
"Windgolven"
Lecture notes b78, Department of Civil Engineering, Delft University of Technology

6. Borgman, L. E. (1967)
"Spectral analysis of ocean wave forces on piling"
Journal of the waterways and harbour division, Vol. 93, no. WW2, May 1967

7. Bouma, A. L. & Esveld, C. (1979)
"Dynamica van constructies"
Lecture notes b15A, Department of Civil Engineering, Delft University of Technology

8. Bouma, A. L. & Esveld, C. (1979)
"Voortgezette dynamica van constructies"
Lecture notes b15B, Department of Civil Engineering, Delft University of Technology

9. Gudmestad, O. & Connor, J. J. (1983)
"Linearization methods and the influence of current on the non-linear hydrodynamic drag force"
Applied Ocean Research, Vol. 5, no. 4, October 1933

10. Hagemeijer, P. M. & Regt, C. T. de (1984)
"Dynamica van een Tension Leg Platform"
Thesis, Department of Civil Engineering, Delft University of Technology

11. Kokkinowrachos, K. (1980)
"Hydromechanik der Seebauwerke"
Rhein.-Westf. Technische Hochschule Aachen, Germany

12. Soest, J. van (1983)
"Elementaire Statistiek"
Lecture notes a92B, Delft University of Technology